Sediment Transport in the Piura River. Piura, Peru.

An application with the HEC-RAS model

Ann Katrin Ladewig Piscoya

Sediment Transport in the Piura River. Piura, Peru.

An application with the HEC-RAS model

By:
Ann Katrin Ladewig Piscoya

Master Thesis

Division of Water Resources Engineering
Department of Building & Environmental Technology
Lund University
Box 118
221 00 Lund, Sweden

Master Thesis
Division of Water Resources Engineering
Department of Building & Environmental Technology
Lund University

Acknowledgements

University Collaboration and Funding

This thesis is a collaboration with the University of Piura. The topic was developed by Jorge Reyes Salazar, lecturer in hydraulics and sediment transport at the University of Piura. Conversation to establish the topic was initially based on the predicted El Niño episode of 2023/2024, during which heavy rainfall was expected. However, the probability for an extreme El Niño episode reduced towards the end of 2023, thereby removing the alert for heavy rainfall. As such, the focus was shifted to sediment transport.

Research for this thesis involved being on- site in Piura. Funding for the trip was provided by The Crafoord Foundation. My time in Piura allowed me to gain insight on the topic, which would hardly have been possible from a distance.

Abstract

This thesis is an investigation of sediment transport in the Piura River in Peru. Years of anthropogenic changes have redirected the river towards the south and have caused changes in the flow regimen (Alvarado Ancieta & Ettmer, 2007). It is suspected that the redirection towards the south has resulted in deposition of sediments which has reduced the capacity of the river in the lower reaches (Reyes Salazar, 2024b). As such, the aim of this thesis is to compare hydraulic conditions of the current route through Virrilá in the south and the original course towards Sechura to assess sediment transport capacity.

HEC-RAS version 6.3.1 is used for hydraulic modelling. The model is calibrated using flow data from the 2017 flood event. Flows of 1,000 m^3/s and 3,200 m^3/s are computed in steady state for velocity, depth, and shear stress profiles as output. Excess shear is used to assess sediment transport capacity. It was found that the general trend for Virrilá is deposition of sediment in the lower reach, while the course towards Sechura produces considerably larger excess shear values, thereby indicating increased capacity for sediment transport.

Glossary

ANA: Autoridad Nacional del Agua- N*ational Authority for Water*

ARCC: Autoridad para la Reconstrucción con Cambios- *Authority for Reconstruction with Change*

ENFEN: Estudio nacional del Fenómeno El Niño- *National Study of El Niño Phenomenon*

ENSO: El Niño southern oscillation

ICEN: Índice Costero el Niño- *El Niño coastal index*

ONI: Oceanic Niño index

PNUD study: study by the National University of Piura and University of Piura (2001)

SENAMHI: Servicio Nacional de Meteorología e Hidrología- *National Meteorology and Hydrology Service*

x

Table of Contents

Appendix A: Field Visits

Appendix B: Geometry Data for Virrilá and Sechura

Appendix C: Output and Calculated Results

List of Figures and Tables

1. Introduction

1.1. General Background

The northern coast of Peru is regularly subject to flooding. The Piura region is consistently among the regions most affected by the floods on a national level together with Tumbes, Lambayeque, and La Libertad (Organización Panamericana de la Salud, 2018) shown in Figure 1. The region covers an area of around 40,580 km^2 (UDEP & UNP, 2001e) and has a population of approximately 1.8 million (ARCC, 2022). The consequences of flooding in the region include loss of agricultural land, destruction of infrastructure, sanitation line failure, and an increase of diseases (SENAMHI, 2014).
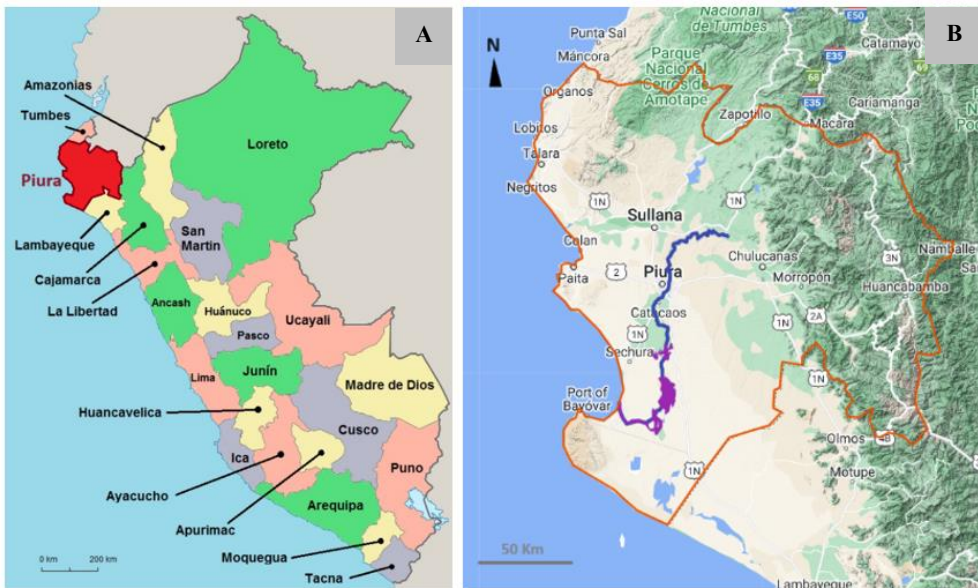
Figure 1a- Overview map of Peru (The Only Guide Peru, n.d.). 1b- Map of Piura Region (Google Maps, 2023)

The capital city of the region, also called Piura, has a population of approximately 517,300 (Atarama & Rashid, 2019) and was founded in 1532 by the Spanish settlers (MGI, n.d.). Piura is partially located in the alluvial fan of the Piura River (Fernández et al., 2021). The river is non-perennial and originates in the highlands to the east at an altitude of 3,370m above sea level (Alvarado Ancieta, 2023) where it then flows west towards the Pacific Ocean and passes through a series of lagoons in the Sechura Desert before exiting into the Virrilá estuary (ARCC, 2022). An overview map of the lower basin is shown in Figure 2.

Figure 2- Overview map of lower basin (Google Earth, 2024)

The semi-arid climate in the lower basin changes during El Niño episodes, during which there is frequent and heavy rainfall for a period of 4-5 months (UDEP & UNP, 2001e). Flood events in Piura are generally linked to the increased precipitation experienced during El Niño. The current river system is incapable of controlling the large quantities of water that develop during this event (UDEP & UNP, 2001e). In the past, flooding occurred due to a lack of urban drainage together with erosion of the riverbed which resulted in the collapse of river infrastructure (Reyes Salazar, 2024b). However, the most recent flood event of 2016-2017 revealed an ongoing process of aggradation which is reducing the capacity of the river (Reyes Salazar, 2024a). Figure 3 shows data collected by the University of Piura for the bottom level and water level for three different years at three different flows. The bottom level in the urban reach has increased 6m since 1998. Consequently, the capacity of the river has decreased.
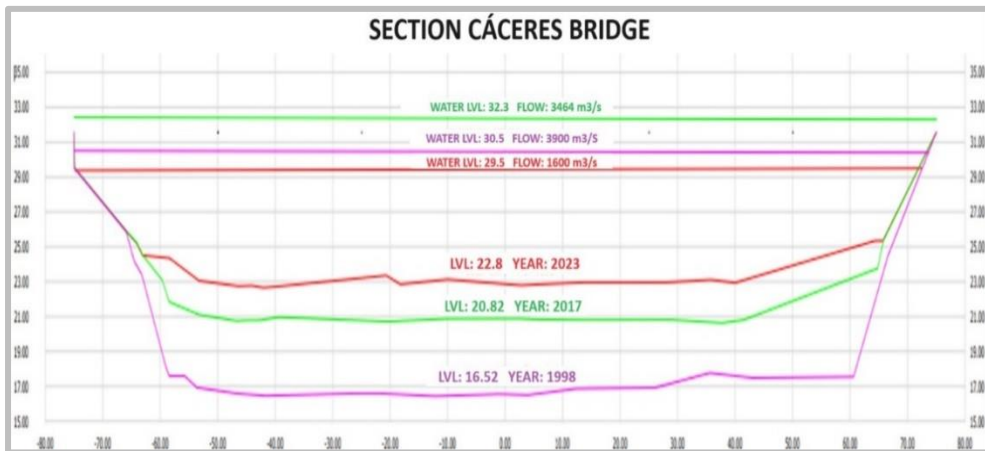
Figure 3- Section Cáceres Bridge showing bottom level development. (adapted from Reyes Salazar, 2024b)

The lower basin has been flooded 6 times in the last 45 years (Castillo Zavaleta, et al., 2019). This has encouraged many investigations and studies concerning vulnerability, urban drainage, El Niño, alleviation plans, and sediment transport. As mentioned, the river flows through a series of lagoons

before exiting into the ocean. For that reason, it should be noted that the Ramón Lagoon has been steadily filling up with sediments. An estimated 30% of the original capacity remains (Reyes Salazar, 2024b), the sedimentation can be observed as shown in Figure 4.

Figure 4- Sedimentation of the Ramón Lagoon (Google Earth, 2024)

Historically, the Piura River flowed through Sechura in the west (Zegarra Dávila, 2024). However, the growing importance of agriculture in the region led to the construction of dikes which resulted in the redirection towards the south (Alvarado Ancieta, 2023). The current route through Virrilá has a smaller slope and is longer than through Sechura (Reyes Salazar, 2024b). As a result, there is less energy in the river and sedimentation occurs (Reyes Salazar, 2024b). Experts suspect that deposition of sediment along some stretches of the river will continue to reduce the capacity and will render the lower basin vulnerable to flooding even during small flows (Reyes Salazar, 2024b).

1.2. Aim

The aim of this thesis is to compare sediment transport in the Piura River for two different river courses. The routes are shown in Figure 5, these are the existing course through the Virrilá Estuary, and a proposed course through Sechura. The software HEC-RAS is used to create a river model for the two routes. Velocity and depth output is used to compare transport capacity.
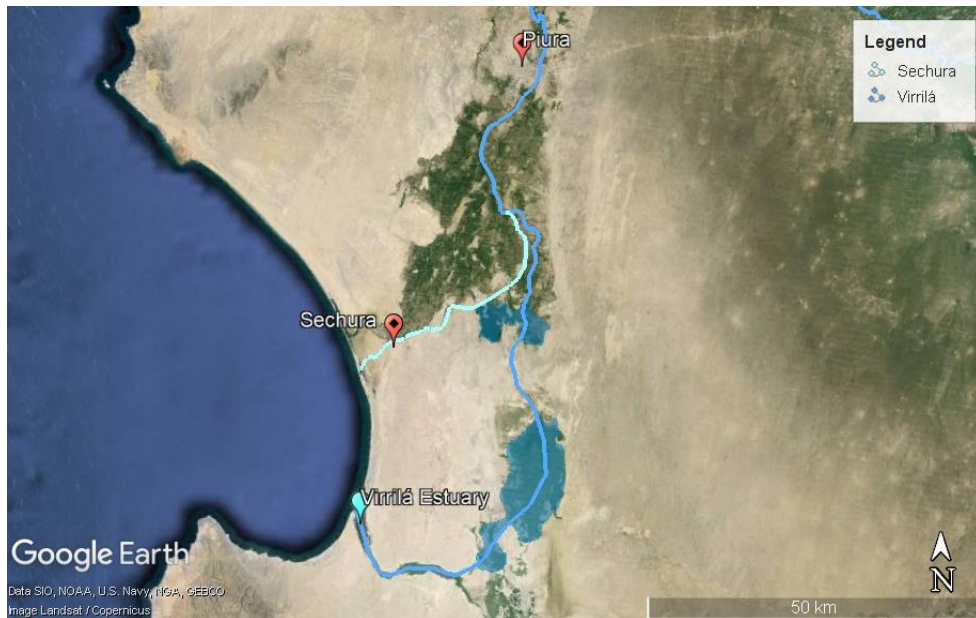
Figure 5- Piura River routes through Virrilá and Sechura (Google Earth, 2024).

The proposed route towards Sechura follows parts of the ancient river course, and is expected to have a larger transport capacity, thereby reducing sedimentation (Zegarra Dávila, 2024). Various proposals are being developed to decrease the vulnerability in the lower basin, therefore describing sediment transport through river modelling can be a useful tool to reinforce suggestions and for planning of future interventions.

1.3. Methodology

This thesis is a collaboration with the University of Piura. Research involved being on site in Piura for improved data acquisition. Information for this thesis was sourced using Google Scholar, company sites, personal communication with experts in the Piura region, field visits, and was provided by the University of Piura. Relevant material included articles, project documents, reports both published and unpublished, and topographic data.

1.4. Thesis Outline

This report consists of 10 chapters. Chapter 1, "Introduction" provides background information, the scope of the study, and objectives. The following chapter "Piura River Catchment" provides information on the study area in terms of flood events, hydrological conditions, and morphology of the river. Chapter 3 "Previous Studies" describes studies and projects related to this research. Chapter 4 "Field Visit" describes the excursion to the Piura River and major observations. Next, Chapter 5 "Theoretical Background" describes theory and the use of HEC-RAS. Continuing in Chapter 6 "Data Employed", data acquired for sediment transport capacity analysis and HEC-RAS modelling is described. Chapter 7 "HEC-RAS Model Set Up and Output Processing" describes input, assumptions, and parameters used in HEC-RAS. The following chapter, "Results" describes calibration, HEC-RAS, and sediment transport capacity results. Next, in Chapter 9 "Discussion and Recommendations" provides insight on the implication of the results, gives suggestions for additional sediment investigation and recommendations for further studies. Finally, Chapter 10 "Conclusion" re-visits the aim of the study in relation to the results. A bibliography and appendices are found at the end of the report.

2. Piura River Catchment

This chapter provides information on the Piura River basin in terms of land use, historical flood events, hydrology, and river morphology.

2.1. Introduction to the Catchment

The Piura River basin has an area of 12,216km^2 (Moreano Segovia & Yauri Quispe, 2008.) which accounts for 31% of the Piura region (CIIFEN, 2020). The river originates in the eastern highlands and runs west where it enters a series of lagoons before indirectly exiting into the Pacific Ocean through the Virrilá estuary, it has a length of 326km (Moreano Segovia & Yauri Quispe, 2008). The catchment is defined by three zones, namely the upper basin, mid-basin, and lower basin as shown in Figure 6.
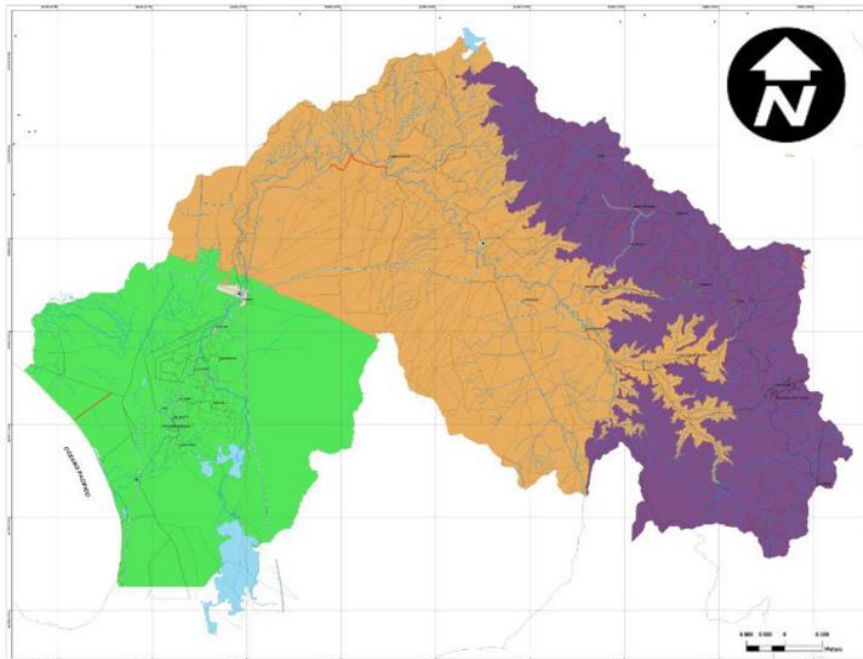
Figure 6- Piura River catchment zones (adapted from Moreano Segovia & Yauri Quispe, 2008)

These are characterized as follows:

- Upper basin- The section of the basin at an altitude between 350-3,650m asl with defined valleys and steep slopes (Moreano Segovia & Yauri Quispe, 2008). The climate is subhumid, and precipitation ranges from 500-1,000mm yearly (Moreano Segovia & Yauri Quispe, 2008). Shown in purple in Figure 6.

- Mid basin- This section ranges from 50–350m asl, it is a hilly landscape with yearly precipitation ranges from 100–500mm (Moreano Segovia & Yauri Quispe, 2008). Shown in orange in Figure 6.

- Lower basin- The lower basin is very flat land with altitudes ranging from 0–50m asl (Moreano Segovia & Yauri Quispe, 2008). It is an arid climate with yearly precipitation at less than 100mm (Moreano Segovia & Yauri Quispe, 2008). Shown in green in Figure 6.

The Piura River is non-perennial. In the highlands the bedrock is closer to the ground and there is more precipitation, as such the river is permanent in the upper basin (Atarama & Rashid, 2019). In the mid basin, the river feeds irrigation canals and recharges an aquifer since the bedrock is deeper (Atarama & Rashid, 2019). Thus, the river regularly runs dry from August to December, especially in years with less rainfall (Atarama & Rashid, 2019). In the lower basin the Piura River is fed by the Chira River to the north at a point 30km upstream of the city of Piura, it provides the lower basin with 60m^3/s of water (PECHP, 2017).

Historical records depict the exit of the Piura River at Sechura, where it discharged into the Pacific Ocean through 2-3 branches (Guererro et al., 2015) as shown by Figure 7 which is a map from 1779 (Zegarra Dávila, 2023).

Figure 7- Map showing the Piura River from 1779 (adapted from Zegarra Dávila, 2023)

During large rain events, a series of lagoons formed further south, namely the Ñapique/Ramón Lagoon and La Niña Lagoon. When exceeded the capacity through Sechura, the river would first overflow into the Ñapique/Ramón Lagoons, then form La Niña Lagoon, and discharge into Virrilá (Zegarra Dávila, 2023). The last overflow route was further south through Reventazón as shown in Figure 8 (Zegarra Dávila, 2023).
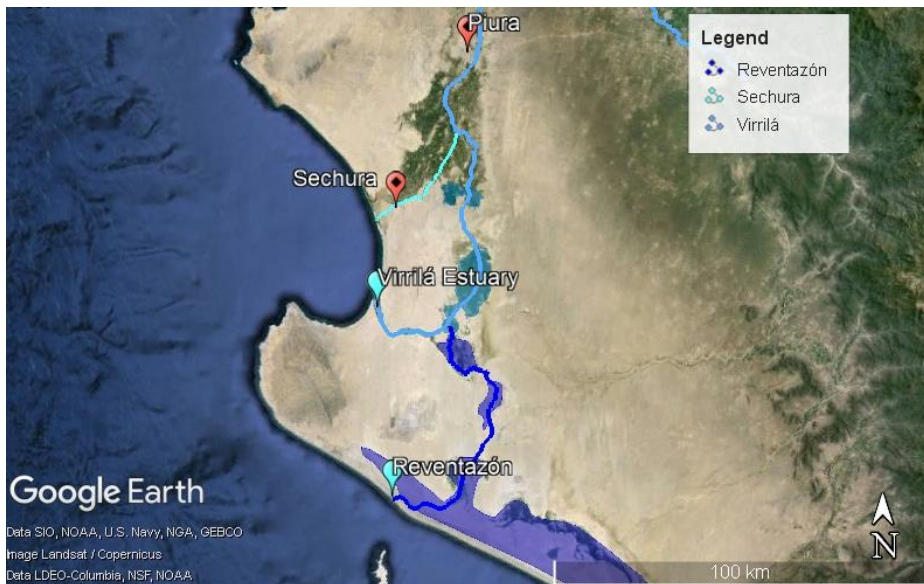
Figure 8- Overflow routes of the Piura River (Google Earth, 2024)

Agriculture plays an important role in the Piura region; it is considered the main reason for regional employment (MGI, n.d.) and makes up 5.7% of the national GVA (CIIFEN, 2020). Consequently, the river has been subject to land use changes due to agricultural activity and human settlements. (Alvarado Ancieta, 2023). At the beginning of the 20th century, the rapid growth of the cotton industry led to the construction of dikes to protect crops in the floodplain during increased flow (Zegarra Dávila, 2023). This was the beginning of a gradual redirection of the river towards the lagoon system in the south through the construction of dikes. Large flows would regularly breach the dikes, consequently these were reinforced in the 1970's and became permanent structures (Azurin Gonzáles, 2010). The location of the dikes is shown in Figure 9.

Figure 9- Dikes in lower basin (Google Earth, 2024)

2.2. Recent Flood Events

As mentioned, flooding in the Piura region is a recurring phenomenon. Flooding in the years 1983, 1998 and 2017 are regularly referred to as the most disastrous flood events the region has experienced. The most significant damages are identified as the destruction of roads, sewer systems, as well as homes and establishments, which caused a disruption in the provision of potable water and other vital goods and services in the region (UDEP & UNP, 2001a).

The flow in 1983 peaked at 3,200m^3/s (Farías Zegada, 2008). This caused overflow in some spans as well as significant erosion along the course of the river (Azurin Gonzáles, 2010). Erosion was notable at various riverine structures and along the banks in the urban zone which were not concreted at the time (Alvarado Ancieta & Ettmer, 2007). The flood resulted in the collapse of approximately 15km of the protective dikes on the west side of the river as well as the collapse of the spillway at the Los Ejidos Dam due to local erosion at the base of both structures (Alvarado Ancieta & Ettmer, 2007) (Reyes Salazar, 2024b). The dike breach on the west side of the river resulted in the river retaking the old course towards Sechura, where it destroyed fields and settlements along the way (Alvarado Ancieta & Ettmer, 2007). The flooding due to the breaches as well as inadequate drainage in the urban areas resulted in losses of around S/12,300 million, which accounted for 11.6% of the country`s GDP (SENAMHI, 2014).

In 1986, following the flood event, dikes were reinforced with concrete along the urban area and with stones and breakwaters along the base (Alvarado Ancieta & Ettmer, 2007). However, no works were conducted to protect against general erosion of the riverbed (Azurin Gonzáles, 2010).

In 1998 the flow in the river reached a peak at $3,900 m^3/s$ (Farías Zegada, 2008). The event had similar impacts as that of 1983 with losses of approximately S/13,100 million, or 6.2% of the GDP (SENAMHI, 2014). During this event, the increased transport of sediments resulted in erosion at the foot of the dikes and breached the left dike, further the bridges San Miguel, Bolognesi, and Independencia collapsed as shown in Figure 10 (Alvarado Ancieta & Ettmer, 2007). The San Miguel and Bolognesi are a part of the urban reach while the Independencia bridge is further downstream of the city Piura as shown in Figure 11.
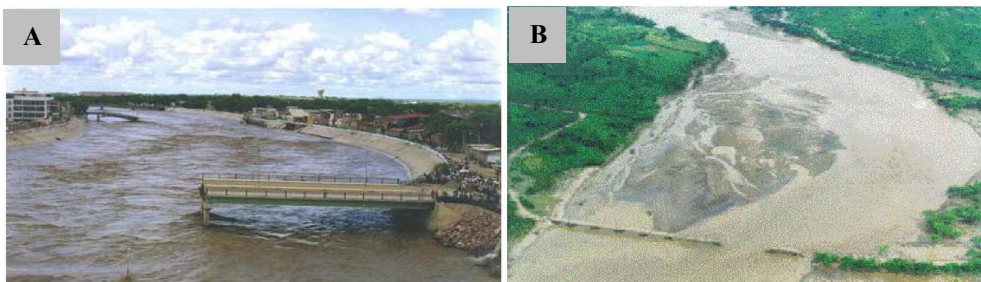
Figure 10a- collapsed San Miguel and Bolognesi Bridges 1998. 10b- collapsed Independencia bridge 1998. (Alvarado Ancieta & Ettmer, 2007)

Figure 11- Location of 1998 collapsed bridges (Google Earth, 2024)

The 2017 flood peaked at 3,468 m^3/s (PECHP, 2017). Although this flow is similar to that of the previous events, the river overflowed in unexpected spans in the urban area (Reyes Salazar, 2024b). In previous years the large flow caused erosion which increased the capacity of the river (Azurin Gonzáles, 2010). However, in 2017 the erosion did not occur thereby causing overflow (Reyes Salazar, 2024b). According to the regional director of health in Piura, Dr Hernán, the region had expected strong rains and low impact floods but did not expect the river to overflow (Organización Panamericana de la Salud, 2018*)*. The flood damaged infrastructure such as health and education establishments, roads, and sewers (Organización Panamericana de la Salud, 2018*)*. It also destroyed thousands of homes, as well as agricultural lands, leaving the Piura region in a state of emergency (Organización Panamericana de la Salud, 2018*)*. In addition to the damage to infrastructure, there was a sudden spread of diseases due to inadequate sanitation as well as a dramatic increase in Dengue, which became a further obstacle for the region (Organización Panamericana de la Salud, 2018*)*.

2.3. Hydrological Conditions and the Role of El Niño

Northwestern Peru is a coastal desert with a dry and tropical climate featuring rainy seasons from December to March (Di Liberto, 2017). The average temperature in the day is 33-35°C and 18-23°C during nighttime (Moreano Segovia & Yauri Quispe, 2008.). The climate along the Peruvian coast is strongly linked to oceanic conditions in the Pacific Ocean (SENAMHI, 2014). Usually, cold water from the Antarctic region is brought up to the South American coast by the Humboldlt Current while trade winds blowing towards the west push warm water away from the coast and towards Asia (Welt Hunger Hilfe, n.d.). Some years trade winds weaken, and this allows kelvin waves carrying warm water to move back into the eastern pacific (NOAA, 2023c)

(SENAMHI, 2014). This increase in temperature in the eastern pacific is known as El Niño and is the warm phase of the El Niño Southern Oscillation (ENSO) pattern which recurs every two to seven years (NOAA, 2023c). ENSO is monitored in the pacific in two zones as shown in Figure 12.
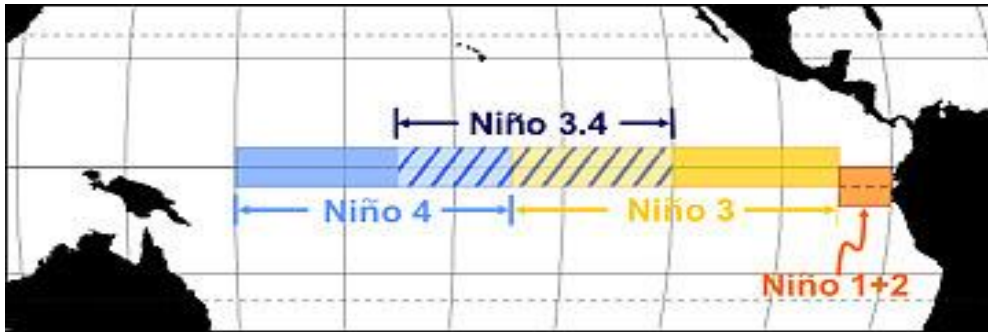
Figure 12- ENSO monitoring zones (NOAA, 2023b)

Zone Niño 3.4 is used to monitor the Oceanic Niño Index (ONI). This index is measured as an average of temperature anomalies during three consecutive months in the region Niño 3.4. Cold and warm episodes are indicated when a threshold of ±0.5°C is exceeded (NOAA, 2023b). When the threshold is exceeded for a minimum of five consecutive months, an El Niño (warm) or La Niña (cold) episode is defined (NOAA, 2023b). Further, the National Study of El Niño (ENFEN), a multisectoral committee in charge of studying El Niño in Peru, has developed an index to describe the variation in temperature in Niño region 1+2 called ICEN (SENAMHI, 2014). The index is calculated in the same way as the ONI and indicates the occurrence of an El Niño event on the coast of Peru, known as El Niño Costero. The ONI index is shown for 1950-2023 in Figure 13 together with threshold values for El Niño classification. Figure 14 shows the El Niño Costero (ICEN) occurrence since 1950.
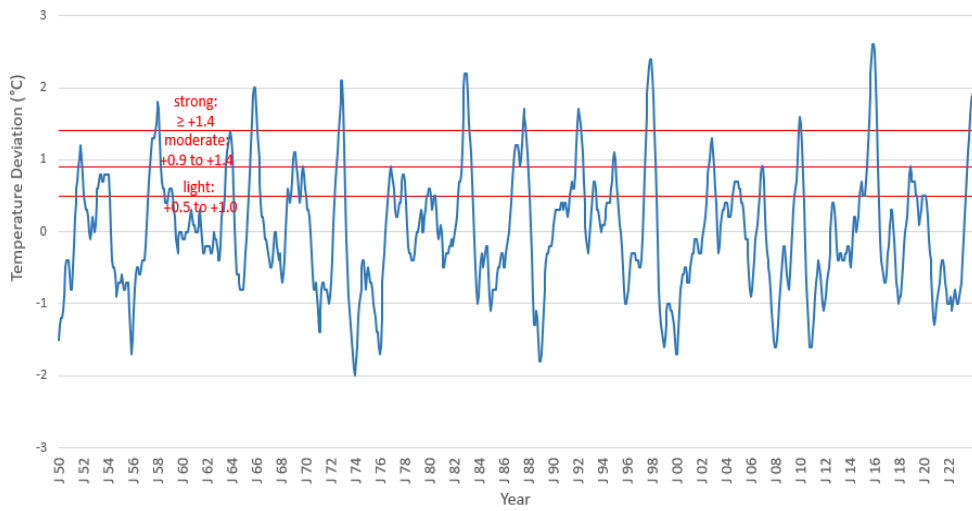
Figure 13- ONI values for Niño Zone 3.4 for 1950-2023. Temperature deviation for averages of 3 consecutive months. Thresholds at neutral -0.5 to +0.5, light +0.5 to +1.0, moderate +0.9 to +1.4, and strong > +1.4 (SENAMHI, 2014). *(NOAA, 2023a)*
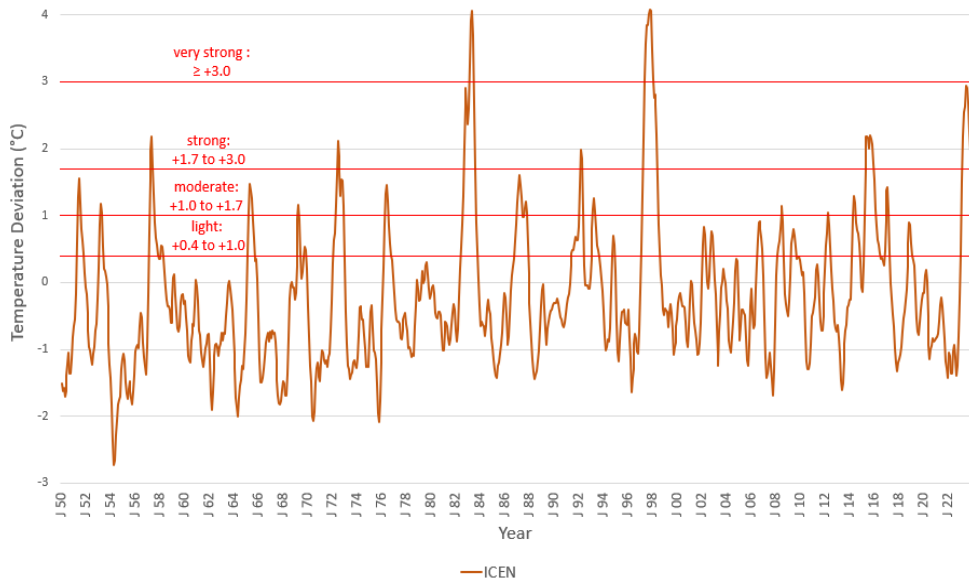
Figure 14- ICEN values for Niño Zone 1+2 for 1950-2023. Temperature deviation for averages of 3 consecutive months. Thresholds at neutral -1.0 to +0.4, light +0.4 to + 1.0, moderate +1.0 to 1.7, strong +1.7 to +3.0, and very strong > +3.0. (Instituto Geofísico del Perú, 2023)

Figure 15 shows that the events of 1983 and 1998 were characterized as 'strong' El Niño events on the ONI scale, the 2017 event was below the El Niño thresholds. However, the ICEN value indicating temperature anomalies in El Niño zone 1+2 coast show that there was a temperature increase locally along the coast, which created the conditions for the increased precipitation and flow experienced in 2017 although Zone 3.4 was in La Niña (cold) conditions.
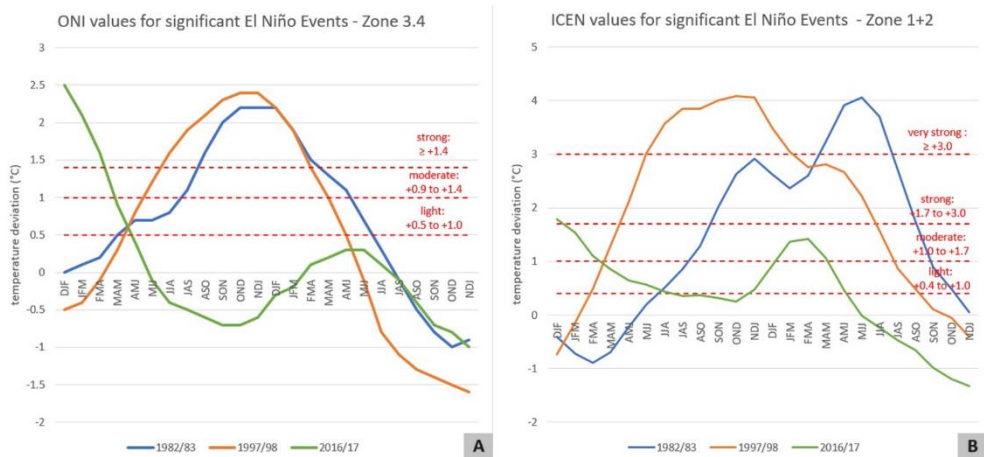
Figure 15a- ONI values for El Niño Events 1982/83, 1997/98, and 2016/17. Temperature deviation for averages of 3 consecutive months (NOAA, 2023a). 15b- ICEN values for El Niño Events 1982/83, 1997/98, and 2016/17. Temperature deviation for averages of 3 consecutive months (Instituto Geofísico del Perú, 2023).

In the Piura region El Niño affects the pluviometry and hydrological regimen of the river basin (Moreano Segovia & Yauri Quispe, 2008.). The arid climate is due to the cool coastal air above the pacific which provides a protective barrier against offshore storms (Di Liberto, 2017). However, during El Niño episodes, the coastal air heats up and allows for an increase in precipitation along the coastal region (Di Liberto, 2017). In general, the average yearly precipitation is around 50-100mm (Azurin Gonzáles, 2010) (Moreano Segovia & Yauri Quispe, 2008.). In years with a 'light' El Niño episode, average yearly precipitation is around 135mm while years with a 'strong' event feature yearly

precipitation of around 3,000mm (Azurin Gonzáles, 2010), this is an increase in yearly precipitation by a factor of 30-60. The relationship between precipitation and ONI/ICEN is shown in Figure 16 for stations in the upper and lower Piura River basin for the years 1972-2013. The data ranges to 2013 as this is what was available on the website of the National Meteorological and Hydrological Service (SENAMHI) for chosen stations.
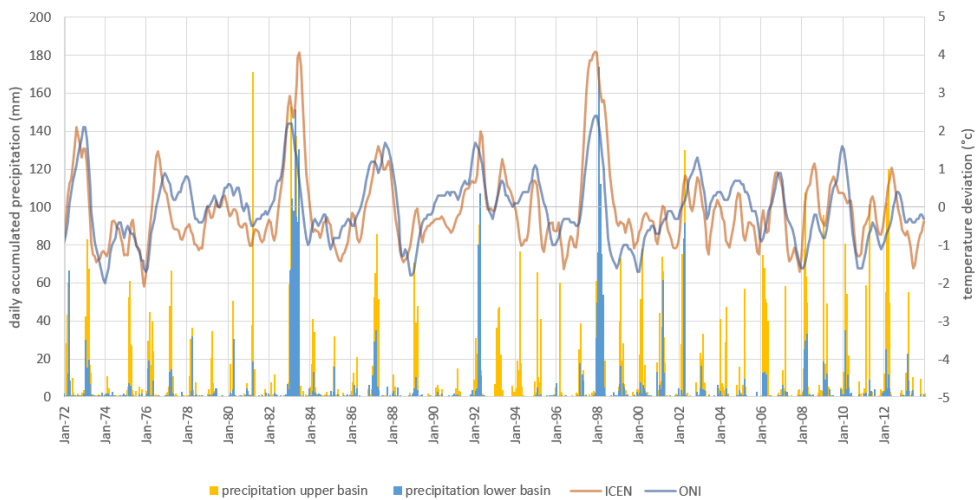
Figure 16- ICEN and ONI values with daily accumulated precipitation values for the upper and lower basin from 1972-2013

2.4. Piura River Morphology

The morphology of a river is governed by shape and hydrology (Guererro et al., 2015). In the case of the Piura River, the shape has been influenced by anthropogenic interventions, and hydrology is largely influenced by ENSO (Guererro et al., 2015).

In the highlands, the river has a large slope of around 15%, after the mountains the slope lowers to around 0.35% and further decreases to 0.08-0.13% in the mid basin (Guererro et al., 2015). In the lower basin, the flat terrain has a slope of around 0.03% (Guererro et al., 2015), which creates conditions for the

formation of an alluvial fan. Research by the University of Piura indicates that flooding of the river used to bring nutrient rich sediment to the floodplains which allowed for vegetative growth (Guererro et al., 2015). However, now the floodplains are restricted to the area within the dikes, this has been made evident by the difference in vegetative coverage inside and outside the dike area as shown in Figure 17.
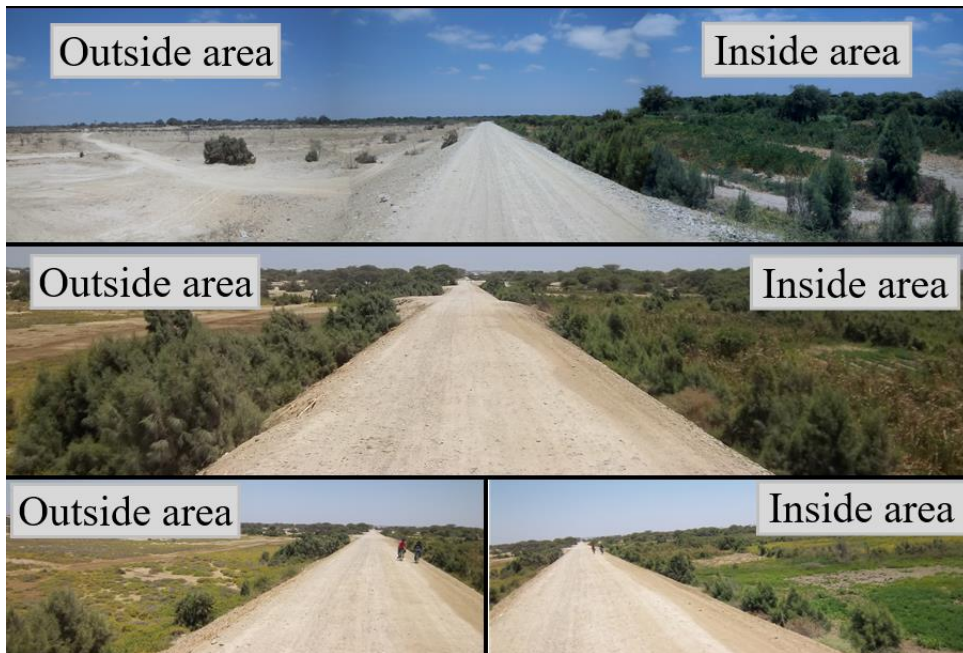
Figure 17- Vegetation difference inside and outside the dikes (Guererro et al., 2015)

As concluded by the Class-Salzgitter study in 2001, this vegetative growth creates resistance to flow, thereby causing an increase in the level within the enclosed zone (Class-Salzgitter, 2001 cited in Córdova Elera, 2020). In combination with the restriction of the flood plain created by the protective dikes, there is a more concentrated accumulation of sediments which creates overflow as shown in Figure 18 (Castillo Zavaleta, et al., 2019).
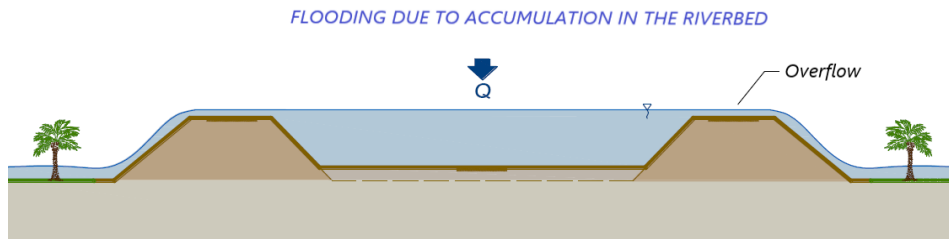
Figure 18- Accumulation of sediments inside the floodplain restricted by dikes (adapted from Castillo Zavaleta, et al., 2019)

The cross section of the Piura River varies throughout the lower basin. In the urban reach from Los Ejidos to the Bolognesi bridge river is channeled and has a width of approximately 130-300m. From the end of the urban area to downstream of Drain 13.08, the river is restricted by protective dikes with a floodplain of a width of 500-800m and a main channel width of 100-200m (Alvarado Ancieta & Ettmer, 2007). After this the flood plain widens to approximately 4km, in this section it is bordered by dikes on the west side and the Panamerican Highway on the east.

According to Alvarado and Ettmer (2007), the sinuosity of the river should be greater than what it currently is considering the slope and the annual average flow, they conclude that the ability of the river to meander is constricted by the dikes (Alvarado Ancieta & Ettmer, 2007) as can also be seen from satellite images where the river frequently meets the dikes as shown in Figure 19. In the years 1982 and 1997, the dikes were breached at these points (Alvarado Ancieta & Ettmer, 2007).
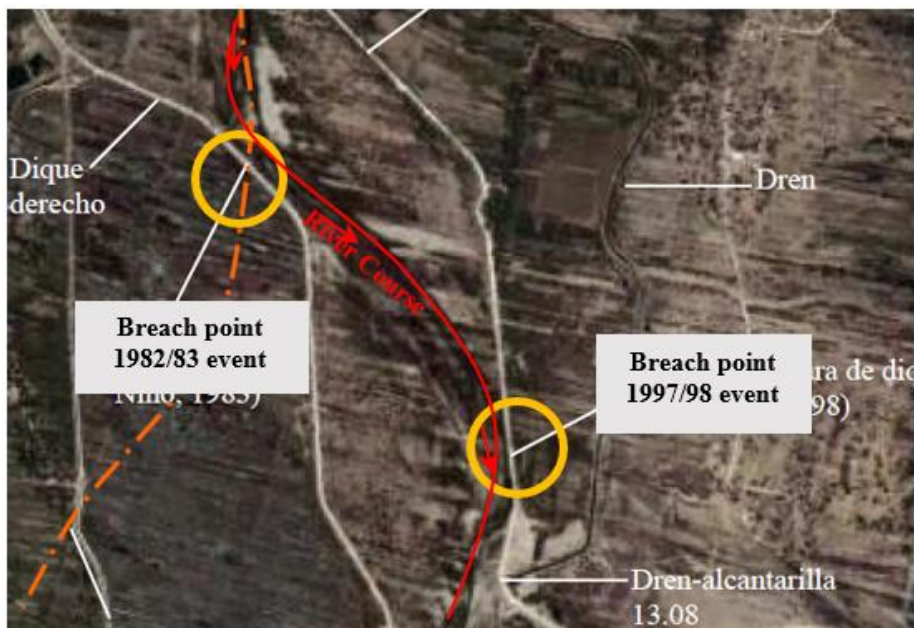
Figure 19- Dike breach points in 1982 and 1997 (adapted from Alvarado Ancieta & Ettmer, 2007)

The morphology of the river is affected by flow through sediment transport. Typically flood events cause general erosion of approximately 6m (Reyes Salazar, 2024b). However, in 2017 the flow had insufficient energy to cause transport of sediments. This decrease in energy is a combination of increased vegetation, breakwater effects by the dikes, and the redirection of the river towards the lagoons (Reyes Salazar, 2024b). The original course of the river had a length of approximately 70km starting at Los Ejidos Dam towards Sechura. However, after the extension towards the south, the river has a length of 118km. This corresponds to an increase of approximately 50km of length across flat terrain. As a result, the river is incapable of controlling the large quantities of water which flow during El Niño event in the same manner as in previous years (UDEP & UNP, 2001e*).

3. Previous Studies

3.1. Studies Concerning the Piura River Flow Regimen

As mentioned, the Piura region is among the most vulnerable during heavy rainfall seasons (ARCC, 2017). As such, this section describes various studies and projects which have been conducted and/or are ongoing related to the flooding of the Piura River.

Among the first and most prominent studies concerning is the "Definitive Study for Reconstruction and Rehabilitation of Defenses in the Lower Piura Basin and Mathematical Model for Prediction of Floods in Real Time in the Piura Basin. Piura, Peru." developed by the Class-Salzgitter consortium in 2001, as well as the "Study for the Integral Plan of the Piura River" developed by the National University of Piura together with the University of Piura also in 2001.

The Class- Salzgitter study focused on the reconstruction and rehabilitation of riverine defenses in the lower Piura basin. The study includes design flows suggested for riverine defenses in different zones along the river, description of sediments in the riverbed, and investigates sediment transport (Class-Salzgitter, 2001 cited in Córdova Elera, 2020). The study shows there are sections in the river experiencing erosion while others tend to aggradation (Class-Salzgitter, 2001 cited in Córdova Elera, 2020). The floodplains in the lower basin were identified as irregular areas with vegetative cover of crops and brush, causing a resistance to flow which has resulted in an increase in the level of the floodplain (Class-Salzgitter, 2001 cited in Córdova Elera, 2020).

The study by the National University of Piura and University of Piura (PNUD study) is an analysis of the parameters which influence the frequency and impact of floods and proposes control measures to reduce the negative impact

of floods and increase riverine security with a focus on the urban Piura and Castilla areas (UDEP & UNP, 2001e*)*. Part of the study includes hydrological investigation for return periods of precipitation and floods, a sediment study, an evaluation of the state of riverine protection in the study year, a numerical and physical model.

Various other studies exist related to the Piura River. These include investigations of flow conditions and precipitation patterns for classification of return periods of flows through the river, vulnerability studies, and hydraulic modeling of the river.

3.2. Projects in the Piura River Basin

One of the most important projects in the Piura River basin is the Chira-Piura Project. It was established in 1981 as a self-governed entity in charge of carrying out a project with the aim of storing and regulating hydraulic resources in the Chira River (UDEP & UNP, 2001a), which is located to the north of the Piura River. The objectives were to improve and stabilize agriculture in the lower basin, this was accomplished through the construction of reservoirs, irrigation channels, and drainage channels (UDEP & UNP, 2001a). In the Piura basin, the Chira-Piura Project included the construction of Los Ejidos dam, the Biaggio Arbulu channel, reinforcement of dikes, and drainage channels (UDEP & UNP, 2001a).

In more recent years following the 2017 flood, works for reconstruction and rehabilitation began for both riverine structures and cities which suffered damage due to the flood. Many projects were executed by the Authority for Reconstruction with Change (ARCC). The objective was to lead an integral plan for rehabilitation for the 13 regions in Peru which were most impacted by the coastal El Niño phenomenon of 2017 (ARCC, 2017). Interventions by the

ARCC can be grouped into three two types, the first being rehabilitation of infrastructure such as roads, sidewalks, sewers, and health and educational establishments (ARCC, 2017). The second is related to preventative measures such as clearing riverbeds, constructing riverine defense systems, urban drainage, and conducting studies in critical basins (ARCC, 2017). The investment necessary for interventions was an estimated S/26,655 million where 77% was dedicated to the first project type, and 21% to the second (ARCC, 2017). In the Piura region, works directly related to the river included clearing the riverbed and reinforcement of river defenses. These interventions accelerated in preparation for the potential El Niño event which was likely to occur in the summer of 2023/24.

Similar to the works conducted by the ARCC, the National Water Authority (ANA) also planned interventions for the potential El Niño event of 2023/24 for seven vulnerable regions in Peru with an investment of approximately S/975 million (Autoridad Nacional del Agua, 2023). In Piura the authority identified 94 critical points which needed intervention and undertook works to clear the riverbed of debris and sediment (Autoridad Nacional del Agua, 2023).

Further works are being undertaken to redirect the river towards the south to exit through Reventazón. This is a part of the ARCC's "Integrated Master Plan for Flood Control and Sediment Transport Management in the Piura River Basin", where a relief channel will be built between Chutuque and Pampa Las Salinas as shown in Figure 20 to improve flow conditions in the lower basin (ARCC, 2022).

Figure 20- Location of Chutuque channel (Google Earth, 2024)

There are also alternative proposals for river redirection and reservoirs being studied. Among these are various proposals suggested by Eduardo Zegarra. In one proposal Zegarra suggests the construction of a reservoir to the east of the city of Piura to redirect water around the city and minimize strain on the Los Ejidos Dam as shown in Figure 21.
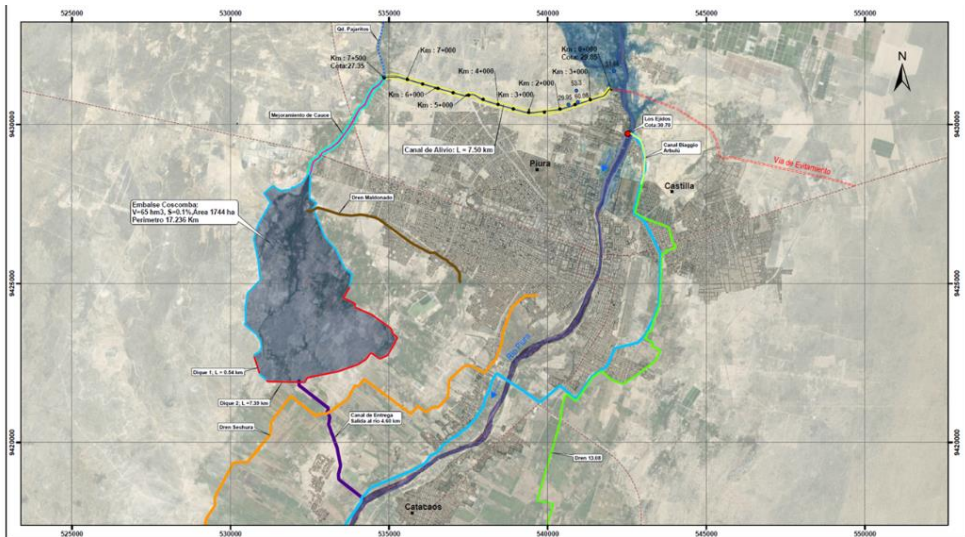
Figure 21- Coscomba Reservoir map (Zegarra Dávila, 2023)

Further, Zegarra presented various potential routes during the Conference for Hydraulic Structures during Flood Events organized by the Colegio de Ingenieros del Peru (Chapter of Civil Engineering of Peru) in 2023. The routes are shown in Figure 22. For Option A2 (yellow) through Sechura, a pilot channel has already been designed to compare to the planned route through Reventazón. Zegarra estimates that the costs for the exit through Sechura are approximately 60% of the investment needed for the exit through Reventazón (Zegarra Dávila, 2023).

Figure 22- Potential routes for Piura River discharge (Zegarra Dávila, 2023)

In this thesis, option A2 (yellow) through Sechura is compared to the current exit through Virrilá. This proposed route was chosen after a virtual meeting with Zegarra during the time in Piura. This proposal already has design parameters since the aforementioned pilot channel was used for cost estimation. As such, a comparison of this route to the existing route using river modelling is a further step to determine the effectiveness of the proposal. The upcoming Chapter 4 describes a field visit following the proposed river course through Sechura.

4. Field visit

In order to create a better understanding of the study area and the Piura River basin, field visits were conducted. Appendix A provides a larger collection of images and information collected during the excursions. This section provides insight into information gathered which is relevant to sediment transport and the alternative river course.

The first excursion entailed a trip following the urban reach of the river from the Los Ejidos dam to the Bolognesi bridge as shown in Figure 23. The field visit to the urban river reach was a part of the University of Piura`s master's program for Water Resources. The excursion was conducted together with participants from the master's program and was led by Jorge Reyes Salazar, lecturer in hydraulics and sediment transport.
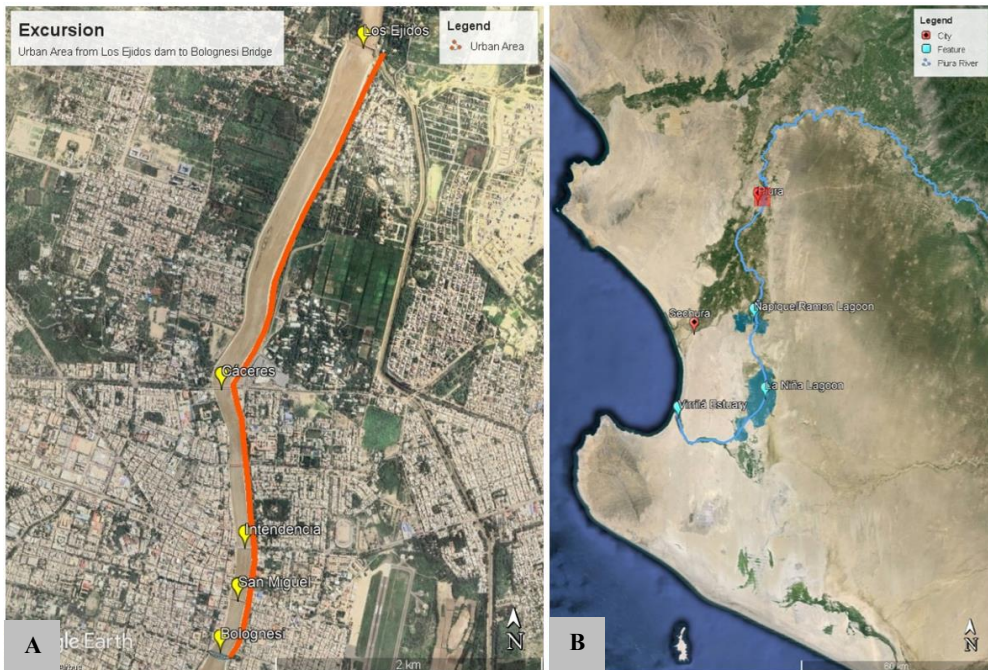
Figure 23a- Excursion to urban river reach. 23b- Overview Map. (Google Earth, 2024)

The excursion began at Los Ejidos Dam located approximately 3km upstream of the city center. The dam is shown in Figure 24 where a weir structure on the left and the gated spillway on the right are visible. The flow through the river on this day was low and consisted primarily of water supplied by the Chira River to the north.

Figure 24- Los Ejidos dam spillway

Sediment in this area was found to be mostly sand with clayey-sand deposits closer to the riverbank. At the dam works have been conducted to remove approximately 3m of accumulated sediment as shown in Figure 25.

Figure 25- Sediments at Los Ejidos dam. 25a- View form bottom. 25b- View form top

The excursion continued through the city where stops were made at different bridges. As mentioned, the river is channeled in the city and the riverbanks are made of concrete. Aggradation is visible along the riverbanks as shown in Figure 26. Further, the areas where sediment has been deposited promote vegetative growth.
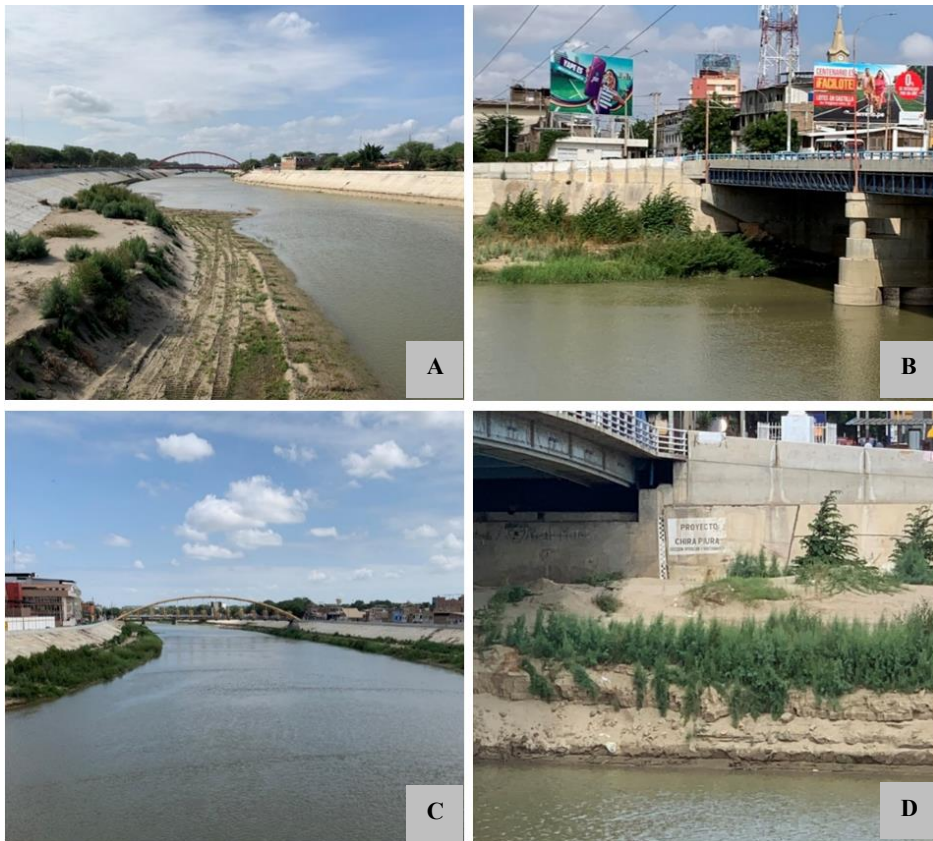
Figure 26- Vegetative growth at riverbanks. 26a- View downstream of Cáceres. 26b- Below Cáceres Bridge. 26c- View upstream of Bolognesi. 26d- Below Bolognesi Bridge

The second visit covered the rural reach of the river starting at the Bolognesi Bridge and following the west (right) dike up to the lagoon system, then following the alternative route towards Sechura as shown in Figure 27. It should be noted that the span along the west dike is not a part of the ancient route but a part of the proposed route. This span provided insight on vegetation cover, irrigation channels, and riverine structures in the lower basin.
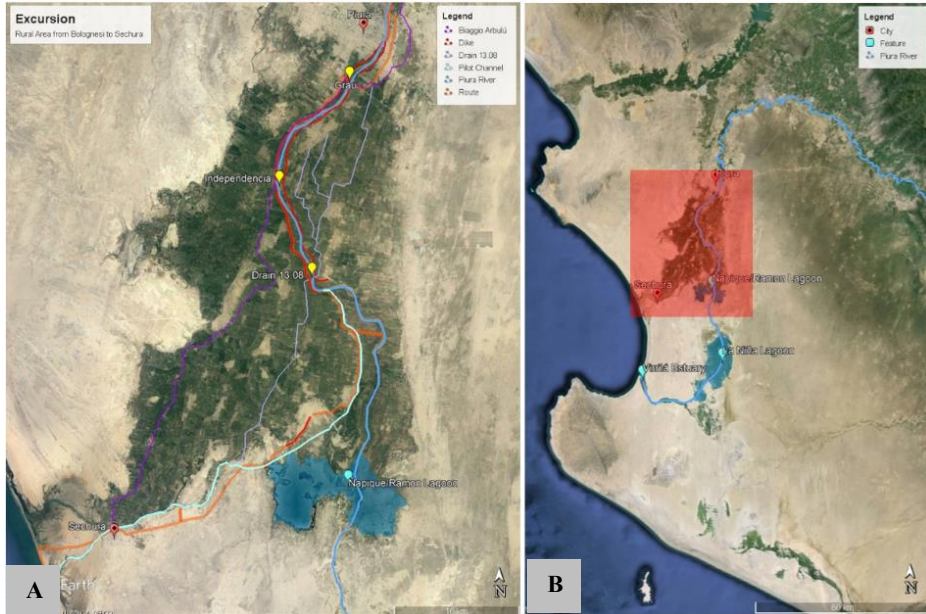
Figure 27a- Excursion to the route through Sechura. 27b- Overview map. (Google Earth, 2024)

The land use starting at the Bolognesi bridge and reaching up to the lagoon system consists primarily of farmland with or without crops and brush as shown in Figure 28. There are fields both inside and outside the floodplain.

Figure 28a- Field without crops. 28b- Dense brush

General aggradation is visible since the level of the floodplain was often observed to be above the level outside of the dikes. However, in some spans erosion is visible. This can be seen in Figure 29, taken close to Drain 13.08

Figure 29- Erosion close to Drain 13.08

The current river course towards Virrilá was followed just upstream of the lagoon system. At this point, a new route towards Sechura was taken to assess land coverage conditions along the ancient river course. The Piura River used to flow west towards Sechura. In this area, the ancient river course is still active and is fed by drainage channels. This river is referred to as Río Loco and is shown in Figure 30.
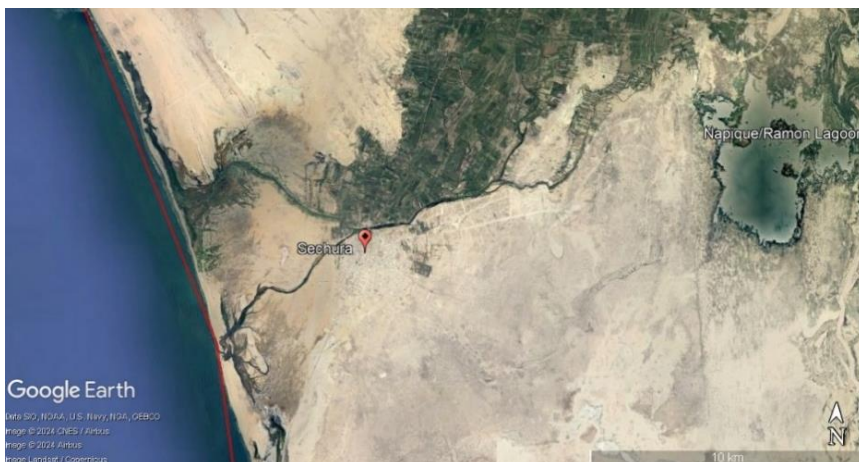
Figure 30- Rio Loco (Google Earth, 2024)

Following the dike on the right side of the river, The Ramón/Ñapique Lagoon is bordered by the dikes as shown in Figure 31. The vegetation differs upstream and downstream of the dike, where the surroundings upstream have more greenery than downstream.

Figure 31a- Ñapique Lagoon dike (Google Earth, 2024). 31b- Upstream of dike.
31c- Downstream of dike

Following this dike, the terrain has less vegetation and becomes more of a desert landscape as shown in Figure 32.

Figure 32- Vegetation between Ñapique Lagoon dike and Río Loco

Río Loco is shown in Figure 33. It passes through Sechura and exits into the Pacific in 3 branches.

Figure 33- Río Loco

5. Theoretical Background

This section describes theory used to compare sediment transport capacity through the current river course (Virrilá), and the alternative course (Sechura). Piura River. Further, an introduction to the software HEC-RAS provides insight into data needed for modelling.

5.1. Sediment Transport

A river is in equilibrium when the amount of sediment being transported in is also transported out (Lane, 1954). According to Lane (1954), for a river to be in complete equilibrium is a rare condition and may only exist momentarily. This is because discharge through a river is not generally constant, and the ratio of high to low flow quantities is very large (Lane, 1954). However, for engineering purposes, equilibrium state is often assumed for a small section of a river although slow aggradation or sedimentation processes may be ongoing (Lane, 1954).

Particles begin to move along the bed when the existing fluid force is larger than the resisting force (Larson, 2023). The critical shear stress is also the resisting force. In this case, Soulsby is used for non-dimensional critical shear stress for non-cohesive sediment using Equations 1 and 2.

$$(1) \qquad \theta_{cr} = \frac{0.3}{1+1.2D_*} + 0.055(1 - exp(-0.02D_*))$$

$$(2) \qquad D_* = (\frac{g(s-1)}{v^2})^{1/3} * d_{50}$$

The critical shields number is given by Equation 1. This is used to find the critical shear stress is τ_{cr} in N/m^2 as shown in Equation 3.

$$(3) \qquad \theta_{cr} = \frac{\tau_{cr}}{\rho g(s-1)d_{50}}$$

The shear stress created by flowing water (τ_b) is calculated using a drag law based on mean velocity (Larson, 2023) as shown in Equation 4.

$$(4) \qquad \tau_b = \rho C_D U^2$$

Transported sediment is classified into bed load, suspended load, and wash load (Larson, 2023). These are defined as follows:

Bed load: Particles are in contact with the riverbed and are transported along the bottom. The shear stress at the bed governs the transport of sediments (Larson, 2023). This can be calculated through numerous equations. In this thesis, Meyer-Peter and Müller is considered.

Suspended load: Particles are carried in the water column through turbulence in the water. Sediment concentration profiles and current velocity are used to describe the load (Larson, 2023).

Wash load: The wash load consists of very fine particles which are evenly distributed through the water column. These are not influenced by the flow properties (Larson, 2023)

5.2. The HEC-RAS Model

HEC-RAS is a river analysis tool developed by the Hydrologic Engineering Center of the U.S. Army Corps of Engineers. This free software allows for one- and two-dimensional flow analysis, steady and unsteady flow calculations, as well as sediment transport and water quality analysis (HEC, 2023). For this thesis, a one-dimensional flow model is set up using steady flow conditions.

Basic profile computations in HEC-RAS are conducted with the standard step method where the Energy Equation is used as shown in Equation 5 to calculate

water surface profiles from cross section to cross section as shown in Figure 34 (HEC, 2024a).

$$(5) \qquad Z_2 + Y_2 + \frac{\alpha_2 V_2^2}{2g} = Z_1 + Y_1 + \frac{\alpha_1 V_1^2}{2g} + h_e$$
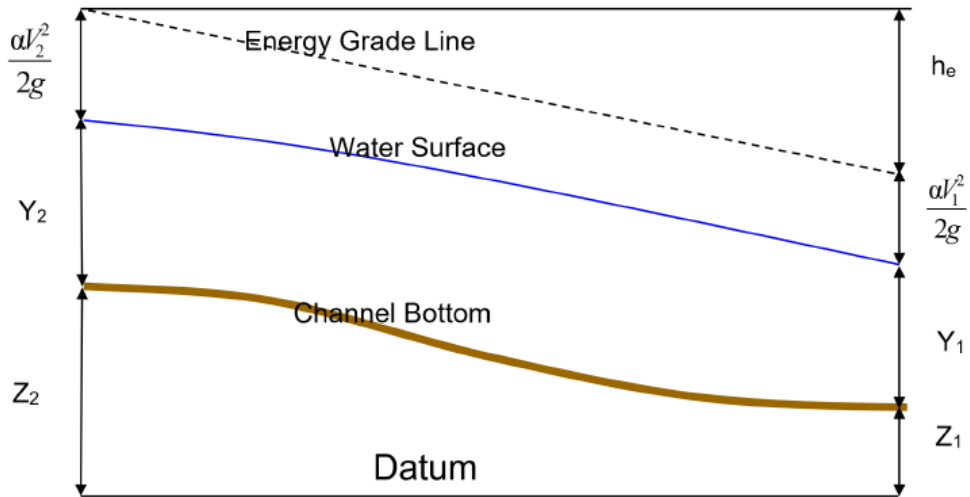
Figure 34- Water surface profile calculation in HEC-RAS (HEC, 2024a)

Further, conveyance, kinetic energy, friction loss, and contraction/expansion losses are computed using various equations and input in form of cross section geometry and Mannings numbers (n) (HEC, 2024a). The program uses an iterative process to calculate water surface using predefined error tolerances (HEC, 2024a). Herein the Mannings n values has a considerable impact on the computed water surface (HEC, 2024a).   Mannings n is a is an indication of the roughness of a terrain. Smooth surfaces have a low Manning's n, while rough surfaces have a high n value.

The following assumptions are used in one-dimensional steady flow analysis according to the HEC-RAS Hydraulic Reference Manual (2024):

- Flow is steady- energy equation does not include time dependent terms.

- Flow is gradually varied- hydrostatic pressure distribution is assumed.

- Flow is one dimensional- velocity components are assumed to be in the same direction as flow under the assumption that total energy head is the same across a cross section.

- Channels have slopes less than 1:10 which implies that vertical pressure head is approximately equal to the depth of the water

Steady flow computations require boundary conditions, flow regime, and discharge information (HEC, 2024a). Flow regime can be defined as subcritical, supercritical, or mixed flow (HEC, 2024a). Boundary conditions can be specified as known water surface elevations, critical depth, normal depth based on the energy slope, or a rating curve where elevation-flow data is entered (HEC, 2024a). Finally, at least one flow value is needed upstream in the river reach (HEC, 2024a).

6. Data Employed

In this section data relevant to the HEC-RAS model set up and sediment transport capacity calculation is described. This includes available flow data, sediment information, observations for Mannings roughness coefficients, topographic data, sea level and a description of the proposal for the course through Sechura provided by Eduardo Zegarra.

6.1. Flow data

As mentioned, the Piura River is non-perennial. The flow through the lower basin is heavily influenced by the presence of El Niño due to the increased precipitation during this weather event. Data for maximum flow through the river has been available since 1926 and is shown in Figure 35. The trendline indicates that the flow through the river is increasing over time.
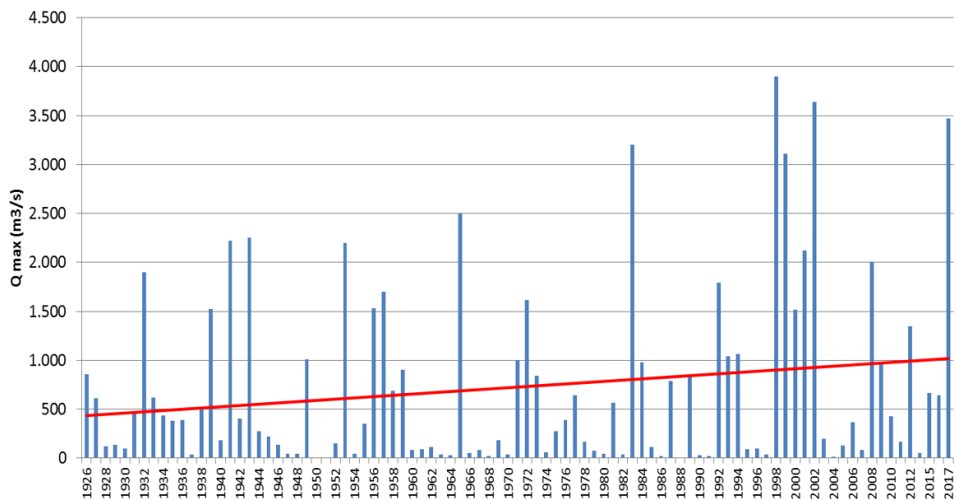
Figure 35- Maximum flows through the Piura River from 1926-2017 (Farías Zegada, 2008)

Data shows that following 1983, maximum flows were larger and more frequent. Statistical analysis of the flows has been conducted in previous studies using different models such as Gamma, Exponential, Person III,

Gumbel, and others. Farías (2018) uses the double Gumbel model to estimate flows. Table 1 shows the maximum flow for different return periods in this double Gumbel investigation. It should be noted that varying values can be found in different literature.

Table 1- Qmax return periods

Tr (years)	Max. flow (m³/s)
2	432
5	2,081
10	2,954
25	4,014
50	4,788
100	5,552

Further, the Piura-Chira Project provides daily flow data since 2015 for five stations along the Piura River (PECHP, 2017). The stations provide flow data for daily average, maximum flow, and precipitation. Of these, the station at the Sánchez Cerro bridge provides flow information for the lower basin. The flood event in March 2017 is shown in Figure 36. The hydrograph shows a peak flow of 3,468 m³/s on March 28th.
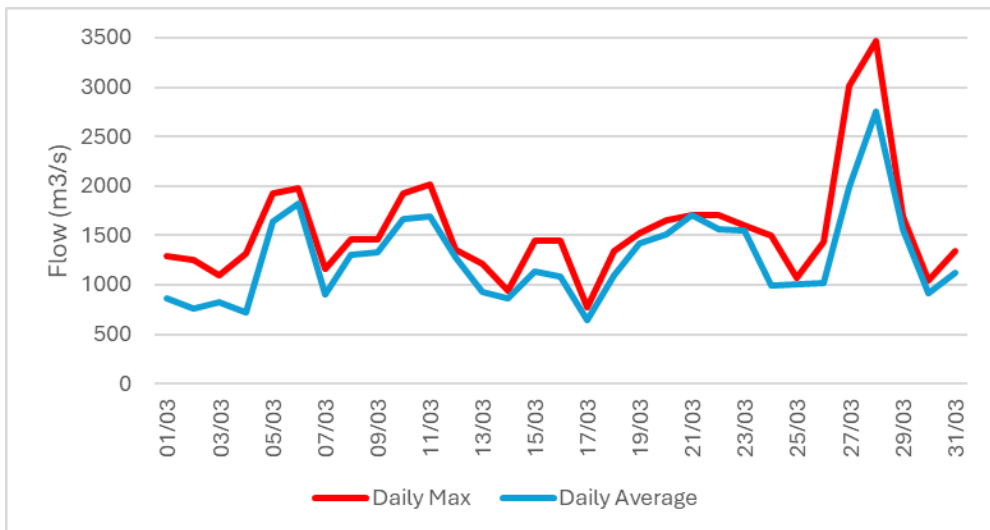
Figure 36- Flow measurements at Sánchez Cerro Bridge for March 2017

6.2. Sea Level

Hourly sea level data from Talara- a port to the north of Piura- was sourced from the University of Hawaii Sea Level Center. Data is available from 31.05.2015 - 30.04.2023, with some missing data, as visible in Figure 37. The mean sea level is found to be at approximately 1.5m with deviations of ±1.2m, resulting in a maximum sea level of 2.7m and a minimum of 0.2m.

Figure 37- Sea Level at Talara, Peru from 31.05.2015 - 30.04.2023

6.3. Sediment data

The study primarily referred to is the study by the National University of Piura and the University of Piura (PNUD study) from 2001 for sediment data. This expansive study covers information relevant for modeling and design of riverine structures. The study gives insight into the geology of the area and provides results for geotechnical evaluations of several samples taken along the river.

The most prominent tertiary formation in the study area is the Zapallal formation (UDEP & UNP, 2001e*)*. In the year this report was written, bedrock (Zapallal formation) was encountered during sediment sampling at Los Ejidos dam, Cáceres Bridge, and Sánchez Cerro bridge (UDEP & UNP, 2001e*)*. The PNUD study mentions that this exposure of bedrock is largely attributed to anthropogenic changes which have influenced the flow regime and caused an increase in sediment transport. Bedrock depth is found to range between 0.5-14.5m (UDEP & UNP, 2001e*)*.

Quaternary sediments are identified as alluvial, fluvial, and eolian sediments (UDEP & UNP, 2001e*)*. Alluvial sediments are found to be coarse sand with fine sand on the top, followed by layers of sand and clay (UDEP & UNP, 2001e). Fluvial sediments are silty-sand sediments and are used for agriculture (UDEP & UNP, 2001e). Following these layers are the eolian sediments which have been transported by wind and form small dunes in some areas (UDEP & UNP, 2001e). The study provides results for soil tests such as grain curves, determination of specific weight, water content, shear strength, and Atterberg limits for samples taken in the riverbed starting at Los Ejidos and ending at the Ramón Lagoon.

The following results points are highlighted from the PNUD study:
- Most samples ranged from silty-sand to fine-sand, however a clay sample was also found in the Ramón Lagoon sample.
- Median sediment grain size (d50) ranges from 0.1-0.3mm
- The specific weight of sediments ranges from 2.55-2.8 t/m^3.

Further, the PNUD report references another study from 1967 in which information for sediment concentration as a rating curve for suspended sediment in tonnes/month versus monthly discharge (Int. Engineering Company & Olazabal y Leon S.A, 1967).

6.4. Manning

Based on observations from the field visit described in Chapter 4, a possible range of values is determined for roughness. Table 2 shows potential Mannings numbers along the river ranging from 0.014 (concrete) to 0.16 (dense brush) based on value suggestions provided by the HEC-RAS Hydraulic Reference Manual (2024).

Table 2- Land cover roughness, Mannings numbers based on observation

Element	Description	Range	Example
Lined channel	Unfinished concrete	0.014-0.02	
Riverbed	Sandy riverbed, short grass, few weeds	0.022-0.033	
Floodplain	Cultivated areas, crops	0.025-0.045	
	Pasture, no brush, short grass	0.025-0.035	
	Scattered brush, heavy weeds	0.035-0.07	
	Dense brush	0.07-0.16	

6.5. Topography

Elevation data is necessary for the area stretching from Los Ejidos Dam to Virrilá and including Sechura as shown in Figure 38. This is the lower basin and has an area of approximately 4,000km^2. The river spans 117km from Los Ejidos to the Virrilá Estuary, and 72km from Los Ejidos to Sechura.
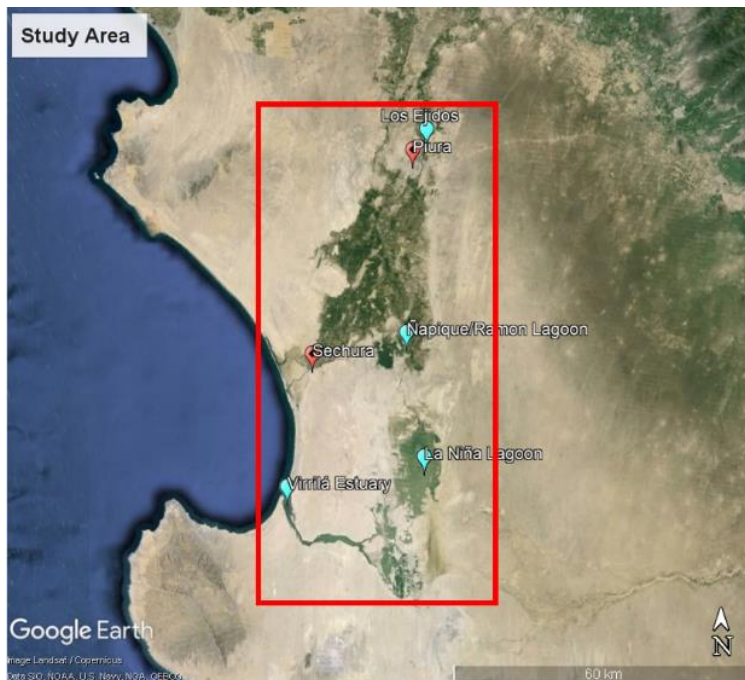
Figure 38- Study area (Google Earth, 2024)

Topographic data is used for geometry creation in HEC-RAS. For this data from a 2015 LIDAR scan by the national water authority (Autoridad Nacional del Agua) was used. The scan covers a length of 50km starting just upstream of Los Ejidos Dam and reaching to the Ñapique/Ramón Lagoon. The width varying from 1.9km to 7.2km to include the floodplains and has an area of approximately 165 km^2 (Peña Valdivia, 2021) the scanned areas are shown in Figure 39. Data from the scan has been preprocessed by students from the University of Piura in previous master thesis studies to create a raster file. This file was used as a GeoTIFF format as input in HEC-RAS, the result is shown in Figure 39.
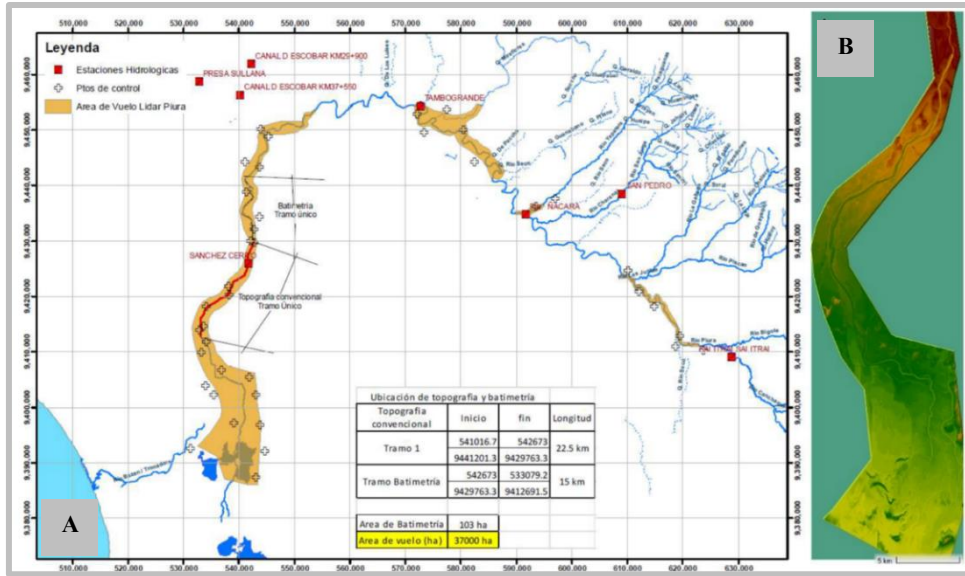
Figure 39a- LiDAR scans by ANA in 2015 (Peña Valdivia, 2021). 39b- GeoTIFF file opened in RAS-Mapper

The study area, however, is larger than what is provided in the LIDAR scan. As such, digital elevation model (DEM) data was obtained through GEO GPS Peru (n.d.), where it was available in GeoTiff format with a resolution of 30m taken in 2008. The file is shown in Figure 40.
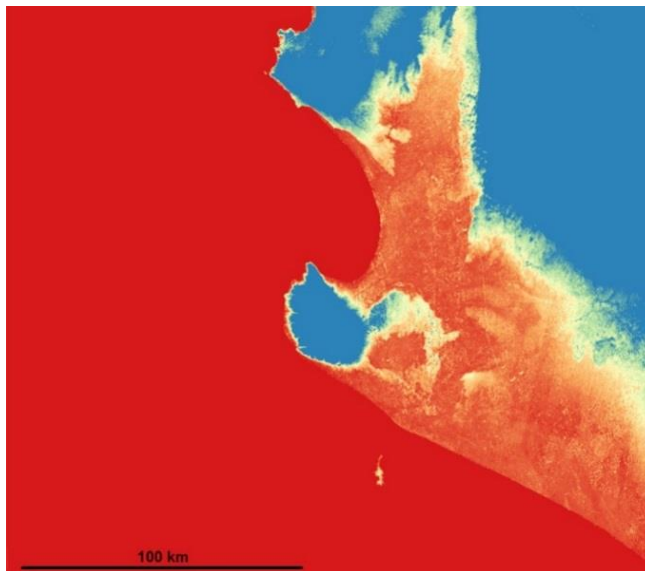
Figure 40- ASTER GDEM Piura region

6.6. River Course through Sechura

The proposed river course through Sechura has a length of approximately 42 km while the course through Virrilá has a length of approximately 87 km from the split point. The new course follows the right dike towards the Ñapique/Ramón Lagoons, then passes through the dike as shown in Figure 41 and rejoins Río Loco after 24km of the split point.
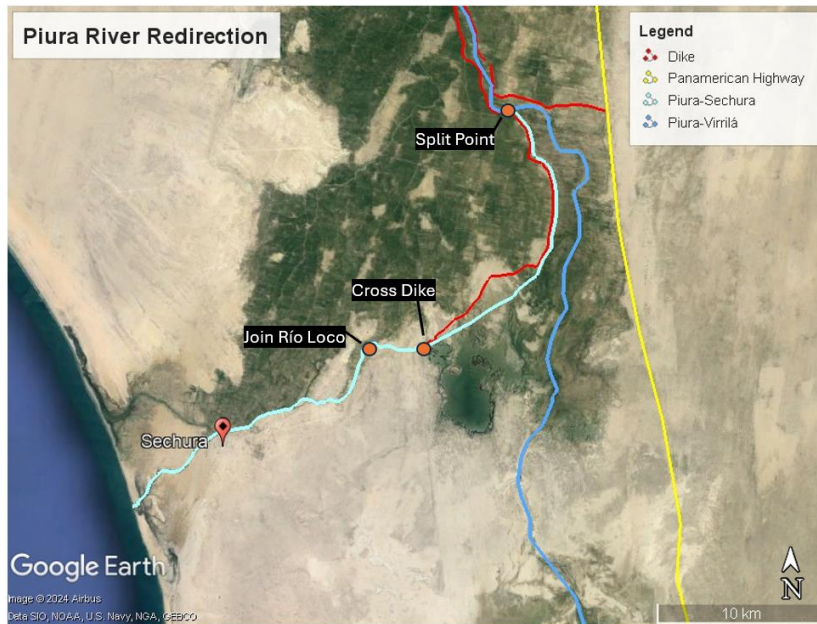
Figure 41- Course through Sechura (Google Earth, 2024)

For the redirection towards Sechura, a pilot channel is to be constructed with a depth of approximately 4m and capacity for 375m^3/s (Zegarra Dávila, 2023). The pilot channel is proposed for the reach from the split point up to the connection to Río Loco. Río Loco is estimated to have a flow capacity of 3,200m^3/s considering that this was the flow of the flood in 1983, and the river contained this flow following the breach of the dikes (Zegarra Dávila, 2023). The small flow capacity is attributed to the idea that this course will have sufficient transport capacity to flush out sediment and thereby begin to widen

overtime without further construction (Zegarra Dávila, 2023). The general section of the proposed pilot channel is shown in Figure 42.
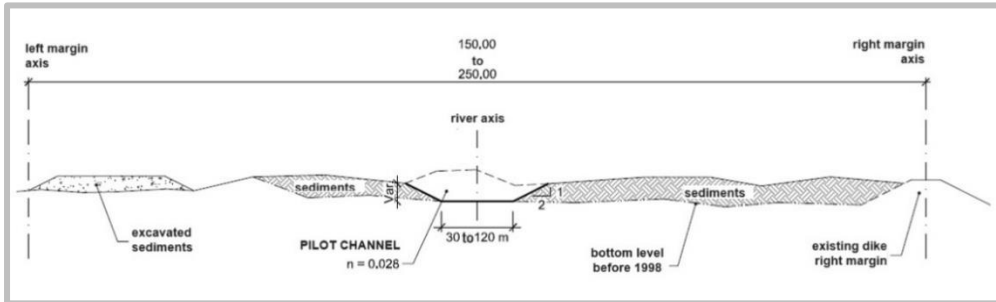
Figure 42- General cross section of the pilot channel through Sechura (Zegarra Dávila, 2023)

Table 3 shows a more detailed description of the pilot channel based on the typical section shown in Figure 43. Station 0+000 is the split point and 24+000 is the connection to Río Loco. In this, the slope of the pilot channel varies depending on the existing terrain.

Table 3- Parameters for the pilot channel

From (stat.)	To (stat.)	L (m)	B (m)	Z (m)	Q (m³/s)	V (m/s)	D (m)	S (m/m)
0+000	6+000	6 000	50	2	300	1.19	VAR	0.0002
6+000	18+400	12400	50	2	300	1.5	VAR	0.0004
18+400	22+000	3600	120	2	300	1.59	VAR	0.0006
22+000	24+000	2000	30	2	300	1.31	VAR	0.0005
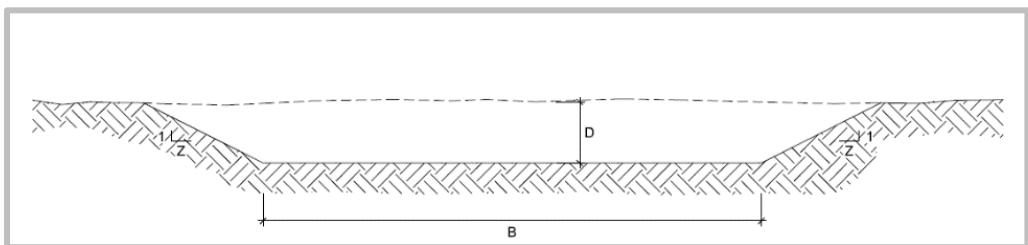
Figure 43- Parameters for the pilot channel (Zegarra Dávila, 2023)

7. HEC-RAS Model Set Up and Output Processing

HEC-RAS Version 6.3.1 was used for the hydraulic model. This chapter describes the setup, parameters, and assumptions used for assessment of the hydraulic conditions in the two river courses. The model is set up as one-dimensional.

7.1. Concept Model

A HEC-RAS model is set up considering elements indicated in Figure 44. Boundary conditions are set in the upstream and downstream sections of the river. These define the behaviour of water entering and exiting the system. The flow through the model is partially limited by dike structures on the left and right as well as the Panamerican Highway which acts as a boundary. The dikes are described as partial boundaries because although they do control flow, there are conditions under which the dikes will be breached. The cross sections are drawn perpendicular to the riverbed and span across the dikes to include the floodplain. Since flood analysis is not the focus of this study, the cross sections will be drawn just beyond the dikes, or just across the riverbed/lagoon in areas where dikes are non-existent.
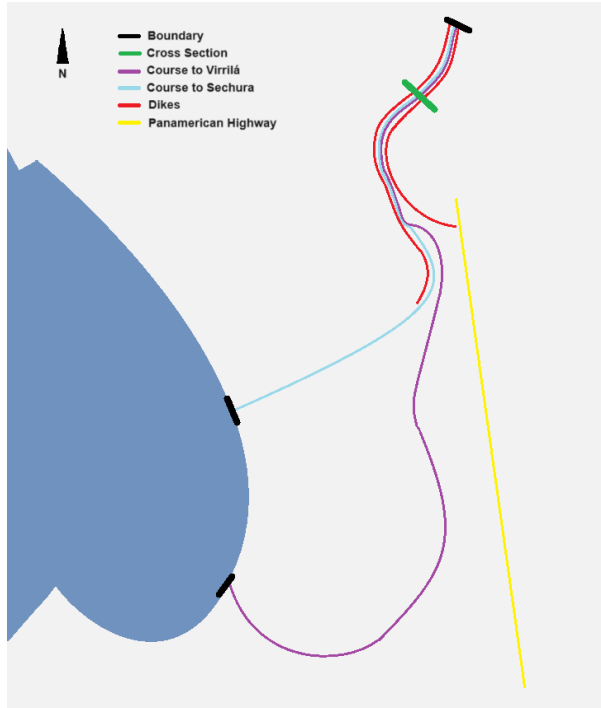
Figure 44- Concept model

In order to run a flow model in HEC-RAS two files are needed; these are a geometry file and a flow file which are combined in a plan file for computation as shown in the scheme in Figure 45.
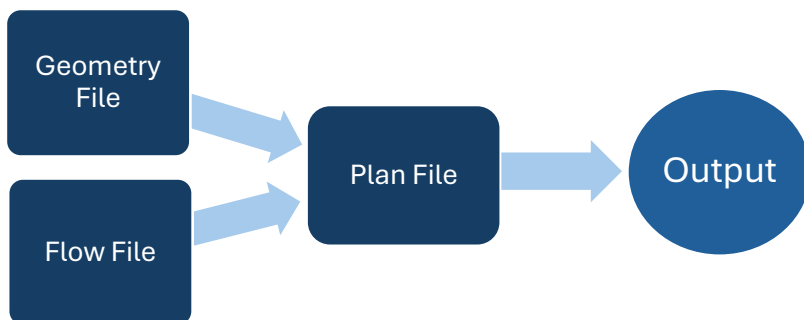
Figure 45- HEC-RAS file setup

7.2. Geometry File

Geometry files for one-dimensional models in HEC-RAS can be set up through manual input of cross section data or through RAS-Mapper. RAS-Mapper is a tool with geospatial capabilities to visualize geometric data and simulation results (HEC, 2024b).

A combination of the two files described in Chapter 6.5 is used to create cross sections in RAS-Mapper. General handling of the files and notable observations are described below:

- While the LIDAR file shows relevant features more clearly, the ASTER file covers a larger area.
- The LIDAR file requires some manipulation for error removal and simplification.
- Although the riverbed is clear in the LIDAR file, the topography data shows elevation differences in large distance steps of approximately 1m. As such the cross sections appear step-like. Nevertheless, considering that the general shape of the sections is clear, it has been deemed appropriate for general hydraulic analysis.
- Features in the ASTER file, such as the riverbed and dikes are not so clear in the ASTER file. However, the file is deemed sufficiently accurate to estimate the slope and approximate shape of the terrain.
- Cross sections created using the ASTER were partially manipulated to create an approximation of the riverbed for both river courses.
- It was found that the elevations of the files are similar in the transition from one to another.

The river centerline has the same shape for both courses up to just downstream of Drain 13.08, after this the geometry differs for both courses. Cross sections are spaced at approximately 500m up to Drain 13.08, then spacing increases

to approximately 1,000m up to the end of the LIDAR topography file. Finally, spacing of cross sections created using the ASTER file are spaced at varying distances. Figure 46 shows the geometry file created using RAS-MAPPER. Detailed spacing and cross section data is provided in Appendix B.
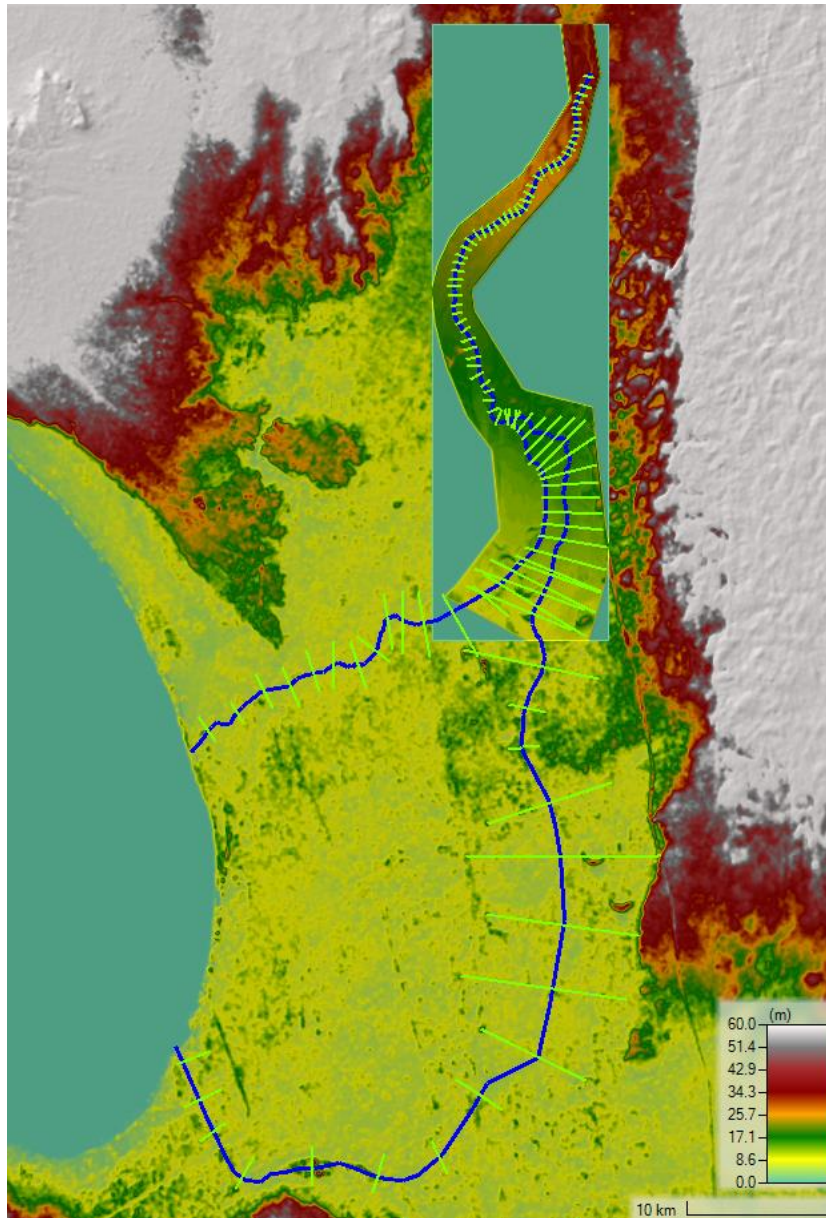
Figure 46- LIDAR topography and ASTER Topography opened in RAS-Mapper

HEC-RAS generates river stationing based on the distance from the most downstream point of the river centerline. As such, the stationing for the courses differs. While Virrilá reaches from station 1+568 downstream to 117+307 upstream, the geometry for the river through Sechura has a downstream river station of 1+870 and upstream station of 71+617.

Upstream of Drain 13.08

This section of the geometry spanning from Los Ejidos to Drain 13.08 is the same for both river courses. The section spans from 117+307 to 87+776 and from 71+617 to 42+086 for Virrilá and Sechura respectively. Cross sections comprise of bank stations, levees and ineffective areas. The riverbanks are approximately placed following the main riverbed. Levee structures are used along the top of the channel in the urban zone as shown in Figure 47 and on top of the dikes in the rural areas as shown in Figure 48.
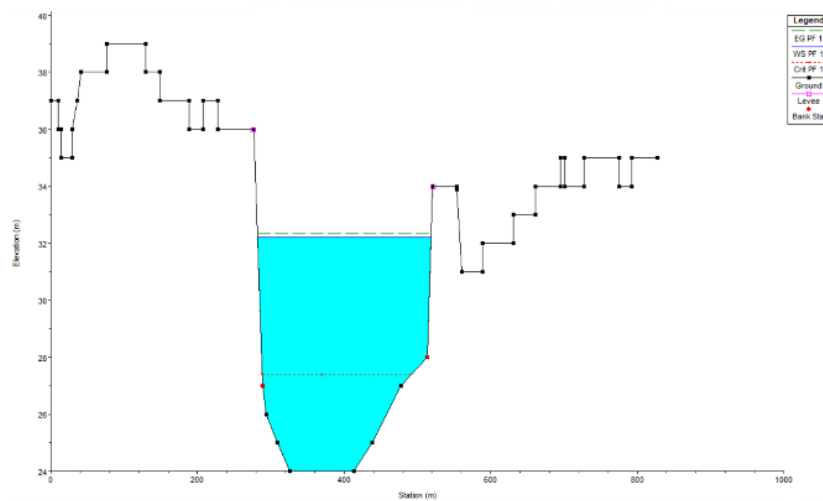
Figure 47- Reach Virrilá: cross section 117+307
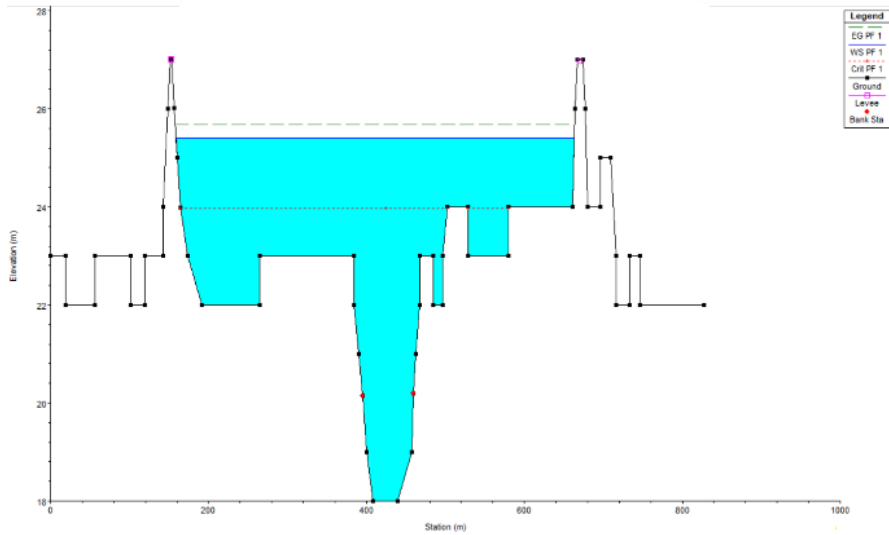
Figure 48- Reach Virrilá: cross Section 103+416

In sections where water is likely to overflow the levees or where flooding is expected to happen, ineffective areas were used outside of the dikes as shown in Figure 49. This ensures that water outside of the floodplain is not contributing to results.
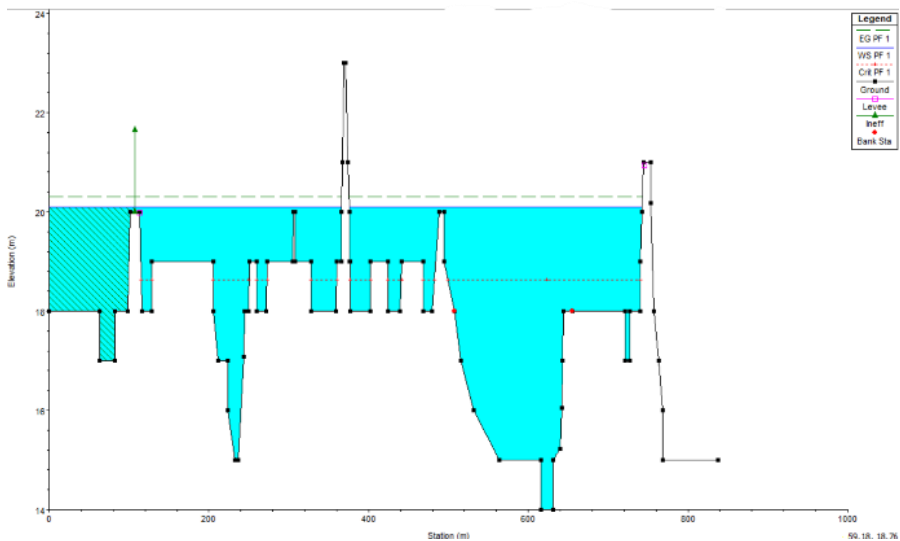
Figure 49- Reach Virrilá: cross section 88+621

Reach to Virrilá

The existing reach to Virrilá follows the same set up as previously described reaching up to the Ñapique/Ramón Lagoon. Levees are used to mark high ground or existing dikes and riverbanks are defined following the main river course. After this the ASTER topography is used and cross sections are drawn to span the width of the riverbed or lagoon. As shown in Figure 50, some features such as high ground, dunes, and the Panamerican highway are visible in the ASTER data. However, the riverbed and estuary are not clear.
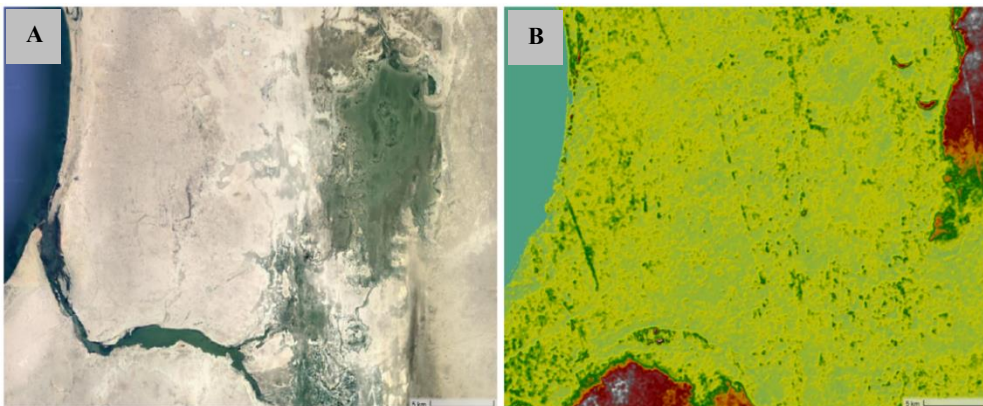
Figure 50a- Virrilá Estuary satelite imagery (Google Earth, 2024). 50b- area of Virrilá Estuary in ASTER data.

The Virrilá estuary is influenced by tidal activity up to approximately 20km upstream and is estimated to have an average depth of 2m (Céspedes, 2005). Since detailed bathymetric data was not available for the estuary, the bottom level in the last cross section 1+568 was calculated to be at -1m based on an assumed slope of 0.2‰ along the estuary. The topography of cross sections along the estuary was modified using this slope of 0.2‰. Similarly, due to the uncertainty in accuracy of the topography in the lagoon area, elevations were adjusted between riverbanks to create a gradual slope towards the estuary as shown in Figure 51 and Figure 52 for a schematic model.
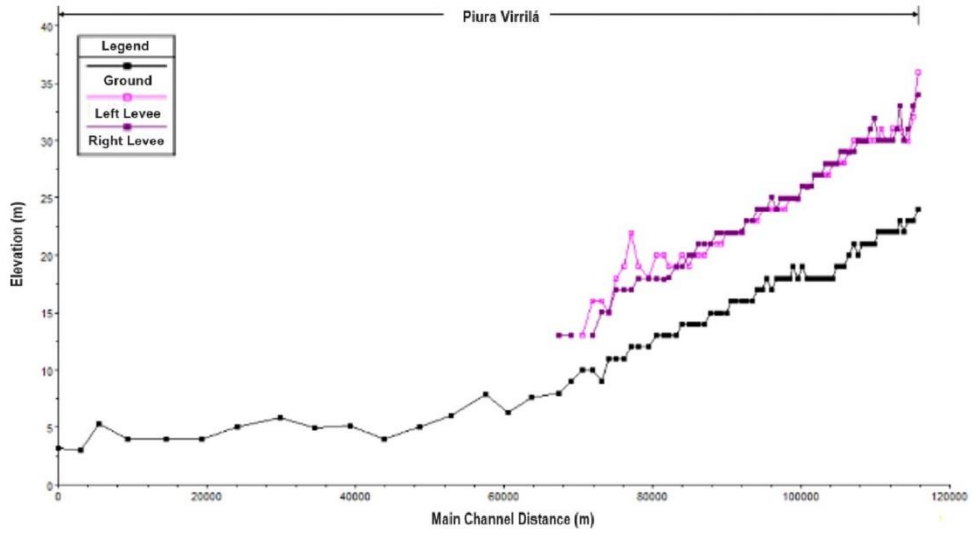
Figure 51- Reach Virrilá: Profile before adjustment
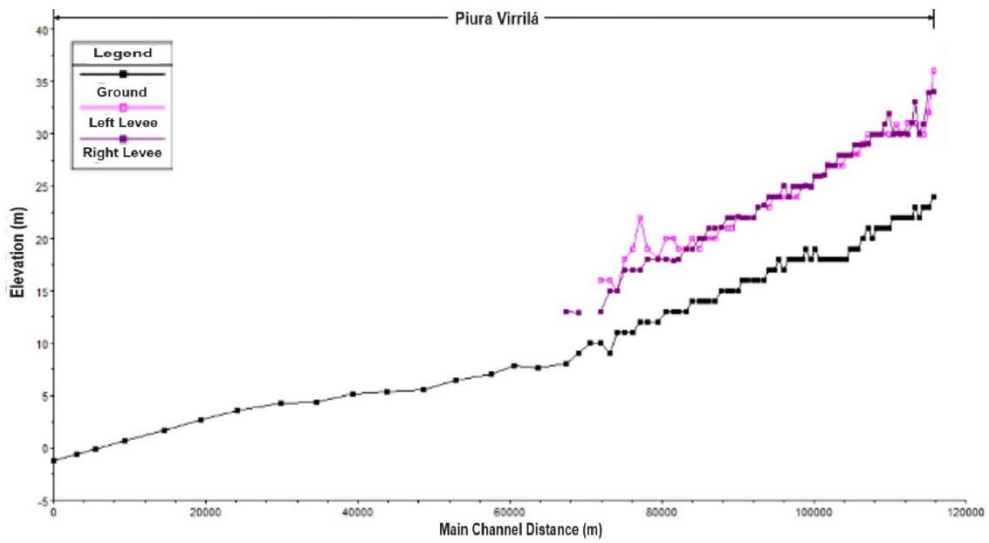
Figure 52- Reach Virrilá: Profile after adjustment

Reach to Sechura

The reach towards Sechura is modelled based on the alternative course description in Chapter 6.6 as well as some assumptions. These are as follows:

- The topography through which the channel passes is adapted to the slope defined in Table 3.

- The slope of the cross sections at Río Loco are modelled with an assumed slope of 0.3‰. to reach a bottom level of around 0. A shallower water level than that at Virrilá is assumed due to observations during the field visit.

- The pilot channel capacity is assumed to increase from 300 m^3/s to 3,200 m^3/s to match the capacity of Río Loco.

- It is assumed that a flow of 3,200 m^3/s will be contained by the channel, as such levees are placed on the top of the inserted channel.

- It is assumed that the Ñapique/Ramón Lagoon will still fill with water in this river course.

- The area outside of the existing dikes is modelled as ineffective zones.

Figure 53 shows a sample section of the channel along the right dike for topography data from the LIDAR scan. The depth of the channel has been assumed to be 4m and the riverbanks have a slope of approximately 1:2. Similar sections are placed on the ASTER topography as shown in Figure 54.
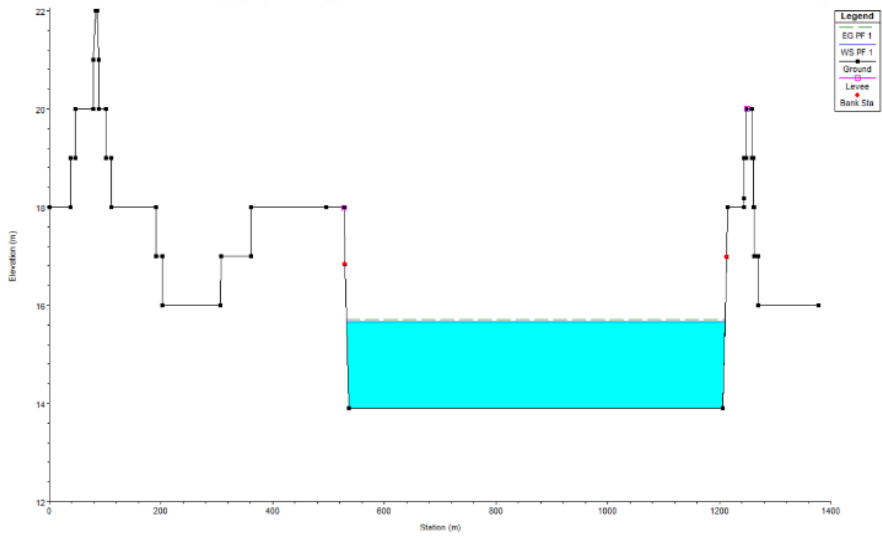
Figure 53- Reach Sechura: cross Section 40+847
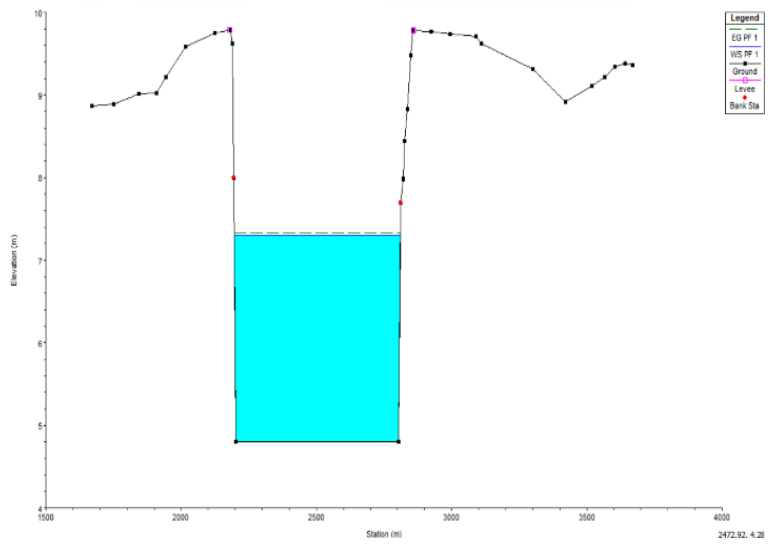
Figure 54- Reach Sechura: cross section 18+624

Manning

Mannings numbers are set for the riverbed and overbanks. As described in Chapter 6.4 the terrain is defined by varying roughness coefficients. Figure 55 indicates approximately where different roughness coefficients are used. The n-value is adjusted during calibration as described in the following section considering the following ranges:

- Riverbed: 0.022-0.033
- Concrete: 0.014-0.02
- Crops/Scattered Brush: 0.025-0.07
- Dense Brush: 0.07-0.016
- Pasture: 0.025-0.035
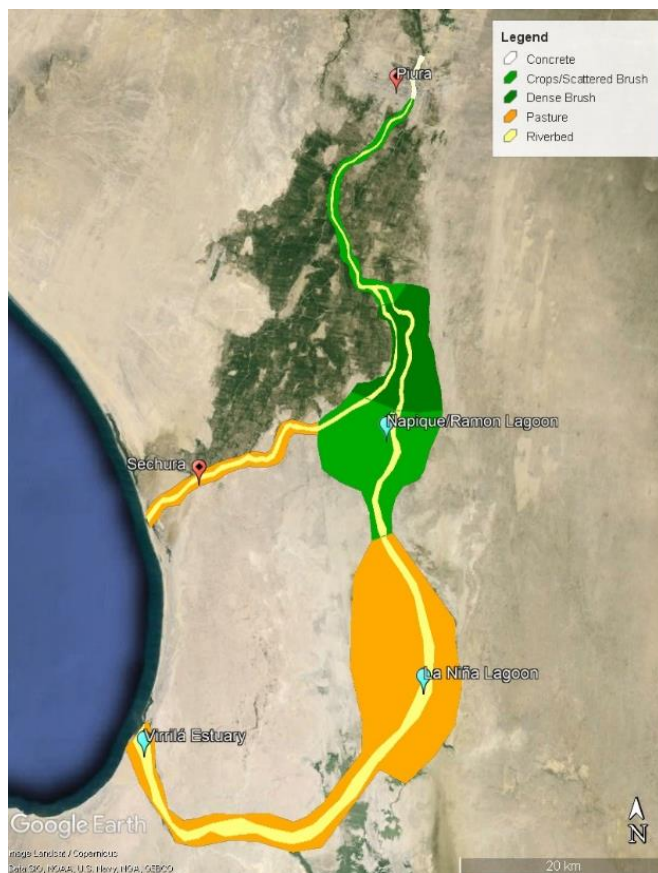
Figure 55- Roughness coefficient regions

7.3. Flow and Plans

Steady flow analysis is used for comparison of the river courses. Steady flow data in HEC-RAS requires upstream and downstream boundary conditions. A sensitivity analysis is conducted to investigate the influence of downstream boundary conditions on velocity. For this, the conditions described in Table 4 are used on a flow of Q= 1,000 m^3/s through Virrilá.

Table 4- Boundary condition in HEC-RAS for sensitivity analysis

Boundary Condition	Value	Description
Normal depth	0.0003 m/m	Depth is calculated using the Manning's Equation based on the friction slope (approximately equal to the surface slope) (HEC, 2024a)
Known water surface	2.7 m	The maximum sea level from Chapter 6.2.
Known water surface	1.5 m	The mean sea level from Chapter 6.2
Known water surface	0.2 m	The minimum sea level from Chapter 6.2
Normal depth + known water surface	0.0003 m/m 1.5 m	The friction slope is set as a boundary condition with an additional known internal water surface of 1.5m set at the downstream-most cross section

As shown in Figure 56, it was found that the boundary condition does not have an impact on upstream stations. The effect of the boundary condition is noted up to approximately 15km from the end of the reach. As such, the known water surface of +1.5m is chosen for simulations as this is the average sea level in the region.
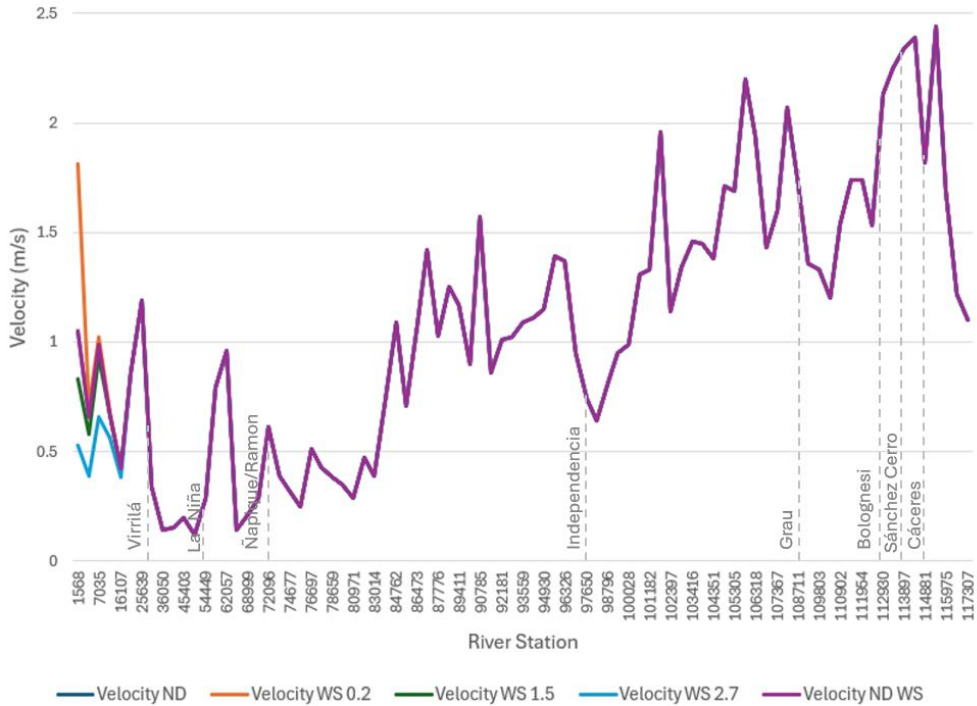
Figure 56- Reach Virrilá: Sensitivity analysis for boundary conditions at Q=1,000m³/s

Flows for assessment of hydraulic conditions were chosen as Q= 3,200 m³/s and Q= 1,000 m³/s and are used as upstream boundary conditions. Since the capacity of Río Loco is estimated to be Q= 3,200 m³/s, this flow is identified as a maximum flow for the alternative course. Larger flows are not expected because it is assumed that flows above 3,200 m³/s will be redirected towards La Niña Lagoon, this spillover concept is not within the scope of the model. Further, a flow of 1,000 m³/s is used for comparison as it is assumed that this is likely to be a recurring maximum flow according to the maximum flows shown in Figure 35 in Chapter 6. Both flow scenarios are computed assuming sub critical conditions due to the small slope along the course of the river.

7.4. Calibration

Before computation of the above-mentioned flow, the model is calibrated using known water surface elevations for a given flow. In this model, the Virrilá reach is calibrated using data from the 2017 flood event. Although the LIDAR topography is from 2015, it is assumed that calibration using 2017 data is appropriate since there were no major floods between the years 2015-2017 thereby no major changes in the topography are expected. A peak flow of 3,468 m^3/s was measured in March 2017 (PECHP, 2017), the water surface elevation was measured for several bridges as shown in Table 5.

Table 5- Maximum water surface for flooding of 2017 (Maza-Sócola, 2019)

Location	Station and downstream distance (Virrilá Geometry)		Water surface elevation (m asl.)
Cáceres Bridge	114+881	128	32.30
Sánchez Cerro Bridge	113+897	392	30.74[*]
Bolognesi Bridge	112+930	230	29.70
Grau Bridge	108+711	553	28.21[*]
Independencia Bridge	97+650	612	24.55

(*) estimated values (Reyes Salazar cited in Maza-Sócola, 2019)

However, additional information is needed to describe the flow regimen further downstream. Since exact water surface elevations are not known, satellite imagery was used to assess the extent of flooding. NASA's EODIS Worldview provides historic satellite images as shown in Figure 57 for the 5th of April 2017. Although the peak flow occurred on March 28th, previous dates showed significant cloud coverage and could not be used for assessment. The resolution of the image is not high; however, the size of the lagoons can be estimated, and the image gives insight into whether flooding occurred in certain regions.

Figure 57- Extent of flooding in 2017. Satellite imagery from
April 5th, 2017 (adapted from Nasa Worldview, 2017)

Mannings n-values are adjusted based on observed water surface elevations and flood extent using a flow of 3,468 m^3/s. The results of calibration are shown in Chapter 8.

7.5. Output Tables

The aim of the simulations is hydraulic comparison as well as an investigation of sediment transport capacity. HEC-RAS output is used for the whole cross section as opposed to analyzing main channel and overbanks separately, this is deemed sufficient for analysis of the general flow regime. Hydraulic depth (m), total velocity (m/s), and total shear (N/m^2) are used as output from HEC-RAS.

8. Results

This chapter shows results for calibration, velocity and depth profiles, as well as sediment transport capacity.

8.1. Calibration

Mannings n-values were adjusted according to the ranges described in Table 2 in Chapter 6. The final n-values are listed in Appendix B. Calibration results of the measured data from 2017 are shown in Table 6, the error found for each station was deemed acceptable.

Table 6- Calibration results for known water surface

Location	Obs. Water Surface	Sim. Water Surface	Error (%)
Cáceres Bridge	32.30	32.39	0.3
Sánchez Cerro Bridge	30.74*	30.83	0.3
Bolognesi Bridge	29.70	29.49	0.7
Grau Bridge	28.21*	28.43	0.8
Independencia Bridge	24.55	24.68	0.5

(*) estimated values (Reyes Salazar cited in Maza-Sócola, 2019)

As mentioned, no precise measurements were available further downstream. However, satellite imagery showing the extent of flooding in 2017 was used for approximation. Namely, the Mannings numbers were adjusted in some areas to allow flooding to occur, or to keep the water level below the levee structures modelled in HEC-RAS. The calibrated model is shown in Figure 58, where the points on the upstream portion indicate the observed water surfaces listed above.
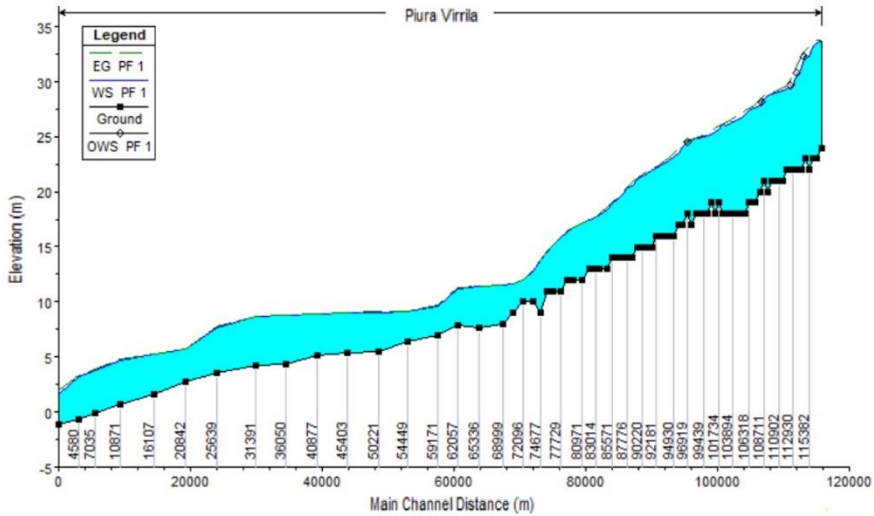
Figure 58- Reach Virrilá: water surface profile for calibration Q=3468m³/s

8.2. HEC-RAS Output: Water Surface Elevation Profiles

Virrilá: Flow Q=1,000 m³/s

Figure 59 shows some increases in depth as between station 25+639 to 31+691 and stations 62+057 to 65+336, which is expected as these are the areas between the lagoons where the river is narrower than the lagoon.
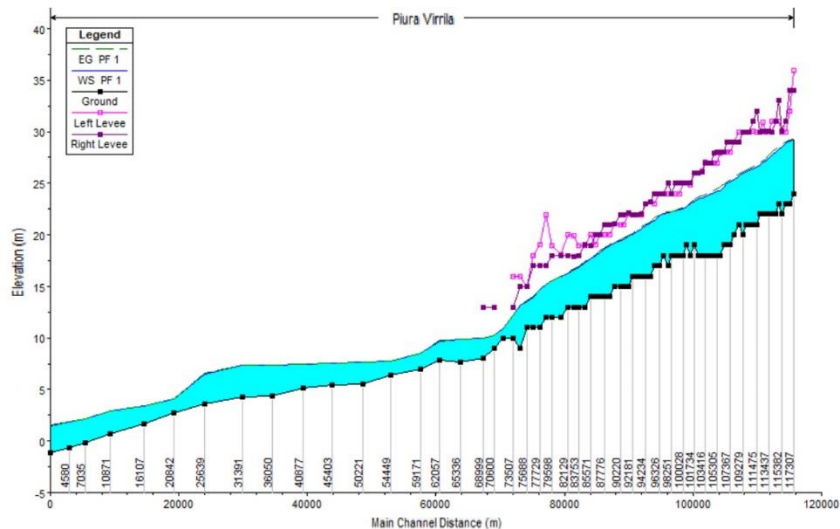
Figure 59- Reach Virrilá: water surface profile for Q=1,000m³/s

Virrilá: Flow Q=3,200 m^3/s

Figure 60 shows the increase in water depth during the larger flow event. Flooding can be seen along some stretches of the river.
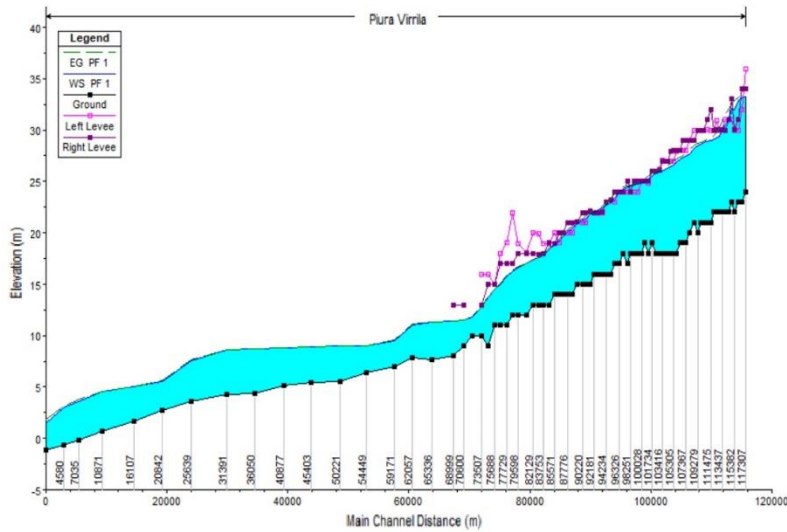
Figure 60- Reach Virrilá: water surface profile Q=3,200m^3/s

<u>Sechura: Flow Q=1,000 m^3/s</u>

The profile in Figure 61 shows the flow through the course towards Sechura. The levees indicated in the lower reach here are not dike structures but are used for modelling purposes. The flow shows a steep drop at around station 40+847, this may be due to the transition from the original river course to the new channel towards Sechura.
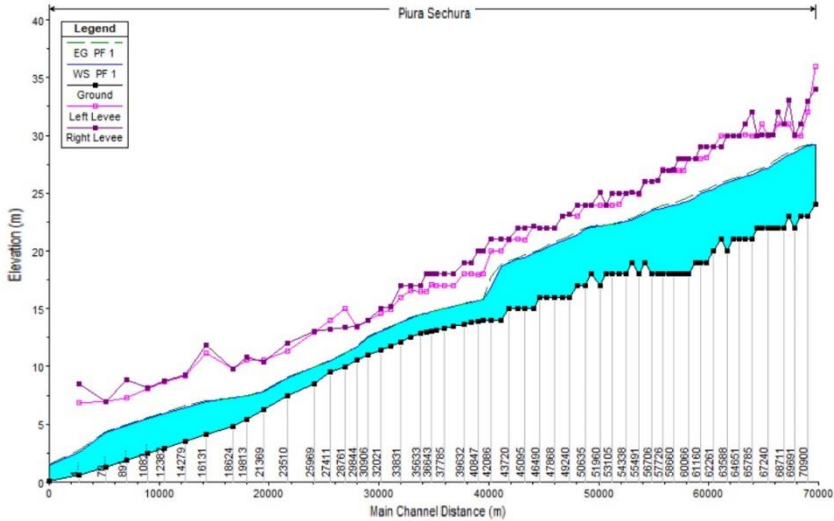
Figure 61- Reach Sechura: water surface profile for Q=1,000m³/s

Sechura: Flow Q=3,200 m³/s

Figure 62 shows the surface profile for a flow of 3,200 m³/s. An increase in depth is seen at station 21+369 as this is the exit of the Ñapique/Ramón Lagoon, since the river is narrower than the lagoon, there is an increase in depth.
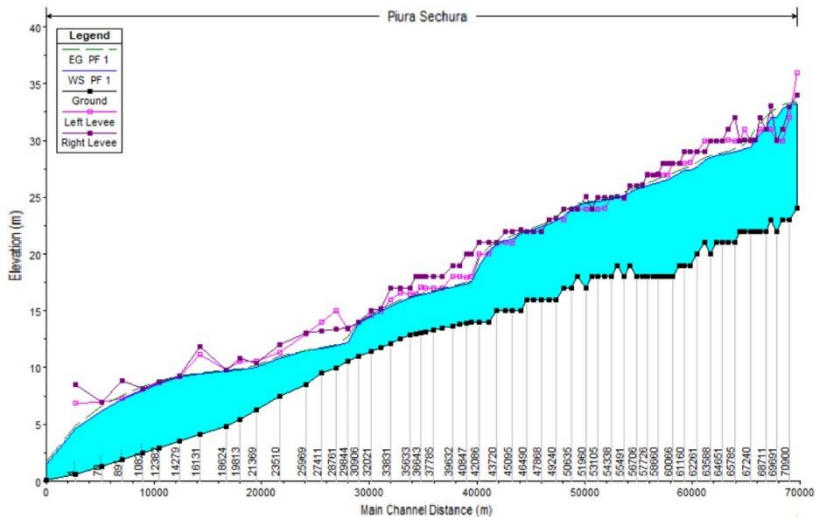
Figure 62- Reach Sechura: water surface profile for Q=3,200m³/s

8.3. HEC-RAS Output: Velocity and Depth Comparison

Figure 63 and 64 show the velocity and depth variation for Q=1,000 m³/s and Q=3,200 m³/s respectively for the course along Virrilá. Velocity and hydraulic depth are average values across each cross section.
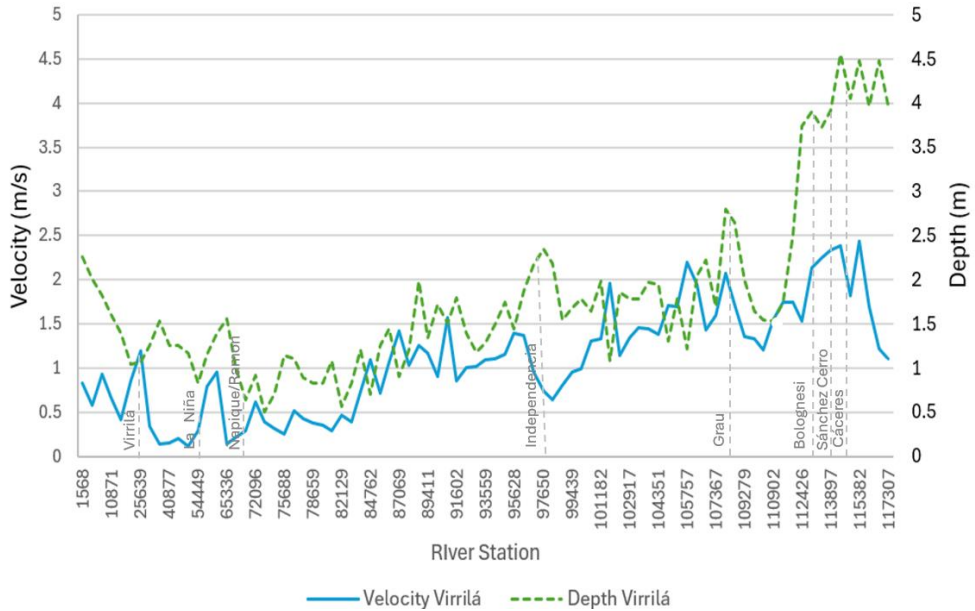
Figure 63- Reach Virrilá: velocity and depth output for Q=1,000m³/s

The course through Virrilá shows velocities reaching from 0.12-2.44 m/s for a flow of 1,000 m³/s. Hydraulic depth and velocity is higher upstream due to the channeling of the river and both decrease towards the lagoons, which is expected due to the expansion of the flood plain.
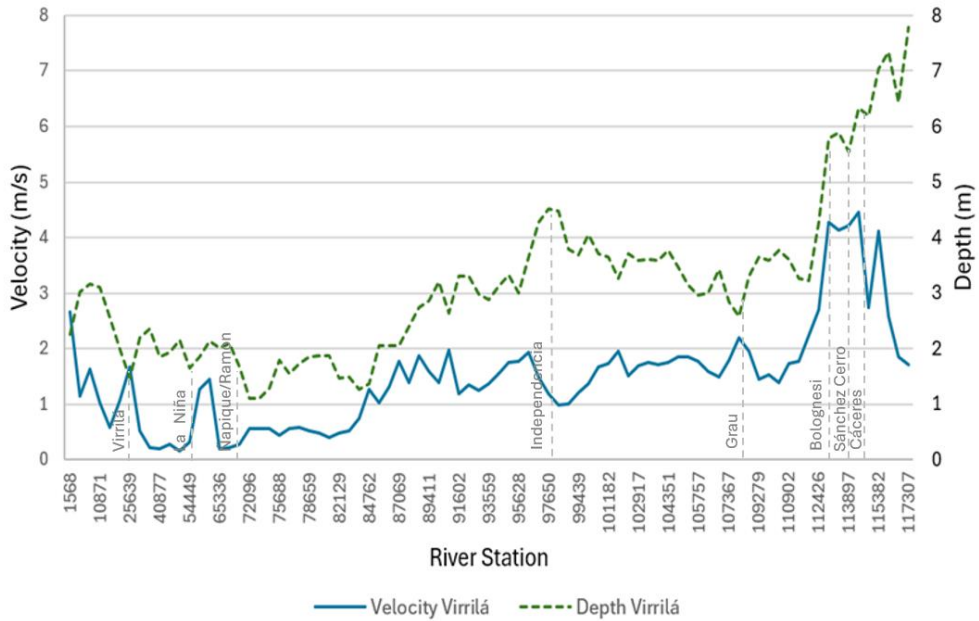
Figure 64- Reach Virrilá: velocity and depth output for Q=3,200m³/s

For a flow of 3,200 m³/s, a range of 0.16-4.46 m/s develops through the river. The same general trend exists where there are larger velocities in the upstream region and very low velocities in the lagoons. However, for this flow, the velocity is approximately twice as large in the peaks. The hydraulic depth relates to the velocity in that when velocity increases, depth decreases and vice versa. This is particularly relevant for narrower reaches such as the urban reach from 117+307-111+954 but is less notable in the lagoons where larger floodplains exist.

Figure 65 and Figure 66 show the velocity and depth variation for Q=1,000m³/s and Q=3,200m³/s respectively for the course along Virrilá. Velocity and hydraulic depth are average values across each cross section.

70
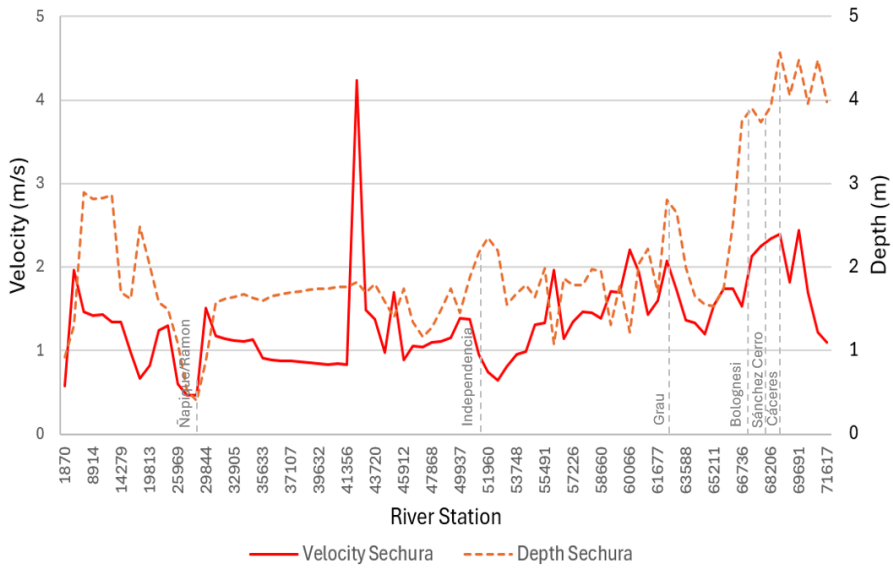
Figure 65- Reach Sechura: velocity and depth for Q=1,000m³/s
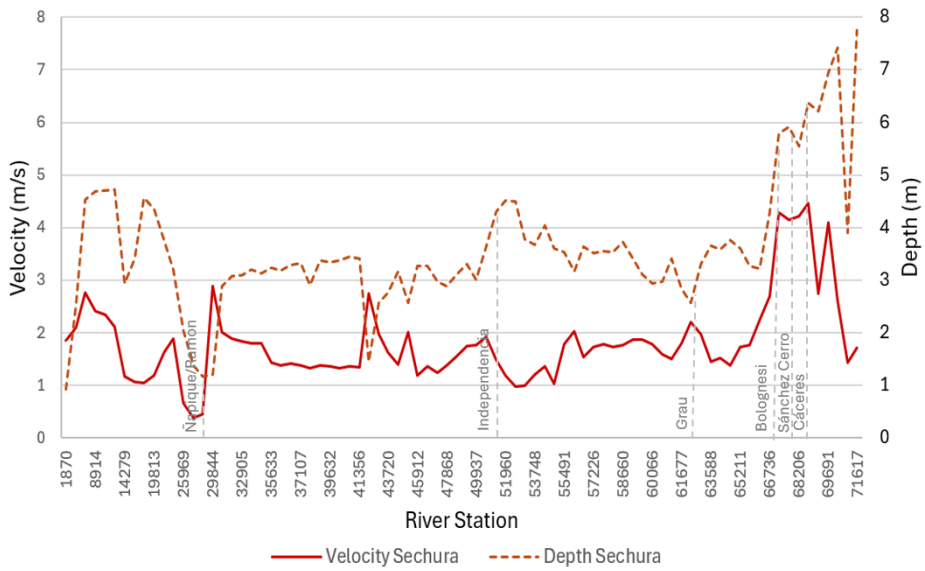
Figure 66- Reach Sechura: velocity and depth for Q=3,200m³/s

71

The course through Sechura shows velocities reaching from 0.46-4.23 m/s for a flow of 1,000 m³/s and a range of 0.38-4.46 m/s for a flow of 3,200 m³/s. Velocity shows a spike in Figure 65, this is due a transition between cross sections where in one cross section the floodplain is flooded and in the next it is contained by the riverbed. This peak is larger for Q=1,000 m³/s than that of Q=3,200 m³/s because the larger flow causes the floodplain to be flooded in both cross sections. However, disregarding the peak, the velocity range for Q=1,000 m³/s would be 0.46-2.44 m/s. This is a similar max velocity to that which develops in the reach through Virrilá, however, the minimum velocity is slightly higher.

The upstream velocity is similar in both courses for both flows. Further downstream the course towards Sechura develops higher velocities than the course through Virrilá as shown in Figure 67 and Figure 68 for comparison of the velocity development.
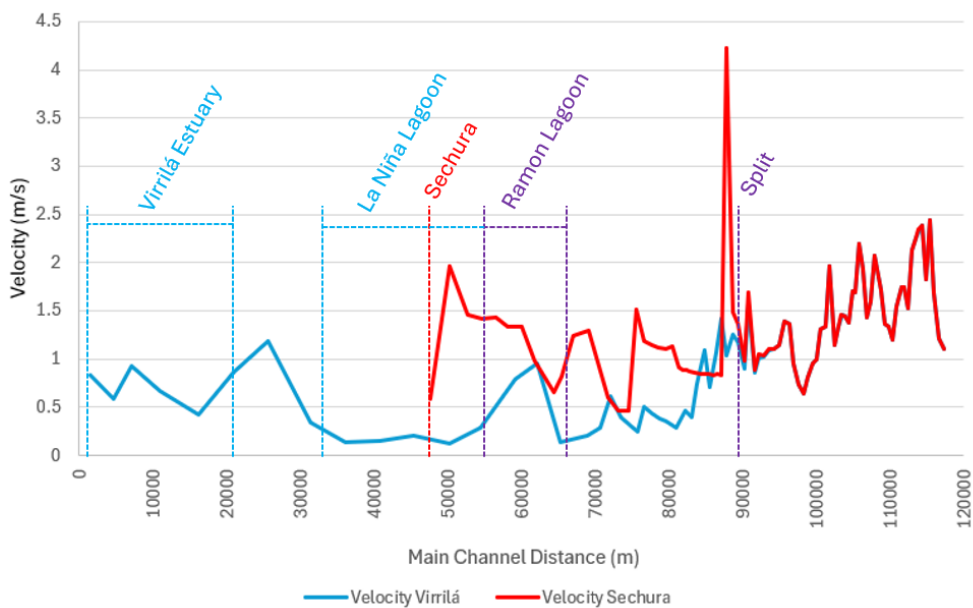
Figure 67- Velocity through Virrilá and Sechura at Q=1,00m³/s
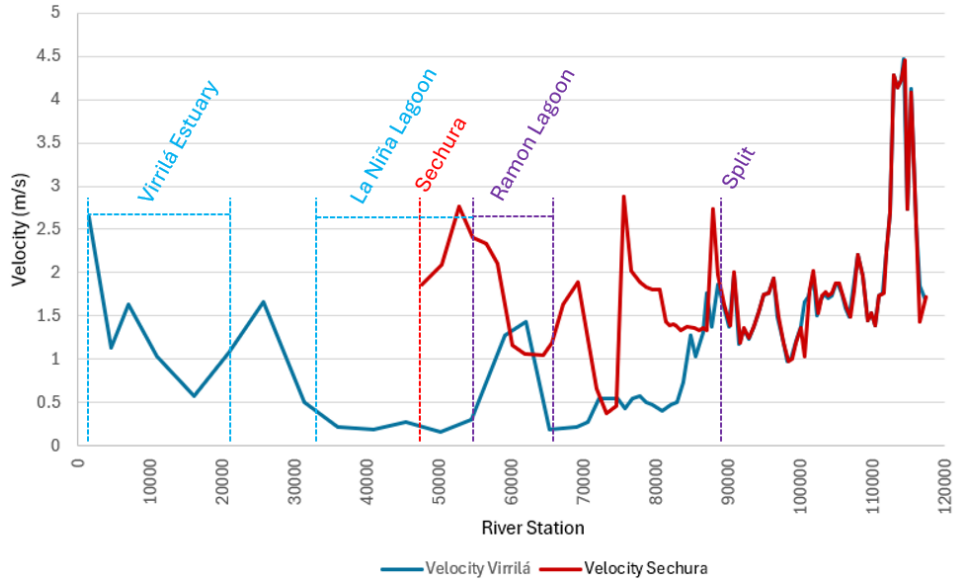
Figure 68- Velocity through Virrilá and Sechura at Q=3,200m³/s

In the next section, velocity and hydraulic depth are used to estimate sediment transport capacity throughout the course of the river.

8.4. Sediment Transport Capacity

HEC-RAS output is applied to the formulas described in Chapter 6 for non-cohesive sediment along the riverbed. As mentioned, shear stress is calculated using a drag law based on mean velocity which accounts for roughness conditions along the riverbed. Shear stress in each cross section is compared to the calculated critical shear stress of $\boldsymbol{\tau_{cr}}$= **0.144 N/m²** for a sediment of mean grain size d_{50}= 0.2mm and water of an assumed temperature of 25°C.

HEC-RAS provides a shear stress value for each cross section based on the hydraulic radius and slope of the cross section. Figure 69 and Figure 70 compare the shear force calculated by the program and shear force calculated using the drag law for a flow of Q=3,200 m³/s for both river courses.

73
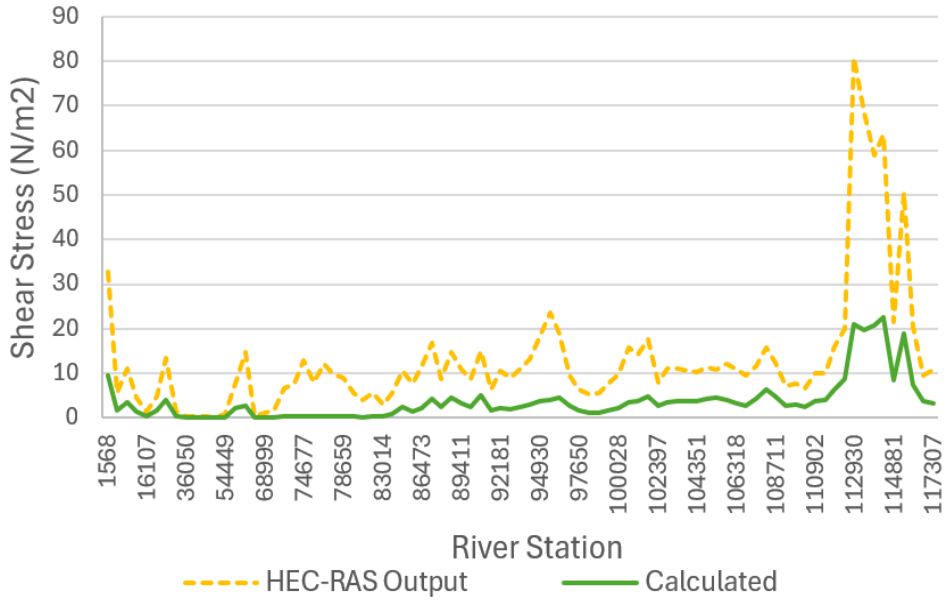
Figure 69- Shear output comparison for Virrilá Q=3,200 m³/s
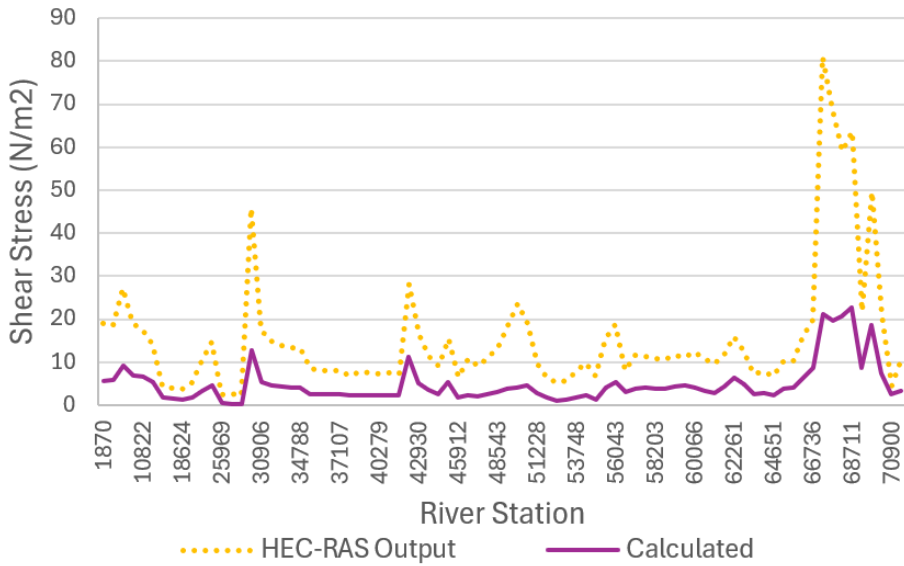
Figure 70- Shear output comparison for Sechura Q=3,200m³/s

The shear stress computed in HEC-RAS is significantly higher than that calculated using the drag law. Figure 71 and Figure 72 show shear stress results for Virrilá and Sechura for calculations based on the drag law and for HEC-RAS output shear stress in relation to the critical shear stress. Values of $\tau_b < \tau_{cr}$ indicate that the section is stable. For clear visualization of results, the y-axis range is reduced from 0-5 considering that the critical shear stress is a small number, it should be noted that exact shear stress values are listed in Appendix C.
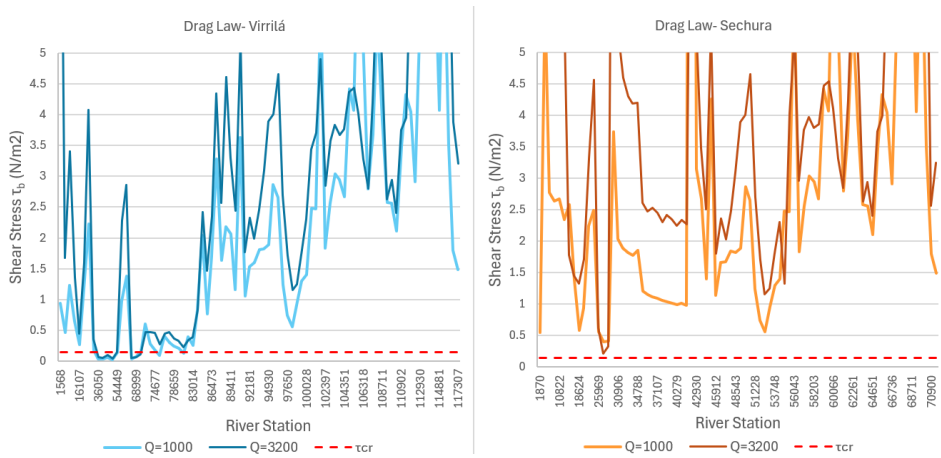
Figure 71- Drag law shear stress and threshold of motion for Q=1,000m³/s and Q=3,200m³/s for Virrilá and Sechura
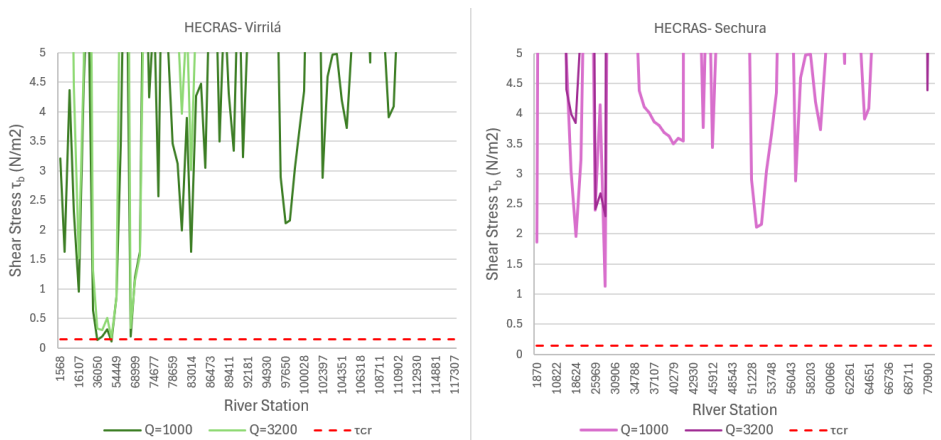
Figure 72- HEC-RAS shear stress output and threshold of motion for Q=1,000m³/s and Q=3,200m³/s for Virrilá and Sechura

The route through Virrilá indicates sections where the calculated shear stress along the bed τ_b is less than τ_{cr}. This implies that the threshold for sediment motion is not exceeded and therefor sediment transport is not expected. The course through Sechura indicates some drops in shear stress but remains above the critical shear stress, therefor indicating that the riverbed is not in a stable state and likely to be eroding. HEC-RAS output does not indicate any sections in stability. The HEC-RAS output is generally larger than that of the drag law calculated shear stress. This is due to the difference in the formulas used for computation where HEC-RAS output is calculated using slope and hydraulic radius (HEC, 2024a) while the drag law is based on bed roughness.

Although the shear stress and critical shear stress comparison gives insight into the sediment transport conditions, the excess shear stress is assumed to be proportional to transport. As such, it can be used to approximate in which sections of the river erosion or deposition is likely to occur. As shown in Figures 73-76, the excess shear is larger along most sections of the river towards Sechura as toward Virrilá. For visual purposes, the y-axis is set from 0-60 for the drag law computations and from 0-140 for the HEC-RAS output results, full results are listed in Appendix C.
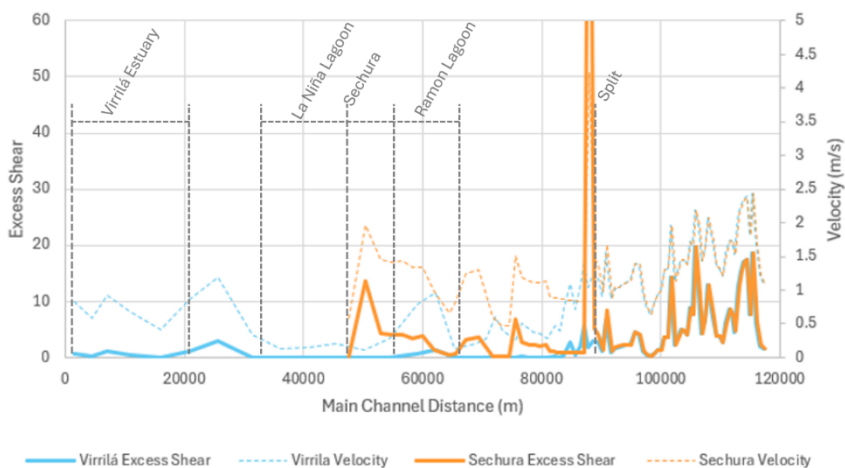
Figure 73- Excess shear based on drag law for Q=1,000m³/s
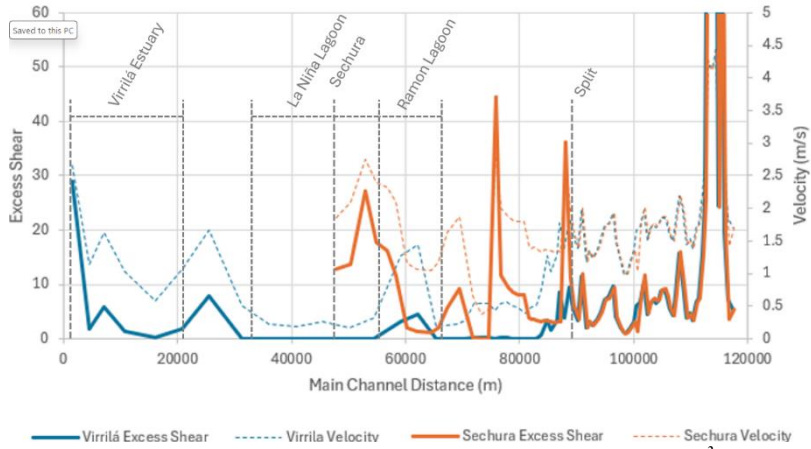
Figure 74- Excess shear based on drag law for Q=3,200m³/s
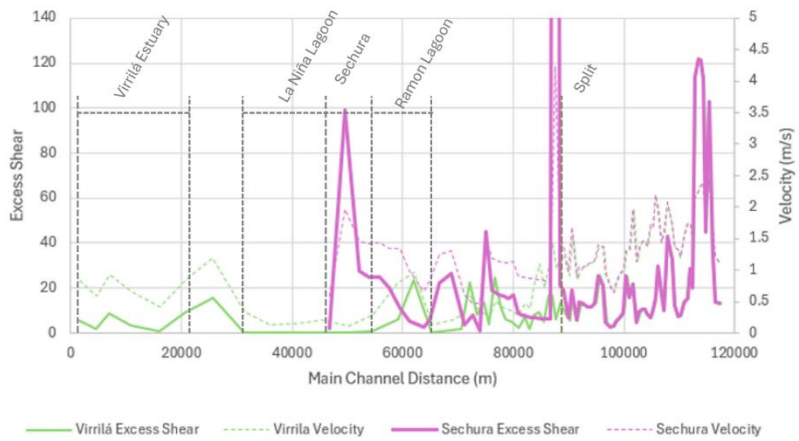
Figure 75- Excess shear based on HEC-RAS output for Q=1,000m³/s
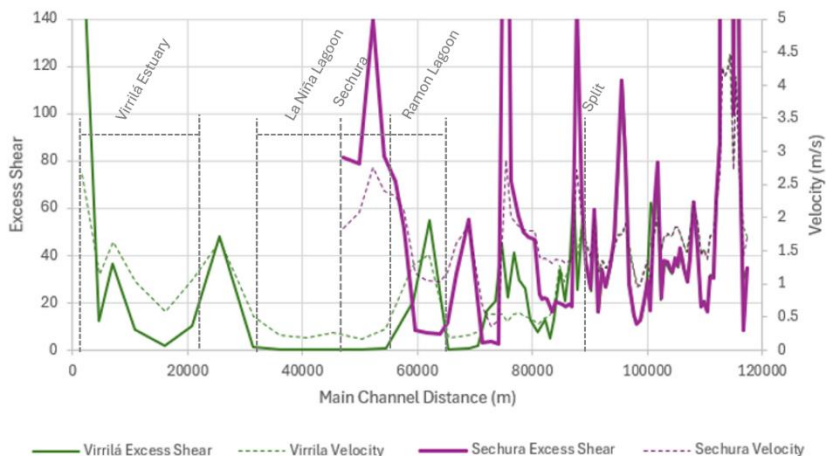
Figure 76- Excess shear based on HEC-RAS output for Q=3,200m³/s

77

Although the shear stress along the course towards Sechura did not go below the critical shear stress, the gradient of excess shear is indicative of erosion or deposition. Erosion occurs when excess shear increases while deposition ocurrs when it decreases. The figures above show various peaks which are likely due to the computation process in HEC-RAS. For analysis of erosion or deposition, trendlines are used to simplify the peaks as shown in Figure 77 for Virrilá and Sechura at a flow of Q=3,200 m³/s for the drag law computation and HEC-RAS shear output. The trendlines are approximations purely created for visualization and are not based on numerical values.
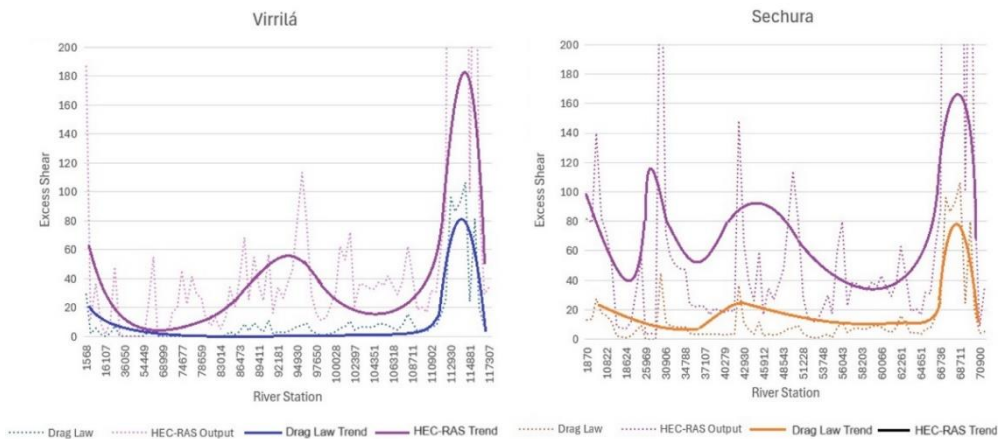
Figure 77- Trend for excess shear along Virrilá and Sechura

Erosion likely occurs immediately downstream of Los Ejidos Dam, then the excess shear drops for both scenarios indicating likely deposition of sediments. Following this, the route towards Virrila shows some smaller peaks but has a decreasing trend due to the decreased transport capacity in the lower reach. The route towards Sechura shows more defined peaks in the lower reach and a general increasing trend in excess shear. There is however a drop in excess shear in the lower reach which is a result of the assumption that the Ramón/Ñapique Lagoon still fills with water. This implies an increased width and a drop in velocity, therefor the excess shear also drops. Comparing both

the HEC-RAS output and the calculated shear stress, the general trend for Virrilá is a decrease in excess shear towards the lower reach while increased larger shear is seen in the course towards Sechura.

As mentioned in Chapter 5, excess shear is related to the Meyer-Peter and Müller bed load transport formula. Bed load transport is calculated for both the shear stress based on the drag law and for the HEC-RAS output shear for a flow of Q=3,200m³/s. As shown in Figures 78 and 79, bed load in load per unit width shows small peaks for the transport through Sechura while it stays quite insignificant for transport through Virrilá. The y-axis was adjusted to 0-0.05 for visualization purposes, full data is provided in Appendix C.
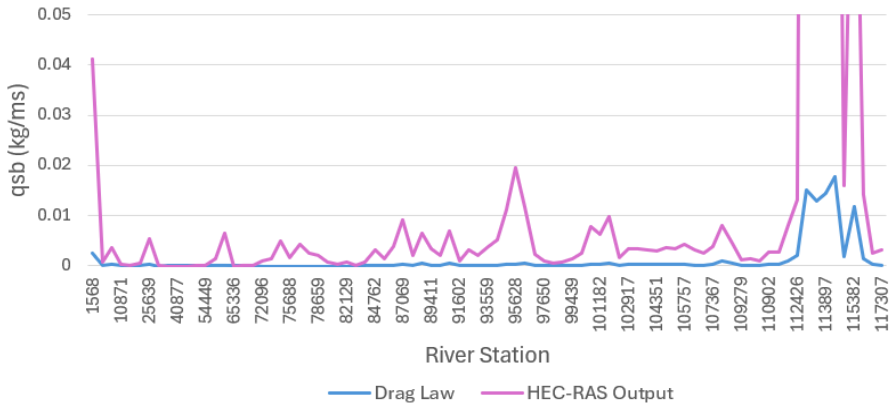
Figure 78- Bed load transport for Virrilá at Q=3,200m³/s
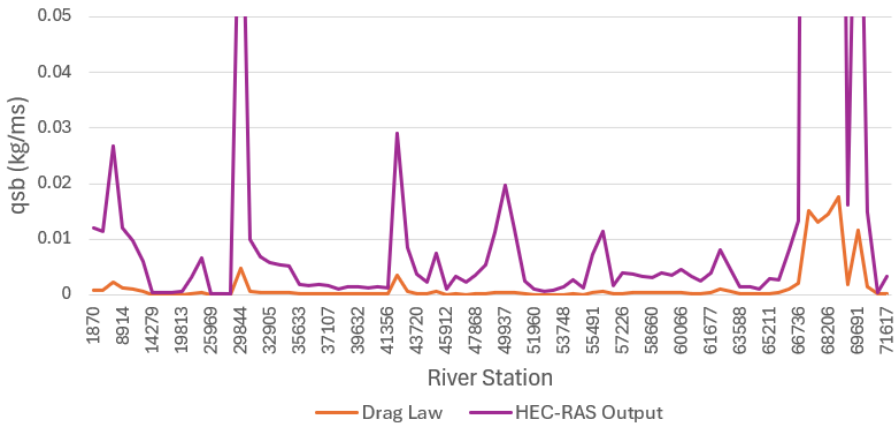
Figure 79- Bed load transport for Sechura at Q=3,200m³/s

9. Discussion and Recommendations

The following chapter describes the significance of the hydraulic conditions occurring in the different river courses, provides suggestions improvement of the study, and comments on potential studies related to the issue of sediment transport in the lower basin.

9.1. Implication of Results

The HEC-RAS model represents the general flow regimen in the two river courses. While conditions upstream of the split point do not vary for different routes, it is evident that the reaches downstream of the split result in conditions that favor sediment transport in the route towards Sechura.

 The course towards Virrilá shows spans totaling to approximately 30km with an excess shear value of 0 using the drag law calculation, and close to 0 using HEC-RAS output, this is an indication of sedimentation. This is expected due to the small slope and resulting low velocities. The lack of transport capacity results in sedimentation in the lagoons which creates an obstacle for flow. Although the lagoons may have a large capacity to hold sediment before filling up, these lagoons are not being filled evenly (Reyes Salazar, 2024b). Instead, there is sedimentation occurring at the upstream section of the Ñapique/Ramón Lagoon which acts as a barrier and reduces the velocity of incoming flows (Reyes Salazar, 2024b). As such, the future behavior of the river is increasingly difficult to predict.

The course towards Sechura has larger velocities and larger excess shear values. This is expected since the general slope of this reach is larger than that towards Virrilá. There is, however, potential for sedimentation in the areas where the excess shear decreases. These areas with local sedimentation are in part also due to the Ñapique/Ramón Lagoon. In the model, it was assumed that

this lagoon fills with water, this however may be different in practice as discussed in the next section and thereby increases the transport capacity in this area.

9.2. Additional Sediment Investigations

Additional investigation of sediment transport can be achieved through comparison of different transport formulas considering the large difference in results from the HEC-RAS shear output based on slope and hydraulic radius compared to the calculated shear stress based on the drag law. The actual transport capacity of the river is difficult to pinpoint since sediment transport may be quite unpredictable. These are only two of the many calculation methods available for shear stress, perhaps a range of potential transport capacity values can be determined using more formulas. However, for the purpose for this investigation, the HEC-RAS output and drag law shear stress provided sufficient information to indicate where sedimentation and erosion is likely to occur.

A detailed analysis of suspended sediment transport is also relevant for the Piura River. The river not only interacts with sediment in the riverbed but also with sediment carried from further upstream (Reyes Salazar, 2024b). This is generally clayey-silty sediment which deposits in the lower spans of the river as seen in the field visits. The influence of the sediment load entering the lower basin from further upstream may also have a significant impact on the quantity of deposited sediment.

Further, the 1967 study (Int. Engineering Company & Olazabal y Leon S.A) mentioned by the PNUD project provides a hydrometer analysis for gradation fine sediments for the Piura River, as well as a rating curve for suspended sediment discharge. This information is useful for sediment modelling in

HEC-RAS, however, suspended sediment quantities in the Piura River are likely to have changed in the since the study due to factors such as deforestation. Deforestation has been an ongoing issue in the upper basin and results in increased runoff going into the river as well as increased sediment transport since there are no roots holding sediment in place (Atarama & Rashid, 2019).

HEC-RAS features sediment transport modelling in one-dimensional models for a quasi-steady flow. In this, the change in the riverbed is considered in the computations and thereby the behavior of sediment can be analyzed over time for a hydrograph. There are many transport equations and a multitude of boundary conditions to be used in varying combinations for computation. These result in varying outputs for the same cross section and sediment data depending on the transport equation combination used. As such, in order to accurately model the sediment movement along the riverbed calibration parameters are necessary for one or many known flows. Calibration data for sediment transport analysis could be in the form of bathymetric data for different years or before and after a large flow event.

9.3. Recommendations

In this model, a simplified version of the river course was created for both the course through Virrilá and Sechura. It was noted that the intervals of 1m in the topography made a difference in whether or not a particular cross section was flooded or not. However, since the areas outside of the dam were marked as ineffective areas, this did not influence the results. Nevertheless, further investigation could include a flood analysis of the two courses using return periods. In this case, a more accurate topography would be necessary.

The Piura River is a complex system with an abundance of potential solutions to reduce vulnerability of surrounding populations. As suggested by Eduardo Zegarra (Zegarra Dávila, 2023), there are multiple routes which can create an increase in energy in the river and allow for adequate sediment transport. The route discussed in this study is one of the several proposals, however, the implications of the other proposals can also be assessed in comparison to the current route through Virrilá in terms of sediment transport capacity.

As mentioned, the Ñapique/Ramón Lagoon was modelled to allow for flooding in the course towards Sechura. However, in order to prevent flows larger than $3,200m^3/s$ from entering Río Loco, a spillway structure can be constructed to control the flow. In this way, flows above $3,200m^3/s$ can be redirected to flood the lagoons in case of extreme events. This spillway structure would require additional investigation for design.

A further investigation would include the effect of maintenance on the course of the river. As mentioned in Chapter 4, during the field visit many reaches were found to be covered in dense brush. The removal of the brush could potentially reduce the roughness of the terrain and allow for faster velocities to develop along the flood plain. An investigation into the effect of river maintenance can also add to the study of sediment transport in the area.

In this research, observations made during field work for land coverage were used to approximate Mannings roughness values. A further investigation could be a systematic analysis of the vegetation in the study area. This can be done by setting a grid for which vegetation type is determined to create a more accurate description of the land coverage, also considering seasonal changes.

A further ongoing investigation is that of upstream reservoirs to control the flow passing through the city of Piura (Reyes Salazar, 2024c). A difficulty encountered with these suggestions, however, is the lack of an integrated

management system for the Piura River. The river crosses several provinces in the region, these however have their own legislation regarding the river; which is often an obstacle for riverine defense design (Reyes Salazar, 2024c). Consequently, there have been efforts to create an entity in charge of risk management against disasters of hydroclimatic origin on a national level which would allow for adequate riverine management (Reyes Salazar, 2024c), however, this entity has yet to be approved.

10. Conclusion

The Piura River regularly poses a threat to Piura and the surrounding agricultural land during El Niño events. Damage or destruction of infrastructure such as roads, communication lines, homes, schools, and health establishments has been a major set pack for the region in the past (Atarama & Rashid, 2019). The ENSO phenomenon causes a dramatic change in the climatic conditions of the Piura region in the form of storms that are transported inland due to increased temperatures along the coast. These storms cause an increase in flow through the non-permanent river. The various anthropogenic changes to the river have resulted in an unstable flow regimen which has increased the vulnerability of populations in the lower basin.

The river generally caused erosion, which allowed for sufficient capacity to be created as large flows passed through the lower basin. However, in the more recent flood of 2017, there was no erosion (Reyes Salazar, 2024b). This resulted in less capacity of the river along some stretches and thereby created an overflow. The extension of the river towards Virrilá in the south instead of through Sechura has moved the river along a route with a smaller slope, thereby causing a reduction in energy (Reyes Salazar, 2024b). Hydraulic conditions were compared for the ancient course towards Sechura and the current course towards Virrilá.

HEC-RAS was used for modeling hydraulic conditions along the different river courses. For this, topography files were used to create a one-dimensional model of the river. The model was calibrated according to data from the 2017 flood event with a flow of Q=3,468m^3/s and observed water surface elevations for the upper reach, as well as satellite imagery to identify the extent of flooding for an approximate calibration in the lower reach. The river courses were then compared at flows of Q=1,000m^3/s and Q=3,200m^3/s in steady state.

The results provided the general water surface, velocity, and shear stress profiles along both courses. The critical shear stress for sediments of a mean grain size of d_{50}= 0.2mm at a water temperature of 25°C was found to be τ_{cr}= 0.144 N/m^2. This was compared to HEC-RAS shear output and shear stress based on the drag law to calculate excess shear as $(\tau_b - \tau_{cr})^{3/2}$. Excess shear was used to indicate whether aggradation or erosion happens along each profile depending on the general trend of the curves. Despite fluctuations in the output, it was found that the course towards Virrilá shows a general trend of sedimentation in the lower reach while the excess shear along Sechura is considerably higher.

The planned redirection of the river towards Reventazón is suspected to aggravate the issue of sediment deposition along the course of the river (Reyes Salazar, 2024c). Not only is the reach longer than the current reach through Sechura, but it also crosses into a different watershed as shown in Figure 80. Experts in the area also argue that this redirection is also more expensive than other alternatives (Zegarra Dávila, 2023). As such, studying alternative proposals is crucial to better understand what the options are for the Piura River.
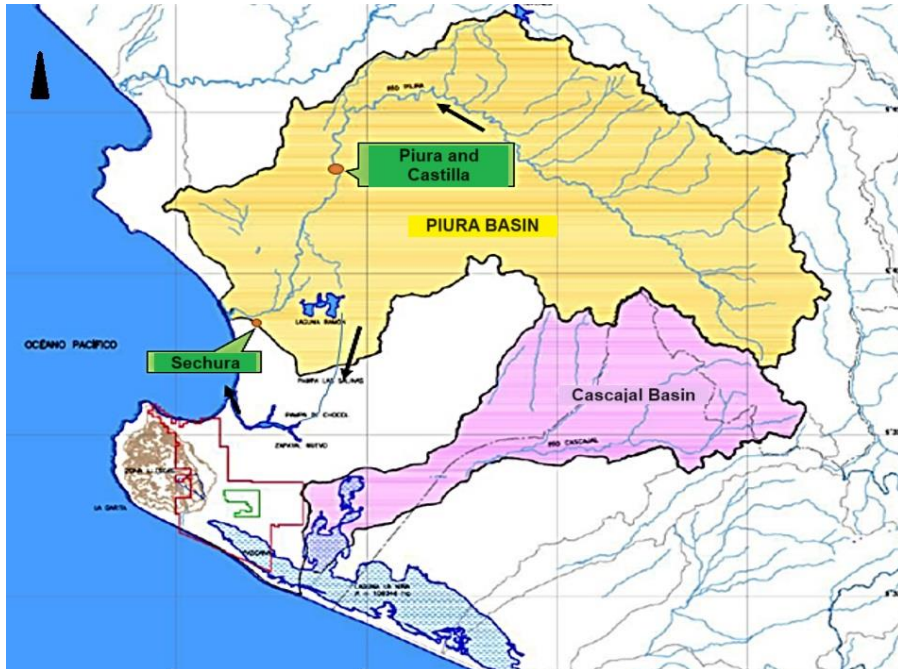
Figure 80- Map showing Piura River basin and Cascajal River basin in Piura Region and Lambayeque (adapted from Zegarra Dávila, 2023)

The non-permanent nature of the Piura River makes for difficult prediction of flow regimen. Redirecting the river towards the original course may allow for a more predictable flow regimen due to the increased velocities and sediment transport capacity. The flow regimen would likely return to general erosion along the riverbed. Damage due to erosion can however be prevented through consideration of the potential velocities during design of riverine structures and through reconstruction of currently damaged structures. To conclude, the Piura region will continue to be affected by the recurring ENSO Phenomenon. As such, it is imperative that the region continues to investigate the flow regimen of the Piura River to better prepare for dramatic increases in flow and strive to increase resilience.

Bibliography

Alvarado Ancieta, C. & Ettmer, B., 2007. *Control del fenómeno de agadación-degradación del Río Piura mediante realiniamiento del cauce principal inferior. Fenómeno El Niño, Piura, Perú*. [pdf] Available at: <https://www.researchgate.net/publication/343046376_CONTROL_DEL_FENOMENO_DE_AGRADACION_-_DEGRADACION_DEL_RIO_PIURA_MEDIANTE_REALINEAMIENTO_DEL_CAUCE_PRINCIPAL_INFERIOR_FENOMENO_EL_NINO_PIURA_PERU> [Accessed November 2023]

Alvarado Ancieta, C., 2023. *Fluvial-geomorphological and anthropogenic changes of Piura River- La Niña anthropogenic basin- El Niño, Peru.* Towards 2048: the next 25 years of river studies: NCR DAYS 2023 Proceedings. s.l.:Netherlands Centre for River Studies Publication 51-2023, pp. 26-27 [pdf]

ARCC, 2017. *Plan Integral de la Reconstrucción con Cambios*. [pdf] Available at: <https://www.congreso.gob.pe/Docs/comisiones2017/CEProcesoReconstruccionFenomeno/files/a_plan-integral-de-reconstrucci%C3%B3n-con-cambios-aprobada-0609.pdf> [Accessed December 2023]

ARCC, 2022. *Integrated Master Plan for Flood Control and Sediment Transport Management in the Piura River Basin*. [pdf] Available at: <https://www.rcc.gob.pe/2020/wp-content/uploads/2023/06/piura-river-masterplan.pdf> [Accessed October 2023]

Atarama, E. & Rashid, M., 2019. *Integral Management for Piura River Basin in Peru.* [pdf] Available at: <https://www.iahr.org/library/infor?pid=3414> [Accessed October 2023]

Autoridad Nacional del Agua, 2023. *Plan de Intervenciones*. [pdf] Ministerio de Desarollo Agrario y Riego. Available at: <https://www.ana.gob.pe/sites/default/files/normatividad/files/PLAN%20DE%20INTERVENCIONES.pdf> [Accessed December 2023]

Azurin Gonzáles, C., 2010. *Elboración: "Estudio para la conformación de un programa de inversión pública que permita disminuir la vulnerabilidad frente al incremento de caudales originados por precipitaciones extremas en la cuenca Media y Baja del río Piura". Informe Final Definitivo.* [pdf] Autoridad Nacional del Agua. Available at: <https://repositorio.ana.gob.pe/handle/20.500.12543/711> [Accessed April 2024]

Caldwell, P. C., et al., 2015. *Sea level measured by tide gauges from global oceans — the Joint Archive for Sea Level holdings (NCEI Accession 0019568)*, Version 5.5, NOAA National Centers for Environmental Information, Dataset, doi:10.7289/V5V40S7W. Talara 31.05.2015-31.04.2024. Available at: <https://uhslc.soest.hawaii.edu/data/> [Accessed May 2024]

Castillo Zavaleta, P., 2024. Discussion during excursion to rural area following course through Sechura. (personal communication February 2024)

Castillo Zavaleta, P., et al., 2019. *Propuesta Para Reducir la Vulnerabilidad Fisica a Indundaciones por Avenidas Extremas en El Bajo Piura, Peru.* Master. Eadic Escuela Técnica.

Céspedes, C., 2005. *Análisis de amenazas del estuario de Virrilá*. [pdf] Lima: Asociación Perú Verde y Comité Holandés de la IUCN. Available at: <https://rsis.ramsar.org/RISapp/files/54275910/documents/PE2455_lit210522_6.pdf> [Accessed May 2024]

CIIFEN, 2020. *Actualización de la Información Climática en el Sector Agrario en Subcuencas Seleccionadas de las Regiones de Áncash, Cajamarca, y Piura. Producto 6. Informe final de la consultoría. Estimación del riesgo ante los efectos del cambio climático*. [pdf] Lima: Ministerio del Ambiente, Ministerio de Agricultura y Riego.

Córdova Elera, Y., 2020. *Análisis del comportamiento hidráulico-sedimentológico del río Piura, Tramo Presa los Ejidos- Sector Corillera, Perú. Problemática actual y propuestas de solución*. Master. Universitat Politècnica de València.

Di Liberto, T., 2017. *Heavy summer rains flood Peru*. [online] NOAA. Available at: <https://www.climate.gov/news-features/event-tracker/heavy-summer-rains-flood-peru> [Accessed November 2023]

Farías Zegada, M., 2008. *Hidrología e Hidráulica del Río Piura.* ITDSAC.

Farías Zegada, M., 2018. *Hidrología del Río Piura.* University of Piura, unpublished.

Fernández, T., et al., 2021. *Summary report of the full technical city profile Piura within the Morgenstadt Global Initiative*. [pdf] Available at: <https://mgi-iki.com/wp-content/uploads/2022/03/MGI-City-Lab-Piura-Summary-Report-EN_WEB-2.pdf> [Accessed January 2023]

GEO GPS Peru, n.d. *Descargar Imagenes ASTER GDEM*. Fuente NASA & METI. [online] Available at:

<https://www.geogpsperu.com/2018/08/descargar-imagenes-aster-gdem-aster.html> [Accessed February 2024]

Google Earth, 2024. Piura Region, various maps created, 5°33'18.19"S, 80°31'03.36"W [Accessed 2024]

Google Maps, 2023. [online] Available at: <https://www.google.com/maps/d/u/0/edit?mid=1HPcX5XR3AxjoWDABbz9J4zxG8T2zdDk&ll=-5.380871968575887%2C-79.49069643242406&z=8> [Accessed December 2023]

Guerrero, L., et al., 2015. *Changing in Morphodynamics of the Ephemeral Piura River due to ENSO*. The 9th Symoposium on River, Coastal and Estuarine Morphodynamics, RCEM 2015.

HEC, 2023. *HEC-RAS User's Manual.* v6.4.1. Exported October 2023. [pdf] US Army Corps of Engineers. Available at: <https://www.hec.usace.army.mil/software/hec-ras/documentation/HEC-RAS%20User's%20Manual-v6.4.1.pdf> [Accessed May 2024]

HEC, 2024a. *HEC-RAS Hydraulic Reference Manual.* v6.5. Exported March 2024. [pdf] US Army Corps of Engineers. Available at: <https://www.hec.usace.army.mil/software/hec-ras/documentation/HEC-RAS_Hydraulic_Reference_Manual_v6.5.pdf> [Accessed May 2024]

HEC, 2024b. *HEC-RAS River Analysis System. HEC-RAS Mapper User's Manual.* v6.5. Exported March 2024. [pdf] US Army Corps of Engineers. Available at: <https://www.hec.usace.army.mil/software/hec-ras/documentation/HEC-RAS_Hydraulic_Reference_Manual_v6.5.pdf> [Accessed June 2024]

Instituto Geofísico del Perú, 2023. *Índice Costero El Niño*. [online] Available at: <http://met.igp.gob.pe/datos/icen.txt> [Accessed December 2023]

Int. Engineering Company & Olazabal y Leon S.A, 1967. *Estudio de Planificacion aprovechamiento de agua de las cuencas Piura y Chira. Estudio de factibilidad valle de Chira desarrollado.* Tomo II. Anexos I a T. [pdf] Republica del Peru, Instituto Nacional de Planificacion y Ministerio de Fomento y Obras Públicas.

Lane, E. W., 1954. *The importance of fluvial morphology in hydraulic engineering*. Hydraulic Laboratory Report No. 372. [pdf] Denver, Colorado. Available at: <https://semspub.epa.gov/work/01/554355.pdf> [Accessed April 2024]

Larson, M., 2023. *Basic Sediment Transport and Boundary Layer Theory. Bed Load and Suspended Load, Sediment Transport Formulas*. Environmental Hydraulics VVRN40 Lectures 11&12. Lund University, unpublished.

Maza-Sócola, J., 2019. *Análisis del comportamiento hidráulico del Río Piura, en el tramo los Ejidos- Puente Independencia.* Master. Universidad de Piura.

MGI, n.d. *Piura, Peru- Extreme Climate Events and Long-Term Urban Planning*. [pdf] Available at: <https://mgi-iki.com/en/city/piura-peru/> [Accessed November 2023]

Moreano Segovia, J. F. & Yauri Quispe, H., 2008. *Estudio de Estimación de Riesgos Distrito de Morropón- Chulucanas. Proyecto Preparativos a Nivel Local Frente a Riesgos Asociados al Fenómeno "El Niño" en la Cuenca del Río Piura*. [pdf] SIREDECI & CRDC.

Nasa Worldview, 2017. Historic Map of April 5th, 2017, Piura Region. [online] NASA. Available at: <https://worldview.earthdata.nasa.gov/?v=-81.87993702967032,-6.248156849130042,-79.315429322922,-5.031351369521857&t=2017-04-05-T18%3A38%3A34Z> [Accessed May 2024]

NOAA, 2023a. *Cold & Warm Episodes by Season.* [online] Available at: <https://origin.cpc.ncep.noaa.gov/products/analysis_monitoring/ensostuff/ONI_v5.php> [Accessed December 2023]

NOAA, 2023b. *El Niño/Southern Oscillation (ENSO).* [online] Available at: <https://www.noaa.gov/jetstream/tropical/enso#:~:text=Sea%20surface%20temperatures%20are%20monitored,%C2%B0N%2D5%C2%B0S)> [Accessed October 2023]

NOAA, 2023c. *What are El Niño and La Niña?* [online] Available at: <https://oceanservice.noaa.gov/facts/ninonina.html#:~:text=than%20La%20Ni%C3%B1a.-,El%20Ni%C3%B1o,Pacific%20Ocean%20in%20the%201600s.> [Accessed October 2023]

Organización Panamericana de la Salud, 2018. *Fenómeno EL Niño- Región Piura, Perú.* [pdf] Lima: Organización Panamericana de la Salud. Available at: <https://iris.paho.org/bitstream/handle/10665.2/34889/OPSPER18005_spa.pdf?sequence=1&isAllowed=y> [Accessed October 2023]

PECHP, 2017. *Informe Diario Del Estado Hidrometeorológico*. Marzo 2017. [online] Available at: <https://servicios.regionpiura.gob.pe/datosh> [Accessed February 2024]

Peña Valdivia, 2021. *Zonificación del riesgo por inundación en el tramo urbano del río Piura en situaciones de FEN*. Master. Universidad de Piura.

Reyes Salazar, J. D., 2024b. *Análisis de la Agradación del Tramo Los Ejidos-Puente Independencia del Río Piura*. [pdf] University of Piura, unpublished.

Reyes Salazar, J., 2024a. *Clase en morfología fluvial y transporte de sedimentos*. Maestríá en Recursos Hídricos. Universidad de Piura, unpublished.

Reyes Salazar, J., 2024c. Discussion during excursion to urban area in Piura. (personal communication February 2024)

SENAMHI, 2014. *El Fenómeno El Niño en el Perú*. [pdf] Ministerio del Ambiente. Available at: <https://www.minam.gob.pe/wp-content/uploads/2014/07/Dossier-El-Ni%C3%B1o-Final_web.pdf> [Accessed October 2023].

The Only Guide Peru, n.d. *Peru Map- Regions*. [online] Available at: <https://www.theonlyperuguide.com/peru-travel-information/maps/peru-map-regions/> [Accessed November 2023]

UDEP & UNP, 2001a. *Estudio Para el Tratamiento Integral del Rio Piura, Proyecto PNUD*. Gobierno PER 98/018. CTAR Piura. Apéndice A: Comportamiento del río Piura durante el Fenómeno El Niño 98. [pdf] CEREN-PNUD.

UDEP & UNP, 2001b. *Estudio Para el Tratamiento Integral del Rio Piura, Proyecto PNUD*. Gobierno PER 98/018. CTAR Piura. Apéndice D: Hidrología. [pdf] CEREN-PNUD.

UDEP & UNP, 2001c. *Estudio Para el Tratamiento Integral del Rio Piura, Proyecto PNUD*. Gobierno PER 98/018. CTAR Piura. Apéndice E: Sedimentología. [pdf] CEREN-PNUD.

UDEP & UNP, 2001d. *Estudio Para el Tratamiento Integral del Rio Piura, Proyecto PNUD*. Gobierno PER 98/018. CTAR Piura. Apéndice H: Modelo Matemático de Flujo. [pdf] CEREN-PNUD.

UDEP & UNP, 2001e. *Estudio Para el Tratamiento Integral del Rio Piura, Proyecto PNUD.* Gobierno PER 98/018. CTAR Piura. Informe Final.[pdf] CEREN-PNUD

Welt Hunger Hilfe, n.d. *El Niño- The Origin & Impact of the Climate Pattern.* [online] Available at: <https://www.welthungerhilfe.org/our-work/focus-areas/climate-change/el-nino> [Accessed January 2024]

Zegarra Dávila, E. A., 2023. *La salida del Río Piura por su desembocadura original.* Foro: Las Obras Hidráulicas ante las Grandes Avenidas Conferencias Magistrales. Capítulo de Ingeniería Civil Comité de Obras Hidraulicas.

Zegarra Dávila, E. A., 2024. Discussion on alternative route towards Sechura. (personal communication February 2024)

Master Thesis
TVVR 24/5008

Appendix A

Field visits

Contents

Introduction to Field Visits

Field visits were conducted to gain perspective on the study area. Insight was gained on sediment types, vegetative coverage, riverine structures, as well as the state of protective structures. This appendix presents images taken during the excursions and summarizes comments and discussions held during the visits. Figure 1 shows the route the urban area covered, and Figure 2 shows the route through the rural area.

Figure 1- Overview map rural area (Google Earth, 2024)
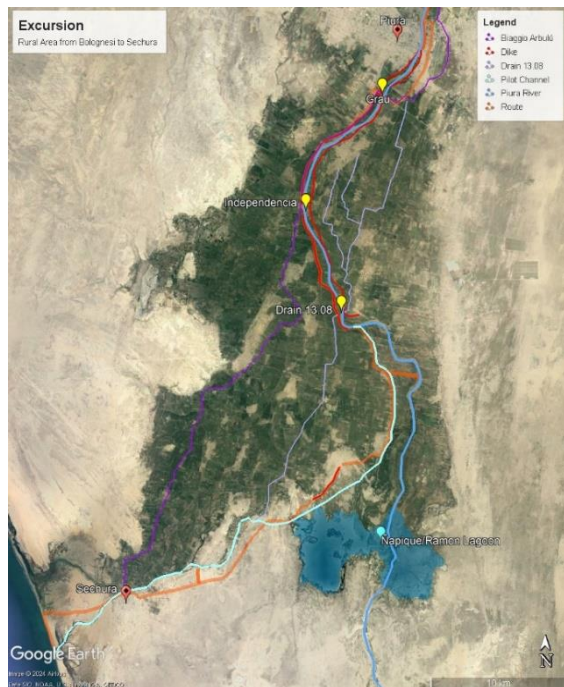
Figure 2- Overview map rural area (Google Earth, 2024)

Urban Area

Field visit: 07.02.2024

The first visit was conducted to the urban reach of the river. The field visit to the urban river reach was a part of the University of Piura`s master's program for Water Resources. The visit was led by Jorge Reyes Salazar, lecturer in hydraulics and sediment transport.

<u>Los Ejidos Dam</u>

The visit began at Los Ejidos Dam. Figure 3 shows the gated spillway on the right and the weir structure (which collapsed in the 80s) on the left. The Los Ejidos Dam is situated approximately 3km from Piura city center.

Figure 3- Los Ejidos Dam

Figure 4- Ramp into the floodplain at Los Ejidos

The floodplain just downstream of the dam shows some of the riverbed clearance works which have been conducted. Sediment accumulated at approximately 3m in height as shown in Figures 3 and 4. It has been/is in the process of being removed.

Figure 5- Sediment build up at Los Ejidos view from bottom

Figure 6- Sediment build up at Los Ejidos view from top

Sediment in the floodplain in this area was found to be mostly sandy, and also clayey/silty-sand closer to the riverbed as shown in the figures below.

Figure 7- Sandy sediment at Los Ejidos

Figure 8- Clayey sediment at Los Ejidos

The dam is fed by a channel from the Chira River which provides a steady flow of 60m3/s. On the day of the excursion, a low flow was observed, which may have been exclusively from the Chira River. The gauge at Los Ejidos indicating potential water levels which can be reached is shown in Figure 9.

Figure 9- Gauge at Los Ejidos

Starting at Los Ejidos, the river through the urban area is channeled by concrete banks as shown in Figure 10. The dry side of the bank is constructed of compacted sediment. However, local erosion can be seen which exists in different scales and often causes holes large enough to cause instability of the banks, as shown in Figure 11.

Figure 10- Concrete riverbank

Figure 11- Hole on 'dry side' of riverbank

Cáceres Bridge

The channel section at the Cáceres bridge is approximately 140m.

Figure 12- Cáceres Bridge

Some sedimentation and vegetative growth is visible at the left bank of the Cáceres bridge as shown below in the view downstream of the bridge in Figure 13.

Figure 13- View downstream of Cáceres Bridge

Sánchez Cerro Bridge

The channel section at the Sánchez Cerro Bridge is approximately 130m.

Figure 14- Sánchez Cerro Bridge

As was seen at the Cáceres Bridge, there is significant vegetative growth along the right bank as shown in Figure 15. A gauge was also found at this point of the river.

Figure 15- Below Sánchez Cerro Bridge

Figure 16- Gauge at Sánchez Cerro

Bolognesi Bridge

The channel section at the Bolognesi Bridge is approximately 150m.

Figure 17- Bolognesi Bridge

The Bolognesi Bridge marks the end of the Urban zone of the river. Similar to the other bridges, there is aggradation occurring close to the concrete banks with some vegetative growth as shown below in the upstream view of the bridge in Figure 18.

Figure 18- View upstream of Bolognesi Bridge

The gauge on the right bank is partially covered by sediments as shown in Figure 19.

Figure 19- Gauge at Bolognesi Bridge

Figure 20- Below Bolognesi Bridge

Rural Area & Exit through Sechura

Field Visit: 28.02.2024

<u>Biaggio Arbulú Channel</u>

The Biaggio Arbulú channel flows along the right side of the river in the rural area, it provides a steady supply of water for irrigation in the lower basin.

Figure 21- Biaggio Arbulú Channel

Figure 22- Biaggio Arbulú Channel

Figure 23- Biaggio Arbulú Channel

Independencia

The Indpenendencia bridge has a width of approximately 360m.

Figure 24- Independencia Bridge

On the bridge, there is a lot of sandy sediment which has been deposited by the wind. Following the riverbanks comes there is vegetation as shown in Figure 25.

Figure 25- Eolian Sediment on Bridge

Figure 26- View upstream of Bolognesi

Figure 27- Downstream of Bolognesi

Figure 28- Old station point

Between Independencia and Drain 13.08

Figures 29 and 30 show farmland inside the flood plain. There are small irrigation channels along the dikes.

Figure 29- Farmland

Figure 30- Farmland

Drain 13.08

The drain 13.08 drains water from Castilla. The sediment around the river in this section is very clayey as shown in Figure 32.

Figure 31- Drain 13.08 on right side of river
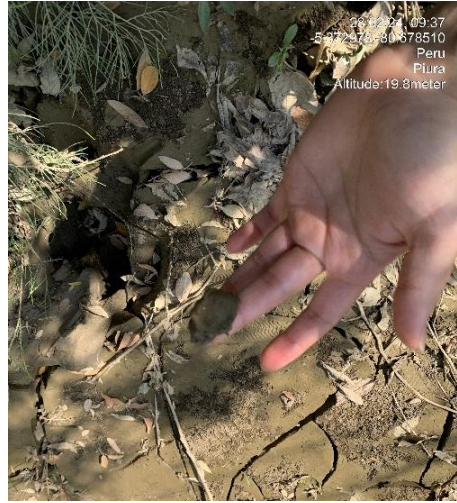
Figure 32- Clayey sediment at Drain 13.08

The drain crosses the Piura River in a pipeline. The location of the pipeline is visible across the Piura River. This may be due to erosion in this section of the river. As shown in Figure 34 many rows of the river defense have been revealed due to transport of sediment. This may put the pipeline in risk of failure.

Figure 33- Drain 13.08 crossing through Piura River

Figure 34- Erosion close to Drain 13.08

This section is just upstream of the lagoon system.

Figure 35- Just upstream of Ramon Lagoon

The banks are very sandy. Some clayey sediments are also present again. The deposition in this area is evident as seen by this dried sediment with a thickness of approximately 15cm as shown in Figure 37.

Figure 36- Sandy riverbank

Figure 37- Clayey sediment deposit

The vegetation up to this point just inside of the dikes is very dense in some stretches. Following this section the pilot channel changes course towards Sechura.

Figure 38- Dense vegetation

Old dikes along the lagoons

The lagoon system is protected by dikes. These feature a very steep slope of 1:1 and are made of large stones. However, this may be deemed unnecessary for the current system since the flow in this section is less aggressive.

Figure 39- Old dikes along Lagoon

The location where the river used to pass towards Sechura is shown in Figures 40 and 41 where Figure 40 is inside of the dike and Figure 41 is outside towards Sechura. The two sides are separated by the dike structure shown in Figure 42 and could be easily reconnected.

Figure 40- Upstream of dike, in Lagoon
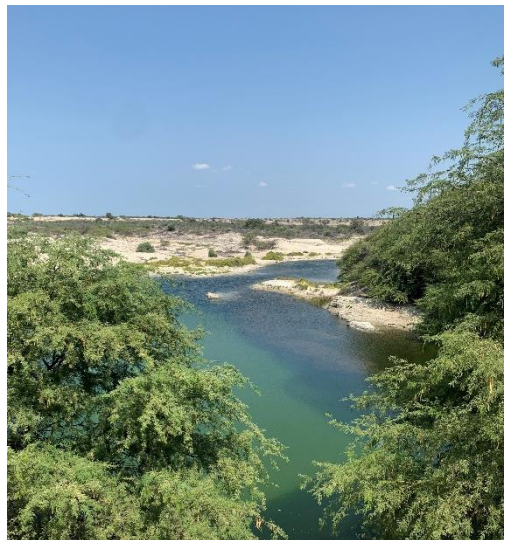
Figure 41- Downstream of dike, outside of the Lagoon

Figure 42- Dike bordering Lagoon

Terrain from Lagoon to Río Loco

The terrain to cross from the lagoon system to the old river course is desert-like with sparse vegetation and some salt plains.

Figure 43- Desert terrain
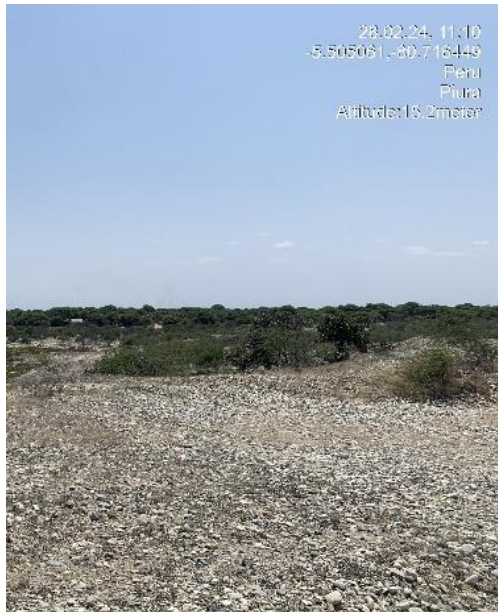
Figure 44- Desert terrain

Figure 45- Salt plain

Río Loco

The old river course is called Río Loco and is currently fed by agricultural discharge and by Drain 13.08. This section of the river is influenced by tidal activity as visible in Figure 47 where around 20cm of sediment is moist.

Figure 46- Río Loco

Figure 47- Tidal influence at Río Loco

Sechura

Río Loco passes through Sechura. The Sechura bridge is shown in Figure 48.

Figure 48- Sechura Bridge

Figure 49- Downstream view at Sechura Bridge

Figure 50- Upstream view at Sechura Bridge

Chulliyache

Río Loco currently discharges into the Pacific Ocean through three branches. The pilot channel is designed to exit through Chulliyache.

Figure 51- River exit at Chulliyache

Figure 52- Chulliyache sign

Figure 53- Upstream view at exit

Master Thesis

TVVR 24/5008

Appendix B

Geometry Data for Virrilá and Sechura

Contents

Table 1- Geometry data for Virrilá

Station	Reach Length	Manning			Bottom Level
		LOB	Channel	ROB	
117307	717.1	0.018	0.028	0.018	24
116590	615.3	0.018	0.028	0.018	23
115975	593	0.018	0.028	0.018	23
115382	501.1	0.018	0.028	0.018	22
114881	479.5	0.018	0.028	0.018	23
114401	504.6	0.018	0.028	0.018	22
113897	459.4	0.018	0.028	0.018	22
113437	506.8	0.02	0.03	0.02	22
112930	504.1	0.02	0.033	0.02	22
112426	472.6	0.025	0.025	0.025	22
111954	478.5	0.025	0.025	0.025	22
111475	573.5	0.025	0.025	0.025	21
110902	560.5	0.025	0.025	0.025	21
110341	538.3	0.025	0.025	0.025	21
109803	524.1	0.025	0.025	0.025	21
109279	568.2	0.025	0.025	0.025	20
108711	759.3	0.025	0.025	0.025	21
107951	584.3	0.03	0.025	0.03	20
107367	517	0.03	0.025	0.03	19
106850	532.5	0.03	0.025	0.03	19
106318	560.9	0.03	0.025	0.03	19
105757	452.1	0.03	0.025	0.03	18
105305	454.3	0.03	0.022	0.03	18
104850	499.6	0.03	0.022	0.03	18
104351	457.2	0.03	0.022	0.03	18
103894	477.4	0.03	0.022	0.03	18
103416	499.2	0.03	0.022	0.03	18
102917	520.5	0.03	0.022	0.03	18
102397	662.8	0.03	0.022	0.03	18
101734	552.2	0.035	0.025	0.035	19
101182	640.9	0.035	0.025	0.035	18
100541	512.3	0.035	0.025	0.035	19
100028	589.7	0.035	0.025	0.035	18
99439	642.5	0.035	0.025	0.035	18
98796	544.8	0.035	0.025	0.035	18
98251	601.1	0.05	0.025	0.05	18
97650	731.3	0.05	0.025	0.05	17
96919	593.3	0.05	0.025	0.05	18
96326	697.7	0.05	0.025	0.05	17
95628	697.8	0.05	0.025	0.05	17
94930	696.1	0.05	0.025	0.05	16
94234	675.4	0.035	0.025	0.035	16
93559	729.9	0.035	0.025	0.035	16
92829	647.6	0.035	0.025	0.035	16

92181	578.8	0.035	0.025	0.035	16
91602	816.9	0.03	0.025	0.03	15
90785	565.5	0.03	0.025	0.03	15
90220	809.2	0.03	0.025	0.03	15
89411	790.2	0.03	0.025	0.03	15
88621	844.2	0.03	0.025	0.03	14
87776	707.2	0.03	0.025	0.03	14
87069	595.9	0.035	0.025	0.035	14
86473	902.7	0.035	0.025	0.035	14
85571	808.7	0.035	0.025	0.035	14
84762	1008.5	0.035	0.025	0.035	13
83753	739.6	0.04	0.025	0.04	13
83014	884.6	0.04	0.025	0.04	13
82129	1157.9	0.06	0.025	0.06	13
80971	1373.1	0.06	0.025	0.06	12
79598	939.5	0.06	0.025	0.06	12
78659	930.1	0.08	0.025	0.08	12
77729	1032	0.08	0.025	0.08	11
76697	1008.3	0.08	0.025	0.08	11
75688	1011.7	0.08	0.025	0.08	11
74677	1169.8	0.08	0.025	0.08	9
73507	1411.3	0.06	0.025	0.05	10
72096	1495.1	0.06	0.025	0.05	10
70600	1601.5	0.06	0.025	0.05	9
68999	3663.3	0.06	0.025	0.06	8
65336	3278.7	0.04	0.025	0.04	7.63
62057	2885.9	0.04	0.025	0.04	7.88
59171	4721.9	0.04	0.025	0.04	7
54449	4227.9	0.04	0.025	0.04	6.42
50221	4817.7	0.035	0.025	0.035	5.53
45403	4526.9	0.035	0.025	0.035	5.38
40877	4827.1	0.035	0.025	0.035	5.18
36050	4658.9	0.035	0.025	0.035	4.37
31391	5752	0.03	0.025	0.03	4.23
25639	4796.9	0.03	0.025	0.03	3.6
20842	4734.8	0.03	0.025	0.03	2.7
16107	5235.8	0.03	0.025	0.03	1.66
10871	3835.8	0.03	0.025	0.03	0.71
7035	2454.9	0.03	0.025	0.03	-0.13
4580	3011.9	0.03	0.025	0.03	-0.64
1568		0.03	0.025	0.03	-1.17

Table 2- Geometry data for Sechura

Station	Reach Length	Manning			Bottom Level
		LOB	Channel	ROB	
71617	717.1	0.018	0.028	0.018	24
70900	615.3	0.018	0.028	0.018	23
70284	593	0.018	0.028	0.018	23
69691	501.1	0.018	0.028	0.018	22
69190	479.5	0.018	0.028	0.018	23
68711	504.6	0.018	0.028	0.018	22
68206	459.4	0.018	0.028	0.018	22
67747	506.8	0.02	0.03	0.02	22
67240	504.1	0.02	0.033	0.02	22
66736	472.6	0.025	0.025	0.025	22
66263	478.5	0.025	0.025	0.025	22
65785	573.5	0.025	0.025	0.025	21
65211	560.5	0.025	0.025	0.025	21
64651	538.3	0.025	0.025	0.025	21
64112	524.1	0.025	0.025	0.025	21
63588	568.2	0.025	0.025	0.025	20
63020	759.3	0.025	0.025	0.025	21
62261	584.3	0.03	0.025	0.03	20
61677	517	0.03	0.025	0.03	19
61160	532.5	0.03	0.025	0.03	19
60627	560.9	0.03	0.025	0.03	19
60066	452.1	0.03	0.025	0.03	18
59614	454.3	0.03	0.022	0.03	18
59160	499.6	0.03	0.022	0.03	18
58660	457.2	0.03	0.022	0.03	18
58203	477.4	0.03	0.022	0.03	18
57726	499.2	0.03	0.022	0.03	18
57226	520.5	0.03	0.022	0.03	18
56706	662.8	0.03	0.022	0.03	18
56043	552.2	0.035	0.025	0.035	19
55491	640.9	0.035	0.025	0.035	18
54850	512.3	0.035	0.025	0.035	19
54338	589.7	0.035	0.025	0.035	18
53748	642.5	0.035	0.025	0.035	18
53105	544.8	0.035	0.025	0.035	18
52561	601.1	0.05	0.025	0.05	18
51960	731.3	0.05	0.025	0.05	17
51228	593.3	0.05	0.025	0.05	18
50635	697.7	0.05	0.025	0.05	17
49937	697.8	0.05	0.025	0.05	17
49240	696.1	0.05	0.025	0.05	16
48543	675.4	0.035	0.025	0.035	16
47868	729.9	0.035	0.025	0.035	16
47138	647.6	0.035	0.025	0.035	16

46490	578.8	0.035	0.025	0.035	16
45912	816.9	0.03	0.025	0.03	15
45095	565.5	0.03	0.025	0.03	15
44529	809.2	0.03	0.025	0.03	15
43720	790.2	0.03	0.025	0.03	15
42930	844.2	0.03	0.025	0.03	14
42086	729.9	0.03	0.025	0.03	14
41356	508.4	0.035	0.025	0.035	14
40847	568.9	0.035	0.025	0.035	13.9
40279	646.8	0.035	0.025	0.035	13.78
39632	1028.4	0.035	0.025	0.035	13.66
38603	818.7	0.04	0.025	0.04	13.45
37785	677.6	0.04	0.025	0.04	13.29
37107	464.3	0.06	0.025	0.06	13.15
36643	439.3	0.06	0.025	0.06	13.06
36204	570.5	0.06	0.025	0.06	12.97
35633	845.2	0.08	0.025	0.08	12.86
34788	956.7	0.08	0.025	0.08	12.52
33831	926.5	0.08	0.025	0.08	12.1
32905	883.9	0.08	0.025	0.08	11.76
32021	1114.8	0.08	0.025	0.08	11.41
30906	1061.5	0.06	0.025	0.05	10.96
29844	1083.2	0.06	0.025	0.05	10.54
28761	1350.5	0.06	0.025	0.05	10
27411	1441.8	0.06	0.025	0.06	9.57
25969	2458.7	0.03	0.025	0.03	8.5
23510	2141.1	0.03	0.025	0.03	7.51
21369	1555.9	0.03	0.025	0.03	6.23
19813	1188.9	0.025	0.025	0.025	5.4
18624	2493.6	0.025	0.025	0.025	4.8
16131	1852.2	0.025	0.025	0.025	4.1
14279	1896.7	0.025	0.025	0.025	3.5
12382	1559.5	0.025	0.025	0.025	2.9
10822	1908.2	0.025	0.025	0.025	2.5
8914	1858.6	0.025	0.025	0.025	1.9
7056	2501.6	0.025	0.025	0.025	1.3
4554	2683.7	0.025	0.025	0.025	0.6
1870		0.025	0.025	0.025	0.08

Table 3- Reference point cross sections

Refence Point	Route Virrilá	Route Sechura
Cáceres Bridge	114881	61190
Sánchez Cerro Bridge	113897	68711
Bolognesi Bridge	112930	67240
Grau Bridge	108711	63020
Independencia Bridge	97650	51960
Drain 13.08	89411	43720
Start Ñapique/Ramon	68999	25969
End Ñapique/Ramon	62057	23510
Start La Niña	54449	-
End La Niña	31391	-
Virrilá Estuary	25639	-

Note: listed cross sections are closest upstream section to the reference point and are not exactly at the reference point.

Appendix C

Output and Calculated Results

Contents

Critical Shear Stress

The parameters in Table 1 are assumed to calculate critical shear stress using Equations 1-3

$$(1) \quad \theta_{cr} = \frac{0.3}{1+1.2D_*} + 0.055(1 - exp(-0.02D_*))$$

$$(2) \quad D_* = (\frac{g(s-1)}{v^2})^{1/3} * d_{50}$$

$$(3) \quad \theta_{cr} = \frac{\tau_{cr}}{\rho g(s-1)d_{50}}$$

Table 1- Critical shear stress parameters

Parameter	Value	Unit	Note
Sediment			
ρs	2600	kg/m^3	UDEP & UNP 2001c
d50	0.0002	m	UDEP & UNP 2001c
Water			
ρw	997	Kg/m^3	at 25°C
υ	0.893*10^{-6}	m^2/s	at 25°C
S		-	ρs/ρw
General			
ƙ	0.4	-	Karmann
g	9.81	m/s^2	Gravity

Critical shear stress is found to be **τcr=0.144 N/m²**

Drag Law Shear Stress

Shear stress is calculated using Equations 4-7 assuming a rough bed condition.

$$(4) \quad \tau_b = \rho C_D U^2$$

$$(5) \quad C_D = \frac{ƙ}{1+ln(\frac{z_0}{h})}^2$$

$$(6) \quad z_0 = \frac{k_s}{30}$$

$$(7) \quad k_s = 2.5 * d_{50}$$

The following tables give output result and calculation results for Q=1,000m³/s and Q=3,200m³/s for Virrilá and Sechura.

Output and Calculation

Table 2- Output and results for Virrilá

	General Output			Drag Law Calculation					Bed Load Calculation			HEC Output			Bed Load Calculation		
Station	Q Total (m3/s)	Hyd Depth (m)	Vel tot (m/s)	z0/h	Cf	tb (N/m2)	tb><cr	(tb-tcr)^3/2	Θb	8*(Θb-Θcr)^3/2	qsb (kg/ms)	Shear Tot (N/m2)	tb><cr	(tb-tcr)^3/2	Θb	8*(Θb-Θcr)^3/2	qsb (kg/ms)
1568	1000	2.26	0.83	7.37E-06	0.00137	0.94	erosion	0.71	0.226	0.857	9.63E-06	3.21	erosion	5.37	1.707	17.845	2.00E-04
4580	1000	2.01	0.58	8.29E-06	0.00140	0.47	erosion	0.19	0.059	0.114	1.28E-06	1.63	erosion	1.81	0.576	3.499	3.93E-05
7035	1000	1.82	0.93	9.16E-06	0.00142	1.23	erosion	1.13	0.359	1.720	1.93E-05	4.36	erosion	8.66	2.753	36.537	4.10E-04
10871	1000	1.61	0.67	1.04E-05	0.00146	0.65	erosion	0.36	0.115	0.313	3.52E-06	2.32	erosion	3.21	1.021	8.251	9.27E-05
16107	1000	1.39	0.42	1.20E-05	0.00150	0.26	erosion	0.04	0.013	0.012	1.36E-07	0.95	erosion	0.72	0.230	0.884	9.93E-06
20842	1000	1.04	0.86	1.60E-05	0.00159	1.17	erosion	1.04	0.331	1.521	1.71E-05	4.5	erosion	9.09	2.891	39.324	4.42E-04
25639	1000	1.07	1.19	1.56E-05	0.00158	2.23	erosion	3.01	0.957	7.485	8.41E-05	6.44	erosion	15.80	5.023	90.071	1.01E-03
31391	1000	1.25	0.34	1.33E-05	0.00153	0.18	erosion	0.01	0.002	0.001	7.31E-09	0.64	erosion	0.35	0.111	0.297	3.33E-06
36050	1000	1.53	0.14	1.09E-05	0.00147	0.03	stable	0.00	0.000	0.000	0.00E+00	0.13	stable	0.00	0.000	0.000	0.00E+00
40877	1000	1.26	0.15	1.32E-05	0.00153	0.03	stable	0.00	0.000	0.000	0.00E+00	0.19	erosion	0.01	0.003	0.001	1.60E-08
45403	1000	1.25	0.2	1.33E-05	0.00153	0.06	stable	0.00	0.000	0.000	0.00E+00	0.31	erosion	0.07	0.022	0.025	2.85E-07
50221	1000	1.17	0.12	1.42E-05	0.00155	0.02	stable	0.00	0.000	0.000	0.00E+00	0.11	stable	0.00	0.000	0.000	0.00E+00
54449	1000	0.83	0.29	2.01E-05	0.00166	0.14	stable	0.00	0.000	0.000	0.00E+00	0.87	erosion	0.62	0.197	0.698	7.85E-06
59171	1000	1.15	0.79	1.45E-05	0.00156	0.97	erosion	0.75	0.238	0.928	1.04E-05	3.43	erosion	5.96	1.894	20.856	2.34E-04
62057	1000	1.39	0.96	1.20E-05	0.00150	1.38	erosion	1.37	0.436	2.300	2.58E-05	8.39	erosion	23.68	7.529	165.282	1.86E-03
65336	1000	1.56	0.14	1.07E-05	0.00147	0.03	stable	0.00	0.000	0.000	0.00E+00	0.19	erosion	0.01	0.003	0.001	1.60E-08
68999	1000	1.01	0.21	1.65E-05	0.00160	0.07	stable	0.00	0.000	0.000	0.00E+00	1.19	erosion	1.07	0.340	1.588	1.78E-05
70600	1000	0.64	0.29	2.60E-05	0.00175	0.15	erosion	0.00	0.000	0.000	3.98E-11	1.63	erosion	1.81	0.576	3.499	3.93E-05
72096	1000	0.92	0.61	1.81E-05	0.00163	0.60	erosion	0.31	0.099	0.250	2.80E-06	8.11	erosion	22.48	7.149	152.922	1.72E-03
73507	1000	0.5	0.39	3.33E-05	0.00185	0.28	erosion	0.05	0.016	0.016	1.82E-07	4.24	erosion	8.29	2.636	34.239	3.85E-04
74677	1000	0.7	0.32	2.38E-05	0.00172	0.18	erosion	0.01	0.002	0.001	6.92E-09	5.76	erosion	13.31	4.232	69.647	7.82E-04
75688	1000	1.14	0.25	1.46E-05	0.00156	0.10	stable	0.00	0.000	0.000	0.00E+00	2.57	erosion	3.78	1.202	10.538	1.18E-04
76697	1000	1.11	0.51	1.50E-05	0.00157	0.41	erosion	0.13	0.043	0.071	7.95E-07	8.64	erosion	24.77	7.874	176.770	1.99E-03
77729	1000	0.89	0.43	1.87E-05	0.00164	0.30	erosion	0.06	0.020	0.023	2.54E-07	5.24	erosion	11.50	3.658	55.971	6.29E-04
78659	1000	0.83	0.38	2.01E-05	0.00166	0.24	erosion	0.03	0.009	0.007	8.14E-08	3.46	erosion	6.04	1.920	21.287	2.39E-04
79598	1000	0.83	0.35	2.01E-05	0.00166	0.20	erosion	0.01	0.005	0.002	2.78E-08	3.12	erosion	5.13	1.633	16.688	1.87E-04
80971	1000	1.08	0.29	1.54E-05	0.00157	0.13	stable	0.00	0.000	0.000	0.00E+00	1.99	erosion	2.51	0.798	5.699	6.40E-05
82129	1000	0.56	0.47	2.98E-05	0.00180	0.40	erosion	0.13	0.041	0.065	7.33E-07	3.9	erosion	7.28	2.315	28.174	3.16E-04
83014	1000	0.83	0.39	2.01E-05	0.00166	0.25	erosion	0.04	0.011	0.010	1.08E-07	1.63	erosion	1.81	0.576	3.499	3.93E-05
83753	1000	1.21	0.73	1.38E-05	0.00154	0.82	erosion	0.55	0.176	0.591	6.64E-06	4.27	erosion	8.38	2.665	34.806	3.91E-04
84762	1000	0.7	1.09	2.38E-05	0.00172	2.04	erosion	2.61	0.828	6.032	6.78E-05	4.47	erosion	9.00	2.861	38.717	4.35E-04
85571	1000	1.25	0.71	1.33E-05	0.00153	0.77	erosion	0.49	0.157	0.499	5.60E-06	3.05	erosion	4.95	1.575	15.818	1.78E-04
86473	1000	1.44	1.07	1.16E-05	0.00149	1.70	erosion	1.94	0.617	3.877	4.35E-05	6.64	erosion	16.56	5.265	96.636	1.09E-03
87069	1000	0.9	1.42	1.85E-05	0.00163	3.28	erosion	5.56	1.769	18.829	2.12E-04	6.63	erosion	16.52	5.252	96.302	1.08E-03
87776	1000	1.2	1.03	1.39E-05	0.00154	1.63	erosion	1.81	0.577	3.507	3.94E-05	3.5	erosion	6.15	1.955	21.869	2.46E-04
88621	1000	1.98	1.25	8.42E-06	0.00140	2.18	erosion	2.91	0.926	7.129	8.01E-05	5.87	erosion	13.70	4.357	72.754	8.17E-04
89411	1000	1.34	1.17	1.24E-05	0.00151	2.06	erosion	2.65	0.844	6.200	6.96E-05	4.3	erosion	8.47	2.694	35.378	3.97E-04
90220	1000	1.72	0.9	9.69E-06	0.00144	1.16	erosion	1.03	0.327	1.494	1.68E-05	3.34	erosion	5.71	1.817	19.593	2.20E-04

90785	1000	1.51	1.57	1.10E-05	0.00148	3.63	erosion	6.50	2.066	23.751	2.67E-04	6.66	erosion	16.63	5.289	97.307	1.09E-03
91602	1000	1.8	0.88	9.26E-06	0.00143	1.05	erosion	0.87	0.275	1.155	1.30E-05	3.23	erosion	5.42	1.724	18.108	2.03E-04
92181	1000	1.39	1.01	1.20E-05	0.00150	1.52	erosion	1.62	0.516	2.965	3.33E-05	5.48	erosion	12.33	3.919	62.077	6.97E-04
92829	1000	1.18	1.02	1.41E-05	0.00155	1.61	erosion	1.77	0.562	3.369	3.78E-05	5.52	erosion	12.47	3.964	63.129	7.09E-04
93559	1000	1.28	1.09	1.30E-05	0.00152	1.80	erosion	2.14	0.680	4.490	5.04E-05	5.21	erosion	11.40	3.626	55.233	6.20E-04
94234	1000	1.49	1.11	1.12E-05	0.00148	1.82	erosion	2.16	0.688	4.567	5.13E-05	5.18	erosion	11.30	3.594	54.500	6.12E-04
94930	1000	1.75	1.15	9.52E-06	0.00143	1.89	erosion	2.31	0.735	5.036	5.66E-05	5.76	erosion	13.31	4.232	69.647	7.82E-04
95628	1000	1.45	1.39	1.15E-05	0.00149	2.86	erosion	4.49	1.427	13.632	1.53E-04	8.81	erosion	25.51	8.112	184.828	2.08E-03
96326	1000	1.87	1.37	8.91E-06	0.00142	2.65	erosion	3.97	1.262	11.343	1.27E-04	7.77	erosion	21.06	6.696	138.627	1.56E-03
96919	1000	2.17	0.95	7.68E-06	0.00138	1.24	erosion	1.15	0.365	1.762	1.98E-05	2.89	erosion	4.55	1.447	13.926	1.56E-04
97650	1000	2.35	0.74	7.09E-06	0.00136	0.74	erosion	0.46	0.147	0.450	5.06E-06	2.11	erosion	2.76	0.877	6.567	7.38E-05
98251	1000	2.19	0.64	7.61E-06	0.00138	0.56	erosion	0.27	0.086	0.201	2.26E-06	2.16	erosion	2.86	0.910	6.949	7.81E-05
98796	1000	1.55	0.81	1.08E-05	0.00147	0.96	erosion	0.74	0.235	0.909	1.02E-05	3.04	erosion	4.93	1.567	15.696	1.76E-04
99439	1000	1.68	0.95	9.92E-06	0.00145	1.30	erosion	1.24	0.396	1.991	2.24E-05	3.65	erosion	6.57	2.088	24.130	2.71E-04
100028	1000	1.78	0.99	9.36E-06	0.00143	1.40	erosion	1.40	0.446	2.384	2.68E-05	4.35	erosion	8.63	2.743	36.343	4.08E-04
100541	1000	1.64	1.31	1.02E-05	0.00145	2.48	erosion	3.58	1.139	9.721	1.09E-04	8.73	erosion	25.16	8.000	181.011	2.03E-03
101182	1000	1.98	1.33	8.42E-06	0.00140	2.47	erosion	3.55	1.129	9.600	1.08E-04	6.38	erosion	15.57	4.952	88.151	9.90E-04
101734	1000	1.08	1.96	1.54E-05	0.00157	6.03	erosion	14.29	4.544	77.478	8.70E-04	7.94	erosion	21.77	6.922	145.677	1.64E-03
102397	1000	1.86	1.14	8.96E-06	0.00142	1.84	erosion	2.20	0.701	4.693	5.27E-05	2.88	erosion	4.53	1.439	13.812	1.55E-04
102917	1000	1.78	1.34	9.36E-06	0.00143	2.56	erosion	3.75	1.194	10.436	1.17E-04	4.59	erosion	9.38	2.981	41.175	4.63E-04
103416	1000	1.78	1.46	9.36E-06	0.00143	3.04	erosion	4.93	1.566	15.677	1.76E-04	4.97	erosion	10.60	3.371	49.519	5.56E-04
103894	1000	1.97	1.45	8.46E-06	0.00140	2.94	erosion	4.68	1.487	14.507	1.63E-04	4.98	erosion	10.64	3.382	49.750	5.59E-04
104351	1000	1.95	1.38	8.55E-06	0.00141	2.67	erosion	4.01	1.276	11.524	1.29E-04	4.19	erosion	8.14	2.588	33.306	3.74E-04
104850	1000	1.31	1.71	1.27E-05	0.00152	4.42	erosion	8.85	2.812	37.731	4.24E-04	3.73	erosion	6.79	2.159	25.386	2.85E-04
105305	1000	1.78	1.69	9.36E-06	0.00143	4.07	erosion	7.78	2.475	31.146	3.50E-04	4.94	erosion	10.50	3.340	48.829	5.49E-04
105757	1000	1.22	2.2	1.37E-05	0.00154	7.42	erosion	19.63	6.240	124.705	1.40E-03	6.3	erosion	15.27	4.857	85.627	9.62E-04
106318	1000	2.04	1.94	8.17E-06	0.00139	5.23	erosion	11.47	3.646	55.703	6.26E-04	9.76	erosion	29.82	9.482	233.566	2.62E-03
106850	1000	2.22	1.43	7.51E-06	0.00137	2.80	erosion	4.32	1.374	12.886	1.45E-04	6.8	erosion	17.17	5.460	102.074	1.15E-03
107367	1000	1.7	1.6	9.80E-06	0.00144	3.68	erosion	6.65	2.115	24.613	2.76E-04	4.83	erosion	10.14	3.226	46.346	5.21E-04
107951	1000	2.8	2.07	5.95E-06	0.00131	5.62	erosion	12.80	4.071	65.708	7.38E-04	12.41	erosion	42.96	13.660	403.875	4.54E-03
108711	1000	2.65	1.72	6.29E-06	0.00133	3.92	erosion	7.33	2.330	28.459	3.20E-04	10.41	erosion	32.89	10.459	270.597	3.04E-03
109279	1000	2	1.36	8.33E-06	0.00140	2.58	erosion	3.80	1.209	10.630	1.19E-04	5.44	erosion	12.19	3.875	61.035	6.86E-04
109803	1000	1.65	1.33	1.01E-05	0.00145	2.56	erosion	3.75	1.193	10.421	1.17E-04	3.91	erosion	7.31	2.324	28.343	3.18E-04
110341	1000	1.55	1.2	1.08E-05	0.00147	2.11	erosion	2.75	0.875	6.547	7.35E-05	4.09	erosion	7.84	2.493	31.483	3.54E-04
110902	1000	1.53	1.54	1.09E-05	0.00147	3.48	erosion	6.09	1.937	21.568	2.42E-04	5.85	erosion	13.63	4.334	72.184	8.11E-04
111475	1000	1.75	1.74	9.52E-06	0.00143	4.33	erosion	8.56	2.723	35.947	4.04E-04	6.36	erosion	15.50	4.928	87.516	9.83E-04
111954	1000	2.51	1.74	6.64E-06	0.00134	4.05	erosion	7.72	2.453	30.740	3.45E-04	9.45	erosion	28.39	9.027	216.965	2.44E-03
112426	1000	3.74	1.53	4.46E-06	0.00125	2.91	erosion	4.61	1.466	14.195	1.59E-04	7.54	erosion	20.12	6.396	129.397	1.45E-03
112930	1000	3.9	2.13	4.27E-06	0.00124	5.61	erosion	12.76	4.058	65.399	7.35E-04	23.61	erosion	113.68	36.144	1738.368	1.95E-02
113437	1000	3.73	2.25	4.47E-06	0.00125	6.30	erosion	15.29	4.861	85.746	9.63E-04	24.71	erosion	121.76	38.715	1927.106	2.16E-02
113897	1000	3.92	2.34	4.25E-06	0.00124	6.76	erosion	17.01	5.410	100.655	1.13E-03	24.65	erosion	121.32	38.573	1916.533	2.15E-02
114401	1000	4.56	2.39	3.65E-06	0.00121	6.87	erosion	17.43	5.543	104.391	1.17E-03	23.48	erosion	112.73	35.844	1716.775	1.93E-02
114881	1000	4.05	1.82	4.12E-06	0.00123	4.07	erosion	7.77	2.469	31.040	3.49E-04	12.76	erosion	44.81	14.248	430.267	4.83E-03
115382	1000	4.48	2.44	3.72E-06	0.00121	7.18	erosion	18.66	5.933	115.622	1.30E-03	22.11	erosion	102.95	32.734	1498.285	1.68E-02
115975	1000	3.96	1.69	4.21E-06	0.00124	3.52	erosion	6.20	1.972	22.150	2.49E-04	11.07	erosion	36.12	11.484	311.319	3.50E-03
116590	1000	4.48	1.22	3.72E-06	0.00121	1.79	erosion	2.12	0.675	4.432	4.98E-05	5.93	erosion	13.92	4.426	74.481	8.37E-04
117307	1000	3.98	1.1	4.19E-06	0.00123	1.49	erosion	1.56	0.496	2.798	3.14E-05	5.71	erosion	13.13	4.176	68.260	7.67E-04
1568	3200	2.26	2.65	7.37E-06	0.00137	9.57	erosion	28.36	9.207	223.480	2.51E-03	32.84	erosion	186.96	59.445	3666.597	4.12E-02
4580	3200	3.03	1.14	5.50E-06	0.00130	1.68	erosion	1.90	0.605	3.765	4.23E-05	5.54	erosion	12.54	3.986	63.659	7.15E-04
7035	3200	3.17	1.63	5.26E-06	0.00129	3.41	erosion	5.89	1.873	20.508	2.30E-04	11.14	erosion	36.46	11.594	315.825	3.55E-03

C1	C2	C3	C4	C5	C6	C7	C8	C9	C10	C11	C12	C13	C14	C15	C16	C17	C18
4.28E-04	38.116	2.831	8.91	erosion	4.44	2.52E-05	2.247	0.429	1.35	erosion	1.36	0.00129	5.36E-06	1.03	3.11	3200	10871
3.31E-05	2.943	0.513	1.61	erosion	1.52	1.11E-06	0.099	0.053	0.17	erosion	0.45	0.00134	6.51E-06	0.58	2.56	3200	16107
5.18E-04	46.123	3.215	10.11	erosion	4.82	3.73E-05	3.324	0.557	1.75	erosion	1.60	0.00140	8.33E-06	1.07	2	3200	20842
5.38E-03	479.310	15.311	48.16	erosion	13.38	3.52E-04	31.292	2.483	7.81	erosion	4.08	0.00148	1.14E-05	1.66	1.46	3200	25639
2.28E-05	2.028	0.400	1.26	erosion	1.31	4.96E-07	0.044	0.031	0.10	erosion	0.36	0.00138	7.61E-06	0.51	2.19	3200	31391
3.25E-07	0.029	0.024	0.07	erosion	0.32	0.00E+00	0.000	0.000	0.00	stable	0.07	0.00136	7.06E-06	0.22	2.36	3200	36050
2.47E-07	0.022	0.020	0.06	erosion	0.3	0.00E+00	0.000	0.000	0.00	stable	0.05	0.00142	8.96E-06	0.19	1.86	3200	40877
1.68E-06	0.150	0.070	0.22	erosion	0.51	0.00E+00	0.000	0.000	0.00	stable	0.10	0.00141	8.59E-06	0.27	1.94	3200	45403
4.49E-09	0.000	0.001	0.00	erosion	0.17	0.00E+00	0.000	0.000	0.00	stable	0.14	0.00138	7.75E-06	0.16	2.15	3200	50221
7.61E-06	0.677	0.193	0.61	erosion	0.86	0.00E+00	0.000	0.000	0.00	stable	0.47	0.00145	1.02E-05	0.31	1.64	3200	54449
1.54E-03	136.996	6.644	20.90	erosion	7.73	8.89E-05	7.915	0.993	3.12	erosion	2.28	0.00142	8.96E-06	1.27	1.86	3200	59171
6.60E-03	587.213	17.531	55.14	erosion	14.63	1.52E-04	13.563	1.422	4.47	erosion	2.86	0.00138	7.82E-06	1.44	2.13	3200	62057
4.13E-07	0.037	0.028	0.09	erosion	0.34	0.00E+00	0.000	0.000	0.00	erosion	0.05	0.00140	8.29E-06	0.19	2.01	3200	65336
1.56E-05	1.390	0.311	0.98	erosion	1.13	0.00E+00	0.000	0.000	0.00	erosion	0.07	0.00139	7.97E-06	0.22	2.09	3200	68999
3.58E-05	3.189	0.542	1.70	erosion	1.57	1.32E-06	0.117	0.060	0.19	erosion	0.47	0.00145	9.98E-06	0.28	1.67	3200	70600
1.08E-03	95.968	5.240	16.48	erosion	6.62	1.33E-06	0.118	0.060	0.19	erosion	0.47	0.00157	1.50E-05	0.55	1.11	3200	72096
1.52E-03	134.973	6.578	20.69	erosion	7.68	1.20E-06	0.107	0.056	0.18	erosion	0.46	0.00152	1.52E-05	0.55	1.1	3200	73507
4.94E-03	439.530	14.452	45.45	erosion	12.88	1.70E-07	0.015	0.015	0.05	erosion	0.28	0.00143	1.29E-05	0.44	1.29	3200	74677
1.69E-03	150.342	7.069	22.23	erosion	8.05	1.07E-06	0.095	0.052	0.16	erosion	0.44	0.00147	9.36E-06	0.55	1.78	3200	75688
4.26E-03	379.122	13.096	41.19	erosion	12.07	1.26E-06	0.112	0.058	0.18	erosion	0.47	0.00147	1.08E-05	0.57	1.54	3200	76697
2.63E-03	234.113	9.496	29.87	erosion	9.77	5.58E-07	0.050	0.034	0.11	erosion	0.37	0.00144	9.69E-06	0.51	1.72	3200	77729
2.16E-03	192.594	8.337	26.22	erosion	8.97	3.47E-07	0.031	0.025	0.08	erosion	0.33	0.00142	9.01E-06	0.48	1.85	3200	78659
7.24E-04	64.458	4.019	12.64	erosion	5.57	5.80E-08	0.005	0.007	0.02	erosion	0.23	0.00142	8.91E-06	0.4	1.87	3200	79598
3.30E-04	29.369	2.380	7.48	erosion	3.97	4.16E-07	0.037	0.028	0.09	erosion	0.34	0.00142	8.87E-06	0.48	1.88	3200	80971
7.39E-04	65.802	4.075	12.82	erosion	5.62	6.52E-07	0.058	0.037	0.12	erosion	0.38	0.00148	1.13E-05	0.51	1.47	3200	82129
1.72E-04	15.333	1.543	4.85	erosion	3.01	6.97E-06	0.621	0.182	0.57	erosion	0.83	0.00148	1.13E-05	0.74	1.48	3200	83014
7.61E-04	67.709	4.153	13.06	erosion	5.69	1.03E-04	9.135	1.092	3.44	erosion	2.42	0.00153	1.31E-05	1.27	1.27	3200	83753
3.21E-03	285.649	10.843	34.10	erosion	10.66	3.05E-05	2.714	0.486	1.53	erosion	1.47	0.00151	1.23E-05	1.03	1.36	3200	84762
1.51E-03	134.570	6.565	20.65	erosion	7.67	9.52E-05	8.474	1.039	3.27	erosion	2.35	0.00139	8.09E-06	1.3	2.06	3200	85571
3.88E-03	345.651	12.313	38.73	erosion	11.59	4.07E-04	36.244	2.738	8.61	erosion	4.34	0.00139	8.13E-06	1.77	2.05	3200	86473
9.16E-03	815.878	21.828	68.65	erosion	16.91	1.18E-04	10.514	1.200	3.77	erosion	2.57	0.00135	8.09E-06	1.38	2.06	3200	87069
2.10E-03	186.753	8.168	25.69	erosion	8.85	4.66E-04	41.484	2.996	9.42	erosion	4.60	0.00132	6.94E-06	1.87	2.4	3200	87776
6.59E-03	586.301	17.513	55.08	erosion	14.62	2.14E-04	19.089	1.786	5.62	erosion	3.30	0.00131	6.11E-06	1.59	2.73	3200	88621
3.33E-03	296.144	11.107	34.93	erosion	10.83	1.04E-04	9.269	1.103	3.47	erosion	2.44	0.00128	5.85E-06	1.38	2.85	3200	89411
2.02E-03	180.064	7.972	25.07	erosion	8.71	6.17E-04	54.930	3.613	11.36	erosion	5.20	0.00133	5.19E-06	1.98	3.21	3200	90220
6.89E-03	613.059	18.042	56.74	erosion	14.91	4.82E-05	4.290	0.660	2.08	erosion	1.77	0.00128	6.34E-06	1.18	2.63	3200	90785
1.04E-03	92.666	5.119	16.10	erosion	6.52	9.26E-05	8.245	1.020	3.21	erosion	2.32	0.00128	5.04E-06	1.35	3.31	3200	91602
3.20E-03	284.428	10.812	34.01	erosion	10.64	6.42E-05	5.711	0.799	2.51	erosion	1.99	0.00130	5.05E-06	1.24	3.3	3200	92181
2.20E-03	195.553	8.423	26.49	erosion	9.03	1.05E-04	9.380	1.112	3.50	erosion	2.45	0.00131	5.57E-06	1.37	2.99	3200	92829
3.55E-03	315.825	11.594	36.46	erosion	11.14	1.83E-04	16.269	1.605	5.05	erosion	3.09	0.00129	5.79E-06	1.55	2.88	3200	93559
5.22E-03	464.768	15.000	47.18	erosion	13.2	3.15E-04	28.058	2.308	7.26	erosion	3.89	0.00128	5.32E-06	1.75	3.13	3200	94234
1.11E-02	988.143	24.802	78.00	erosion	18.4	3.38E-04	30.064	2.417	7.60	erosion	4.01	0.00130	5.02E-06	1.76	3.32	3200	94930
1.95E-02	1731.708	36.051	113.38	erosion	23.57	4.78E-04	42.564	3.048	9.59	erosion	4.66	0.00125	5.56E-06	1.93	3	3200	95628
1.17E-02	1043.792	25.725	80.91	erosion	18.85	1.33E-04	11.847	1.299	4.09	erosion	2.70	0.00122	4.57E-06	1.49	3.65	3200	96326
2.41E-03	214.872	8.969	28.21	erosion	9.41	4.39E-05	3.908	0.620	1.95	erosion	1.70	0.00121	3.90E-06	1.19	4.27	3200	96919
9.51E-04	84.691	4.821	15.16	erosion	6.27	1.67E-05	1.483	0.325	1.02	erosion	1.16	0.00121	3.69E-06	0.98	4.52	3200	97650
6.32E-04	56.219	3.669	11.54	erosion	5.25	1.99E-05	1.772	0.366	1.15	erosion	1.24	0.00121	3.73E-06	1	4.47	3200	98251
7.48E-04	66.616	4.108	12.92	erosion	5.65	5.00E-05	4.448	0.676	2.13	erosion	1.80	0.00125	4.41E-06	1.2	3.78	3200	98796
1.53E-03	136.185	6.617	20.81	erosion	7.71	9.11E-05	8.111	1.009	3.17	erosion	2.30	0.00125	4.53E-06	1.37	3.68	3200	99439
2.64E-03	235.209	9.526	29.96	erosion	9.79					erosion		0.00123	4.12E-06		4.05	3200	100028

100541	3200	3.71	1.66	4.49E-06	0.00125	3.43	erosion	5.97	1.898	20.921	2.35E-04	15.83	erosion	62.13	19.754	702.364	7.89E-03
101182	3200	3.64	1.72	4.58E-06	0.00125	3.70	erosion	6.71	2.132	24.907	2.80E-04	14.25	erosion	52.98	16.846	553.122	6.21E-03
101734	3200	3.27	1.96	5.10E-06	0.00128	4.90	erosion	10.36	3.295	47.844	5.37E-04	17.53	erosion	72.50	23.050	885.335	9.95E-03
102397	3200	3.71	1.51	4.49E-06	0.00125	2.84	erosion	4.43	1.409	13.383	1.50E-04	7.85	erosion	21.39	6.802	141.920	1.59E-03
102917	3200	3.59	1.69	4.64E-06	0.00126	3.58	erosion	6.37	2.026	23.068	2.59E-04	11.1	erosion	36.27	11.531	313.246	3.52E-03
103416	3200	3.61	1.75	4.62E-06	0.00126	3.84	erosion	7.09	2.255	27.098	3.04E-04	11.08	erosion	36.17	11.499	311.961	3.50E-03
103894	3200	3.58	1.71	4.66E-06	0.00126	3.67	erosion	6.62	2.103	24.403	2.74E-04	10.58	erosion	33.71	10.720	280.783	3.15E-03
104351	3200	3.77	1.74	4.42E-06	0.00125	3.76	erosion	6.89	2.189	25.912	2.91E-04	10.33	erosion	32.51	10.337	265.876	2.99E-03
104850	3200	3.46	1.86	4.82E-06	0.00127	4.37	erosion	8.67	2.758	36.647	4.12E-04	11.42	erosion	37.87	12.040	334.208	3.75E-03
105305	3200	3.15	1.86	5.29E-06	0.00129	4.44	erosion	8.90	2.831	38.105	4.28E-04	10.86	erosion	35.08	11.154	298.018	3.35E-03
105757	3200	2.97	1.76	5.61E-06	0.00130	4.02	erosion	7.62	2.424	30.191	3.39E-04	12.26	erosion	42.18	13.410	392.847	4.41E-03
106318	3200	3	1.59	5.56E-06	0.00130	3.27	erosion	5.53	1.760	18.677	2.10E-04	10.76	erosion	34.59	10.998	291.797	3.28E-03
106850	3200	3.43	1.49	4.86E-06	0.00127	2.81	erosion	4.34	1.381	12.984	1.46E-04	9.58	erosion	28.99	9.217	223.844	2.51E-03
107367	3200	2.84	1.79	5.87E-06	0.00131	4.19	erosion	8.14	2.587	33.289	3.74E-04	11.51	erosion	38.32	12.184	340.239	3.82E-03
107951	3200	2.58	2.2	6.46E-06	0.00133	6.44	erosion	15.80	5.023	90.049	1.01E-03	15.91	erosion	62.60	19.905	710.450	7.98E-03
108711	3200	3.31	1.96	5.04E-06	0.00128	4.89	erosion	10.33	3.284	47.604	5.35E-04	12.5	erosion	43.43	13.810	410.573	4.61E-03
109279	3200	3.65	1.45	4.57E-06	0.00125	2.63	erosion	3.92	1.245	11.114	1.25E-04	7.25	erosion	18.94	6.023	118.260	1.33E-03
109803	3200	3.58	1.53	4.66E-06	0.00126	2.94	erosion	4.67	1.484	14.458	1.62E-04	7.68	erosion	20.69	6.578	134.973	1.52E-03
110341	3200	3.76	1.39	4.43E-06	0.00125	2.40	erosion	3.39	1.079	8.971	1.01E-04	6.68	erosion	16.71	5.313	97.980	1.10E-03
110902	3200	3.61	1.73	4.62E-06	0.00126	3.75	erosion	6.84	2.176	25.680	2.88E-04	10.14	erosion	31.61	10.049	254.847	2.86E-03
111475	3200	3.27	1.76	5.10E-06	0.00128	3.95	erosion	7.42	2.360	28.998	3.26E-04	10	erosion	30.94	9.839	246.887	2.77E-03
111954	3200	3.22	2.23	5.18E-06	0.00128	6.36	erosion	15.48	4.924	87.399	9.82E-04	16.05	erosion	63.44	20.171	724.723	8.14E-03
112426	3200	4.28	2.69	3.89E-06	0.00122	8.80	erosion	25.45	8.091	184.122	2.07E-03	19.86	erosion	87.55	27.836	1174.893	1.32E-02
112930	3200	5.79	4.28	2.88E-06	0.00116	21.14	erosion	96.18	30.581	1352.904	1.52E-02	80.9	erosion	725.71	230.745	28040.655	3.15E-01
113437	3200	5.89	4.14	2.83E-06	0.00115	19.72	erosion	86.60	27.536	1155.970	1.30E-02	68.59	erosion	566.27	180.050	19327.633	2.17E-01
113897	3200	5.55	4.22	3.00E-06	0.00117	20.70	erosion	93.17	29.625	1289.980	1.45E-02	59	erosion	451.53	143.568	13761.804	1.55E-01
114401	3200	6.34	4.46	2.63E-06	0.00114	22.60	erosion	106.42	33.837	1574.654	1.77E-02	63.5	erosion	504.30	160.344	16243.077	1.82E-01
114881	3200	6.19	2.74	2.69E-06	0.00114	8.56	erosion	24.44	7.770	173.264	1.95E-03	21.64	erosion	99.67	31.689	1427.117	1.60E-02
115382	3200	7.04	4.12	2.37E-06	0.00112	18.95	erosion	81.55	25.931	1056.362	1.19E-02	50.62	erosion	358.62	114.025	9740.654	1.09E-01
115975	3200	7.34	2.58	2.27E-06	0.00111	7.38	erosion	19.46	6.189	123.162	1.38E-03	20.55	erosion	92.18	29.310	1269.436	1.43E-02
116590	3200	6.44	1.85	2.59E-06	0.00114	3.88	erosion	7.22	2.295	27.811	3.12E-04	9.62	erosion	29.17	9.275	225.985	2.54E-03
117307	3200	7.79	1.71	2.14E-06	0.00110	3.21	erosion	5.37	1.707	17.843	2.00E-04	10.77	erosion	34.64	11.014	292.416	3.28E-03

Table 3- Output and results for Sechura

	General Output			Drag Law Calculation					Bed Load Calculation			HEC Output			Bed Load Calculation		
Station	Q Total (m3/s)	Hyd Depth (m)	Vel tot (m/s)	z0/h	Cd	tb (N/m2)	tb>τcr	(tb-τcr)^3/2	θb	8*(θb-θcr)^3/2	qsb (kg/ms)	Shear Tot (N/m2)	tb>τcr	(tb-τcr)^3/2	θb	8*(θb-θcr)^3/2	qsb (kg/ms)
1870	1000	0.92	0.58	1.81159E-05	0.00163	0.55	erosion	0.25	0.081	0.184	2.07E-06	1.86	erosion	2.25	0.715	4.836	5.43E-05
4554	1000	1.3	1.96	1.28205E-05	0.00152	5.82	erosion	13.51	4.296	71.231	8.00E-04	21.55	erosion	99.04	31.491	1413.709	1.59E-02
7056	1000	2.89	1.46	5.76701E-06	0.00131	2.78	erosion	4.28	1.360	12.682	1.42E-04	9.21	erosion	27.30	8.680	204.578	2.30E-03
8914	1000	2.81	1.42	5.9312E-06	0.00131	2.64	erosion	3.95	1.255	11.248	1.26E-04	8.63	erosion	24.72	7.860	176.302	1.98E-03
10822	1000	2.82	1.43	5.91017E-06	0.00131	2.68	erosion	4.03	1.282	11.612	1.30E-04	8.66	erosion	24.85	7.902	177.708	2.00E-03
12382	1000	2.86	1.34	5.82751E-06	0.00131	2.34	erosion	3.27	1.038	8.462	9.51E-05	7.57	erosion	20.24	6.435	130.581	1.47E-03
14279	1000	1.69	1.34	9.86193E-06	0.00144	2.58	erosion	3.81	1.213	10.684	1.20E-04	5.05	erosion	10.87	3.455	51.385	5.77E-04
16131	1000	1.62	0.98	1.02881E-05	0.00146	1.39	erosion	1.40	0.444	2.370	2.66E-05	3.06	erosion	4.98	1.583	15.941	1.79E-04
18624	1000	2.48	0.66	6.72043E-06	0.00134	0.58	erosion	0.29	0.093	0.226	2.54E-06	1.96	erosion	2.45	0.778	5.493	6.17E-05
19813	1000	2.02	0.82	8.25083E-06	0.00140	0.94	erosion	0.71	0.224	0.849	9.54E-06	3.24	erosion	5.45	1.732	18.241	2.05E-04
21369	1000	1.57	1.24	1.06157E-05	0.00146	2.24	erosion	3.05	0.968	7.623	8.56E-05	8.09	erosion	22.40	7.122	152.059	1.71E-03
23510	1000	1.5	1.3	1.11111E-05	0.00148	2.49	erosion	3.59	1.142	9.762	1.10E-04	9	erosion	26.36	8.380	194.070	2.18E-03
25969	1000	1.09	0.6	1.52905E-05	0.00157	0.56	erosion	0.27	0.087	0.204	2.29E-06	2.39	erosion	3.37	1.070	8.860	9.95E-05
27411	1000	0.52	0.47	3.20513E-05	0.00183	0.40	erosion	0.13	0.042	0.069	7.75E-07	4.14	erosion	7.99	2.540	32.387	3.64E-04
28761	1000	0.4	0.46	4.16667E-05	0.00194	0.41	erosion	0.14	0.043	0.072	8.13E-07	1.13	erosion	0.98	0.311	1.390	1.56E-05
29844	1000	0.87	1.51	1.91571E-05	0.00164	3.74	erosion	6.82	2.168	25.531	2.87E-04	12.78	erosion	44.92	14.282	431.804	4.85E-03
30906	1000	1.57	1.18	1.06157E-05	0.00146	2.03	erosion	2.60	0.826	6.000	6.74E-05	7.31	erosion	19.18	6.100	120.519	1.35E-03
32021	1000	1.62	1.14	1.02881E-05	0.00146	1.89	erosion	2.30	0.731	5.002	5.62E-05	6.73	erosion	16.90	5.374	99.675	1.12E-03
32905	1000	1.64	1.12	1.01626E-05	0.00145	1.82	erosion	2.16	0.688	4.562	5.12E-05	6.54	erosion	16.18	5.144	93.321	1.05E-03
33831	1000	1.67	1.11	9.98004E-06	0.00145	1.78	erosion	2.09	0.664	4.329	4.86E-05	6.32	erosion	15.35	4.880	86.254	9.69E-04
34788	1000	1.63	1.13	1.02249E-05	0.00145	1.85	erosion	2.23	0.709	4.778	5.37E-05	6.66	erosion	16.63	5.289	97.307	1.09E-03
35633	1000	1.6	0.91	1.04167E-05	0.00146	1.20	erosion	1.09	0.347	1.638	1.84E-05	4.38	erosion	8.72	2.772	36.929	4.15E-04
36204	1000	1.65	0.89	1.0101E-05	0.00145	1.15	erosion	1.00	0.319	1.440	1.62E-05	4.11	erosion	7.90	2.512	31.843	3.58E-04
36643	1000	1.67	0.88	9.98004E-06	0.00145	1.12	erosion	0.96	0.305	1.351	1.52E-05	4.02	erosion	7.63	2.427	30.240	3.40E-04
37107	1000	1.69	0.87	9.86193E-06	0.00144	1.09	erosion	0.92	0.292	1.266	1.42E-05	3.86	erosion	7.16	2.278	27.504	3.09E-04
37785	1000	1.71	0.86	9.74659E-06	0.00144	1.06	erosion	0.88	0.280	1.185	1.33E-05	3.8	erosion	6.99	2.223	26.515	2.98E-04
38603	1000	1.73	0.85	9.63391E-06	0.00144	1.04	erosion	0.84	0.268	1.108	1.25E-05	3.68	erosion	6.65	2.114	24.597	2.76E-04
39632	1000	1.74	0.84	9.57854E-06	0.00144	1.01	erosion	0.81	0.256	1.039	1.17E-05	3.62	erosion	6.48	2.061	23.668	2.66E-04
40279	1000	1.74	0.83	9.57854E-06	0.00144	0.99	erosion	0.77	0.246	0.975	1.10E-05	3.5	erosion	6.15	1.955	21.869	2.46E-04
40847	1000	1.76	0.84	9.4697E-06	0.00143	1.01	erosion	0.80	0.255	1.033	1.16E-05	3.59	erosion	6.40	2.034	23.211	2.61E-04
41356	1000	1.76	0.83	9.4697E-06	0.00143	0.98	erosion	0.77	0.245	0.970	1.09E-05	3.54	erosion	6.26	1.990	22.460	2.52E-04
42086	1000	1.82	4.23	9.15751E-06	0.00142	25.40	erosion	126.92	40.354	2050.754	2.30E-02	89.99	erosion	851.63	270.781	35646.481	4.00E-01
42930	1000	1.69	1.48	9.86193E-06	0.00144	3.15	erosion	5.22	1.660	17.109	1.92E-04	7.78	erosion	21.10	6.710	139.036	1.56E-03
43720	1000	1.79	1.37	9.31099E-06	0.00143	2.67	erosion	4.02	1.279	11.567	1.30E-04	7.24	erosion	18.90	6.011	117.886	1.32E-03
44529	1000	1.58	0.98	1.05485E-05	0.00146	1.40	erosion	1.41	0.448	2.398	2.69E-05	3.77	erosion	6.91	2.196	26.028	2.92E-04
45095	1000	1.4	1.69	1.19048E-05	0.00150	4.26	erosion	8.36	2.658	34.664	3.89E-04	7.2	erosion	18.74	5.960	116.396	1.31E-03
45912	1000	1.74	0.89	9.57854E-06	0.00144	1.13	erosion	0.99	0.313	1.403	1.58E-05	3.43	erosion	5.96	1.894	20.856	2.34E-04
46490	1000	1.34	1.05	1.24378E-05	0.00151	1.66	erosion	1.87	0.593	3.656	4.11E-05	5.81	erosion	13.49	4.289	71.050	7.98E-04

47138	1000	1.16	1.04	1.43678E-05	0.00155	1.67	erosion	1.89	0.602	3.739	4.20E-05	5.69	erosion	13.06	4.153	67.709	7.61E-04
47868	1000	1.27	1.1	1.31234E-05	0.00153	1.84	erosion	2.21	0.703	4.712	5.29E-05	5.26	erosion	11.57	3.680	56.467	6.34E-04
48543	1000	1.49	1.11	1.11857E-05	0.00148	1.82	erosion	2.16	0.688	4.567	5.13E-05	5.2	erosion	11.37	3.615	54.988	6.18E-04
49240	1000	1.74	1.15	9.57854E-06	0.00144	1.89	erosion	2.31	0.736	5.049	5.67E-05	5.77	erosion	13.35	4.243	69.927	7.85E-04
49937	1000	1.45	1.39	1.14943E-05	0.00149	2.86	erosion	4.49	1.427	13.632	1.53E-04	8.82	erosion	25.56	8.126	185.308	2.08E-03
50635	1000	1.87	1.37	8.91266E-06	0.00142	2.65	erosion	3.97	1.262	11.343	1.27E-04	7.78	erosion	21.10	6.710	139.036	1.56E-03
51228	1000	2.17	0.95	7.68049E-06	0.00138	1.24	erosion	1.15	0.365	1.762	1.98E-05	2.9	erosion	4.58	1.455	14.040	1.58E-04
51960	1000	2.35	0.74	7.0922E-06	0.00136	0.74	erosion	0.46	0.147	0.450	5.06E-06	2.11	erosion	2.76	0.877	6.567	7.38E-05
52561	1000	2.19	0.64	7.61035E-06	0.00138	0.56	erosion	0.27	0.086	0.201	2.26E-06	2.16	erosion	2.86	0.910	6.949	7.81E-05
53105	1000	1.55	0.81	1.07527E-05	0.00147	0.96	erosion	0.74	0.235	0.909	1.02E-05	3.04	erosion	4.93	1.567	15.696	1.76E-04
53748	1000	1.68	0.95	9.92063E-06	0.00145	1.30	erosion	1.24	0.396	1.991	2.24E-05	3.65	erosion	6.57	2.088	24.130	2.71E-04
54338	1000	1.78	0.99	9.3633E-06	0.00143	1.40	erosion	1.40	0.446	2.384	2.68E-05	4.35	erosion	8.63	2.743	36.343	4.08E-04
54850	1000	1.64	1.31	1.01626E-05	0.00145	2.48	erosion	3.58	1.139	9.721	1.09E-04	8.73	erosion	25.16	8.000	181.011	2.03E-03
55491	1000	1.98	1.33	8.41751E-06	0.00140	2.47	erosion	3.55	1.129	9.600	1.08E-04	6.38	erosion	15.57	4.952	88.151	9.90E-04
56043	1000	1.08	1.96	1.54321E-05	0.00157	6.03	erosion	14.29	4.544	77.478	8.70E-04	7.94	erosion	21.77	6.922	145.677	1.64E-03
56706	1000	1.86	1.14	8.96057E-06	0.00142	1.84	erosion	2.20	0.701	4.693	5.27E-05	2.88	erosion	4.53	1.439	13.812	1.55E-04
57226	1000	1.78	1.34	9.3633E-06	0.00143	2.56	erosion	3.75	1.194	10.436	1.17E-04	4.59	erosion	9.38	2.981	41.175	4.63E-04
57726	1000	1.78	1.46	9.3633E-06	0.00143	3.04	erosion	4.93	1.566	15.677	1.76E-04	4.97	erosion	10.60	3.371	49.519	5.56E-04
58203	1000	1.97	1.45	8.46024E-06	0.00140	2.94	erosion	4.68	1.487	14.507	1.63E-04	4.98	erosion	10.64	3.382	49.750	5.59E-04
58660	1000	1.95	1.38	8.54701E-06	0.00141	2.67	erosion	4.01	1.276	11.524	1.29E-04	4.19	erosion	8.14	2.588	33.306	3.74E-04
59160	1000	1.31	1.71	1.27226E-05	0.00152	4.42	erosion	8.85	2.812	37.731	4.24E-04	3.73	erosion	6.79	2.159	25.386	2.85E-04
59614	1000	1.78	1.69	9.3633E-06	0.00143	4.07	erosion	7.78	2.475	31.146	3.50E-04	4.94	erosion	10.50	3.340	48.829	5.49E-04
60066	1000	1.22	2.2	1.36612E-05	0.00154	7.42	erosion	19.63	6.240	124.705	1.40E-03	6.3	erosion	15.27	4.857	85.627	9.62E-04
60627	1000	2.04	1.94	8.16993E-06	0.00139	5.23	erosion	11.47	3.646	55.703	6.26E-04	9.76	erosion	29.82	9.482	233.566	2.62E-03
61160	1000	2.22	1.43	7.50751E-06	0.00137	2.80	erosion	4.32	1.374	12.886	1.45E-04	6.8	erosion	17.17	5.460	102.074	1.15E-03
61677	1000	1.7	1.6	9.80392E-06	0.00144	3.68	erosion	6.65	2.115	24.613	2.76E-04	4.83	erosion	10.14	3.226	46.346	5.21E-04
62261	1000	2.8	2.07	5.95238E-06	0.00131	5.62	erosion	12.80	4.071	65.708	7.38E-04	12.41	erosion	42.96	13.660	403.875	4.54E-03
63020	1000	2.65	1.72	6.28931E-06	0.00133	3.92	erosion	7.33	2.330	28.459	3.20E-04	10.41	erosion	32.89	10.459	270.597	3.04E-03
63588	1000	2	1.36	8.33333E-06	0.00140	2.58	erosion	3.80	1.209	10.630	1.19E-04	5.44	erosion	12.19	3.875	61.035	6.86E-04
64112	1000	1.65	1.33	1.0101E-05	0.00145	2.56	erosion	3.75	1.193	10.421	1.17E-04	3.91	erosion	7.31	2.324	28.343	3.18E-04
64651	1000	1.55	1.2	1.07527E-05	0.00147	2.11	erosion	2.75	0.875	6.547	7.35E-05	4.09	erosion	7.84	2.493	31.483	3.54E-04
65211	1000	1.53	1.54	1.08932E-05	0.00147	3.48	erosion	6.09	1.937	21.568	2.42E-04	5.85	erosion	13.63	4.334	72.184	8.11E-04
65785	1000	1.75	1.74	9.52381E-06	0.00143	4.33	erosion	8.56	2.723	35.947	4.04E-04	6.36	erosion	15.50	4.928	87.516	9.83E-04
66263	1000	2.51	1.74	6.64011E-06	0.00134	4.05	erosion	7.72	2.453	30.740	3.45E-04	9.45	erosion	28.39	9.027	216.965	2.44E-03
66736	1000	3.74	1.53	4.45633E-06	0.00125	2.91	erosion	4.61	1.466	14.195	1.59E-04	7.54	erosion	20.12	6.396	129.397	1.45E-03
67240	1000	3.9	2.13	4.2735E-06	0.00124	5.61	erosion	12.76	4.058	65.399	7.35E-04	23.61	erosion	113.68	36.144	1738.368	1.95E-02
67747	1000	3.73	2.25	4.46828E-06	0.00125	6.30	erosion	15.29	4.861	85.746	9.63E-04	24.71	erosion	121.76	38.715	1927.106	2.16E-02
68206	1000	3.92	2.34	4.2517E-06	0.00124	6.76	erosion	17.01	5.410	100.655	1.13E-03	24.65	erosion	121.32	38.573	1916.533	2.15E-02
68711	1000	4.56	2.39	3.65497E-06	0.00121	6.87	erosion	17.43	5.543	104.391	1.17E-03	23.48	erosion	112.73	35.844	1716.775	1.93E-02
69190	1000	4.05	1.82	4.11523E-06	0.00123	4.07	erosion	7.77	2.469	31.040	3.49E-04	12.76	erosion	44.81	14.248	430.267	4.83E-03
69691	1000	4.48	2.44	3.72024E-06	0.00121	7.18	erosion	18.66	5.933	115.622	1.30E-03	22.11	erosion	102.95	32.734	1498.285	1.68E-02
70284	1000	3.96	1.69	4.20875E-06	0.00124	3.52	erosion	6.20	1.972	22.150	2.49E-04	11.07	erosion	36.12	11.484	311.319	3.50E-03
70900	1000	4.48	1.22	3.72024E-06	0.00121	1.79	erosion	2.12	0.675	4.432	4.98E-05	5.93	erosion	13.92	4.426	74.481	8.37E-04
71617	1000	3.98	1.1	4.1876E-06	0.00123	1.49	erosion	1.56	0.496	2.798	3.14E-05	5.71	erosion	13.13	4.176	68.260	7.67E-04
1870	3200	0.92	1.86	1.81159E-05	0.00163	5.61	erosion	12.78	4.063	65.520	7.36E-04	19	erosion	81.88	26.035	1062.719	1.19E-02
4554	3200	2.54	2.1	6.56168E-06	0.00134	5.88	erosion	13.75	4.373	73.156	8.22E-04	18.63	erosion	79.48	25.272	1016.375	1.14E-02
7056	3200	4.54	2.77	3.67107E-06	0.00121	9.23	erosion	27.39	8.710	205.641	2.31E-03	27.13	erosion	140.19	44.574	2380.750	2.67E-02
8914	3200	4.69	2.41	3.55366E-06	0.00120	6.95	erosion	17.75	5.644	107.258	1.20E-03	19.07	erosion	82.34	26.180	1071.616	1.20E-02
10822	3200	4.7	2.34	3.5461E-06	0.00120	6.55	erosion	16.21	5.153	93.584	1.05E-03	17.4	erosion	71.68	22.792	870.510	9.78E-03
12382	3200	4.73	2.11	3.52361E-06	0.00120	5.32	erosion	11.77	3.743	57.922	6.51E-04	14.06	erosion	51.91	16.506	536.500	6.03E-03

14279	3200	2.94	1.17	5.66893E-06	0.00130	1.78	erosion	2.09	0.665	4.335	4.87E-05	4.4	erosion	8.78	2.792	37.322	4.19E-04
16131	3200	3.42	1.07	4.87329E-06	0.00127	1.45	erosion	1.49	0.473	2.606	2.93E-05	3.99	erosion	7.54	2.398	29.716	3.34E-04
18624	3200	4.56	1.05	3.65497E-06	0.00121	1.33	erosion	1.28	0.408	2.088	2.35E-05	3.84	erosion	7.11	2.260	27.172	3.05E-04
19813	3200	4.35	1.19	3.83142E-06	0.00122	1.72	erosion	1.97	0.627	3.973	4.46E-05	5.33	erosion	11.81	3.755	58.220	6.54E-04
21369	3200	3.76	1.63	4.43262E-06	0.00125	3.30	erosion	5.62	1.786	19.095	2.15E-04	10.37	erosion	32.70	10.398	268.230	3.01E-03
23510	3200	3.2	1.89	5.20833E-06	0.00128	4.57	erosion	9.32	2.962	40.779	4.58E-04	14.71	erosion	55.59	17.676	594.535	6.68E-03
25969	3200	2.05	0.67	8.13008E-06	0.00139	0.62	erosion	0.33	0.106	0.274	3.08E-06	2.41	erosion	3.41	1.085	9.039	1.02E-04
27411	3200	1.39	0.38	1.19904E-05	0.00150	0.22	erosion	0.02	0.006	0.004	4.34E-08	2.67	erosion	4.02	1.277	11.541	1.30E-04
28761	3200	1.17	0.46	1.4245E-05	0.00155	0.33	erosion	0.08	0.025	0.032	3.54E-07	2.29	erosion	3.14	1.000	7.997	8.98E-05
29844	3200	1.21	2.88	1.37741E-05	0.00154	12.74	erosion	44.68	14.207	428.398	4.81E-03	45.79	erosion	308.40	98.056	7767.903	8.73E-02
30906	3200	2.88	2.02	5.78704E-06	0.00131	5.32	erosion	11.78	3.746	58.000	6.52E-04	17.45	erosion	72.00	22.891	876.195	9.84E-03
32021	3200	3.08	1.89	5.41126E-06	0.00129	4.60	erosion	9.41	2.993	41.433	4.65E-04	14.95	erosion	56.97	18.115	616.802	6.93E-03
32905	3200	3.1	1.83	5.37634E-06	0.00129	4.31	erosion	8.50	2.704	35.565	4.00E-04	13.79	erosion	50.41	16.028	513.363	5.77E-03
33831	3200	3.2	1.81	5.20833E-06	0.00128	4.19	erosion	8.15	2.590	33.346	3.75E-04	13.38	erosion	48.16	15.311	479.310	5.38E-03
34788	3200	3.14	1.81	5.30786E-06	0.00129	4.21	erosion	8.19	2.604	33.610	3.78E-04	13.23	erosion	47.34	15.052	467.175	5.25E-03
35633	3200	3.23	1.43	5.15996E-06	0.00128	2.61	erosion	3.88	1.233	10.956	1.23E-04	8.48	erosion	24.07	7.653	169.368	1.90E-03
36204	3200	3.19	1.39	5.22466E-06	0.00128	2.47	erosion	3.56	1.131	9.621	1.08E-04	7.94	erosion	21.77	6.922	145.677	1.64E-03
36643	3200	3.29	1.41	5.06586E-06	0.00128	2.53	erosion	3.69	1.173	10.165	1.14E-04	8.17	erosion	22.74	7.230	155.525	1.75E-03
37107	3200	3.33	1.39	5.00501E-06	0.00127	2.45	erosion	3.51	1.117	9.446	1.06E-04	7.95	erosion	21.81	6.935	146.098	1.64E-03
37785	3200	2.91	1.33	5.72738E-06	0.00131	2.30	erosion	3.17	1.009	8.103	9.10E-05	6.69	erosion	16.75	5.326	98.318	1.10E-03
38603	3200	3.38	1.38	4.93097E-06	0.00127	2.41	erosion	3.42	1.087	9.067	1.02E-04	7.68	erosion	20.69	6.578	134.973	1.52E-03
39632	3200	3.35	1.36	4.97512E-06	0.00127	2.35	erosion	3.27	1.040	8.487	9.53E-05	7.42	erosion	19.63	6.241	124.721	1.40E-03
40279	3200	3.38	1.33	4.93097E-06	0.00127	2.24	erosion	3.04	0.966	7.596	8.53E-05	7.18	erosion	18.66	5.935	115.655	1.30E-03
40847	3200	3.45	1.36	4.83092E-06	0.00127	2.34	erosion	3.24	1.032	8.381	9.41E-05	7.45	erosion	19.75	6.279	125.881	1.41E-03
41356	3200	3.42	1.34	4.87329E-06	0.00127	2.27	erosion	3.10	0.986	7.835	8.80E-05	7.25	erosion	18.94	6.023	118.260	1.33E-03
42086	3200	1.45	2.74	1.14943E-05	0.00149	11.13	erosion	36.41	11.577	315.107	3.54E-03	28.15	erosion	148.21	47.125	2588.014	2.91E-02
42930	3200	2.58	1.98	6.45995E-06	0.00133	5.22	erosion	11.42	3.632	55.377	6.22E-04	16.35	erosion	65.24	20.744	755.840	8.49E-03
43720	3200	2.77	1.63	6.01685E-06	0.00132	3.49	erosion	6.12	1.946	21.714	2.44E-04	11.46	erosion	38.07	12.104	336.881	3.78E-03
44529	3200	3.16	1.4	5.27426E-06	0.00129	2.51	erosion	3.65	1.160	9.996	1.12E-04	9.03	erosion	26.49	8.423	195.553	2.20E-03
45095	3200	2.58	2.01	6.45995E-06	0.00133	5.38	erosion	11.97	3.804	59.366	6.67E-04	15.4	erosion	59.59	18.947	659.784	7.41E-03
45912	3200	3.28	1.19	5.0813E-06	0.00128	1.80	erosion	2.14	0.680	4.489	5.04E-05	6.64	erosion	16.56	5.265	96.636	1.09E-03
46490	3200	3.27	1.36	5.09684E-06	0.00128	2.36	erosion	3.29	1.047	8.575	9.63E-05	10.81	erosion	34.84	11.076	294.898	3.31E-03
47138	3200	2.97	1.25	5.61167E-06	0.00130	2.03	erosion	2.58	0.821	5.955	6.69E-05	9.16	erosion	27.07	8.608	202.048	2.27E-03
47868	3200	2.88	1.38	5.78704E-06	0.00131	2.48	erosion	3.58	1.138	9.712	1.09E-04	11.23	erosion	36.91	11.737	321.671	3.61E-03
48543	3200	3.12	1.55	5.34188E-06	0.00129	3.09	erosion	5.05	1.607	16.291	1.83E-04	13.29	erosion	47.67	15.156	472.008	5.30E-03
49240	3200	3.31	1.75	5.03525E-06	0.00128	3.90	erosion	7.27	2.310	28.093	3.16E-04	18.48	erosion	78.52	24.965	997.913	1.12E-02
49937	3200	3.01	1.76	5.5371E-06	0.00130	4.01	erosion	7.60	2.415	30.022	3.37E-04	23.71	erosion	114.40	36.375	1755.080	1.97E-02
50635	3200	3.64	1.93	4.57875E-06	0.00125	4.66	erosion	9.59	3.050	42.612	4.79E-04	18.9	erosion	81.23	25.828	1050.080	1.18E-02
51228	3200	4.3	1.49	3.87597E-06	0.00122	2.70	erosion	4.08	1.297	11.813	1.33E-04	9.47	erosion	28.48	9.056	218.016	2.45E-03
51960	3200	4.52	1.19	3.68732E-06	0.00121	1.70	erosion	1.95	0.620	3.908	4.39E-05	6.29	erosion	15.24	4.845	85.314	9.58E-04
52561	3200	4.49	0.98	3.71195E-06	0.00121	1.16	erosion	1.02	0.325	1.480	1.66E-05	5.28	erosion	11.64	3.701	56.965	6.40E-04
53105	3200	3.78	1	4.40917E-06	0.00125	1.24	erosion	1.15	0.366	1.772	1.99E-05	5.66	erosion	12.96	4.119	66.888	7.51E-04
53748	3200	3.67	1.2	4.54133E-06	0.00125	1.80	erosion	2.13	0.677	4.453	5.00E-05	7.72	erosion	20.85	6.631	136.590	1.53E-03
54338	3200	4.05	1.37	4.11523E-06	0.00123	2.30	erosion	3.17	1.009	8.111	9.11E-05	9.8	erosion	30.01	9.541	235.758	2.65E-03
54850	3200	3.6	1.03	4.62963E-06	0.00126	1.33	erosion	1.29	0.410	2.104	2.36E-05	6.76	erosion	17.02	5.411	100.699	1.13E-03
55491	3200	3.53	1.79	4.72144E-06	0.00126	4.03	erosion	7.66	2.435	30.396	3.41E-04	15.32	erosion	59.12	18.798	652.026	7.32E-03
56043	3200	3.16	2.03	5.27426E-06	0.00129	5.29	erosion	11.66	3.707	57.091	6.41E-04	18.69	erosion	79.87	25.395	1023.812	1.15E-02
56706	3200	3.64	1.54	4.57875E-06	0.00125	2.97	erosion	4.74	1.507	14.807	1.66E-04	8.16	erosion	22.70	7.217	155.090	1.74E-03
57226	3200	3.52	1.73	4.73485E-06	0.00126	3.77	erosion	6.89	2.191	25.950	2.91E-04	11.54	erosion	38.47	12.232	342.263	3.84E-03
57726	3200	3.55	1.78	4.69484E-06	0.00126	3.98	erosion	7.51	2.389	29.542	3.32E-04	11.44	erosion	37.97	12.072	335.543	3.77E-03

|																	
58203	3200	3.53	1.74	4.72144E-06	0.00126	3.81	erosion	7.01	2.229	26.628	2.99E-04	10.88	erosion	35.18	11.185	299.271	3.36E-03
58660	3200	3.73	1.76	4.46828E-06	0.00125	3.86	erosion	7.16	2.275	27.456	3.08E-04	10.57	erosion	33.67	10.704	280.178	3.15E-03
59160	3200	3.42	1.88	4.87329E-06	0.00127	4.47	erosion	9.00	2.860	38.703	4.35E-04	11.67	erosion	39.13	12.442	351.110	3.94E-03
59614	3200	3.11	1.88	5.35906E-06	0.00129	4.55	erosion	9.24	2.937	40.261	4.52E-04	11.07	erosion	36.12	11.484	311.319	3.50E-03
60066	3200	2.94	1.78	5.66893E-06	0.00130	4.12	erosion	7.92	2.518	31.961	3.59E-04	12.49	erosion	43.38	13.793	409.826	4.60E-03
60627	3200	2.98	1.6	5.59284E-06	0.00130	3.32	erosion	5.66	1.798	19.291	2.17E-04	10.9	erosion	35.28	11.217	300.527	3.38E-03
61160	3200	3.42	1.5	4.87329E-06	0.00127	2.85	erosion	4.44	1.412	13.419	1.51E-04	9.67	erosion	29.40	9.349	228.676	2.57E-03
61677	3200	2.83	1.8	5.88928E-06	0.00131	4.24	erosion	8.29	2.635	34.215	3.84E-04	11.6	erosion	38.78	12.329	346.331	3.89E-03
62261	3200	2.57	2.21	6.48508E-06	0.00134	6.50	erosion	16.04	5.099	92.099	1.03E-03	16.01	erosion	63.20	20.095	720.629	8.09E-03
63020	3200	3.3	1.97	5.05051E-06	0.00128	4.94	erosion	10.50	3.339	48.801	5.48E-04	12.53	erosion	43.59	13.861	412.819	4.64E-03
63588	3200	3.65	1.45	4.56621E-06	0.00125	2.63	erosion	3.92	1.245	11.114	1.25E-04	7.27	erosion	19.02	6.049	119.011	1.34E-03
64112	3200	3.58	1.53	4.65549E-06	0.00126	2.94	erosion	4.67	1.484	14.458	1.62E-04	7.69	erosion	20.73	6.591	135.376	1.52E-03
64651	3200	3.76	1.39	4.43262E-06	0.00125	2.40	erosion	3.39	1.079	8.971	1.01E-04	6.69	erosion	16.75	5.326	98.318	1.10E-03
65211	3200	3.6	1.73	4.62963E-06	0.00126	3.75	erosion	6.85	2.178	25.709	2.89E-04	10.16	erosion	31.70	10.079	255.996	2.88E-03
65785	3200	3.27	1.77	5.09684E-06	0.00128	3.99	erosion	7.55	2.402	29.775	3.34E-04	10.01	erosion	30.99	9.854	247.451	2.78E-03
66263	3200	3.22	2.24	5.17598E-06	0.00128	6.41	erosion	15.70	4.992	89.217	1.00E-03	16.06	erosion	63.50	20.190	725.748	8.15E-03
66736	3200	4.28	2.69	3.89408E-06	0.00122	8.80	erosion	25.45	8.091	184.122	2.07E-03	19.87	erosion	87.61	27.857	1176.235	1.32E-02
67240	3200	5.79	4.28	2.87853E-06	0.00116	21.14	erosion	96.18	30.581	1352.904	1.52E-02	80.94	erosion	726.25	230.916	28071.915	3.15E-01
67747	3200	5.91	4.14	2.82008E-06	0.00115	19.71	erosion	86.53	27.512	1154.462	1.30E-02	68.78	erosion	568.63	180.800	19448.558	2.18E-01
68206	3200	5.55	4.22	3.003E-06	0.00117	20.70	erosion	93.17	29.625	1289.980	1.45E-02	59.01	erosion	451.65	143.604	13767.066	1.55E-01
68711	3200	6.37	4.46	2.61643E-06	0.00114	22.58	erosion	106.29	33.797	1571.816	1.77E-02	63.56	erosion	505.01	160.572	16277.708	1.83E-01
69190	3200	6.21	2.74	2.68384E-06	0.00114	8.56	erosion	24.42	7.763	173.048	1.94E-03	21.71	erosion	100.15	31.844	1437.595	1.61E-02
69691	3200	6.94	4.09	2.40154E-06	0.00112	18.72	erosion	80.06	25.456	1027.492	1.15E-02	49.71	erosion	348.96	110.955	9349.984	1.05E-01
70284	3200	7.42	2.6	2.24618E-06	0.00111	7.48	erosion	19.87	6.319	127.076	1.43E-03	20.97	erosion	95.04	30.219	1328.980	1.49E-02
70900	3200	3.9	1.44	4.2735E-06	0.00124	2.56	erosion	3.76	1.196	10.458	1.17E-04	4.39	erosion	8.75	2.782	37.125	4.17E-04
71617	3200	7.76	1.72	2.14777E-06	0.00110	3.25	erosion	5.47	1.740	18.367	2.06E-04	10.86	erosion	35.08	11.154	288.018	3.35E-03
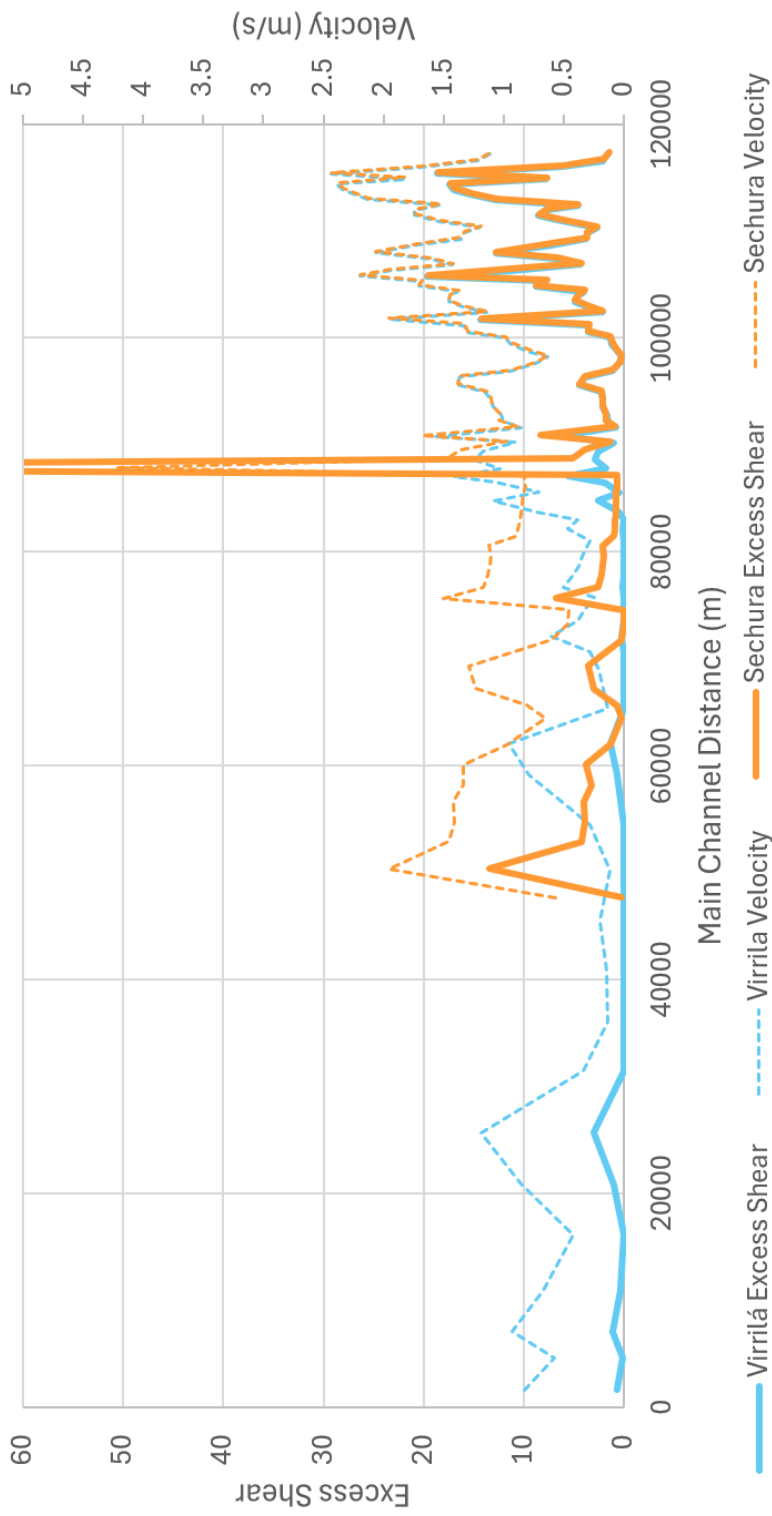
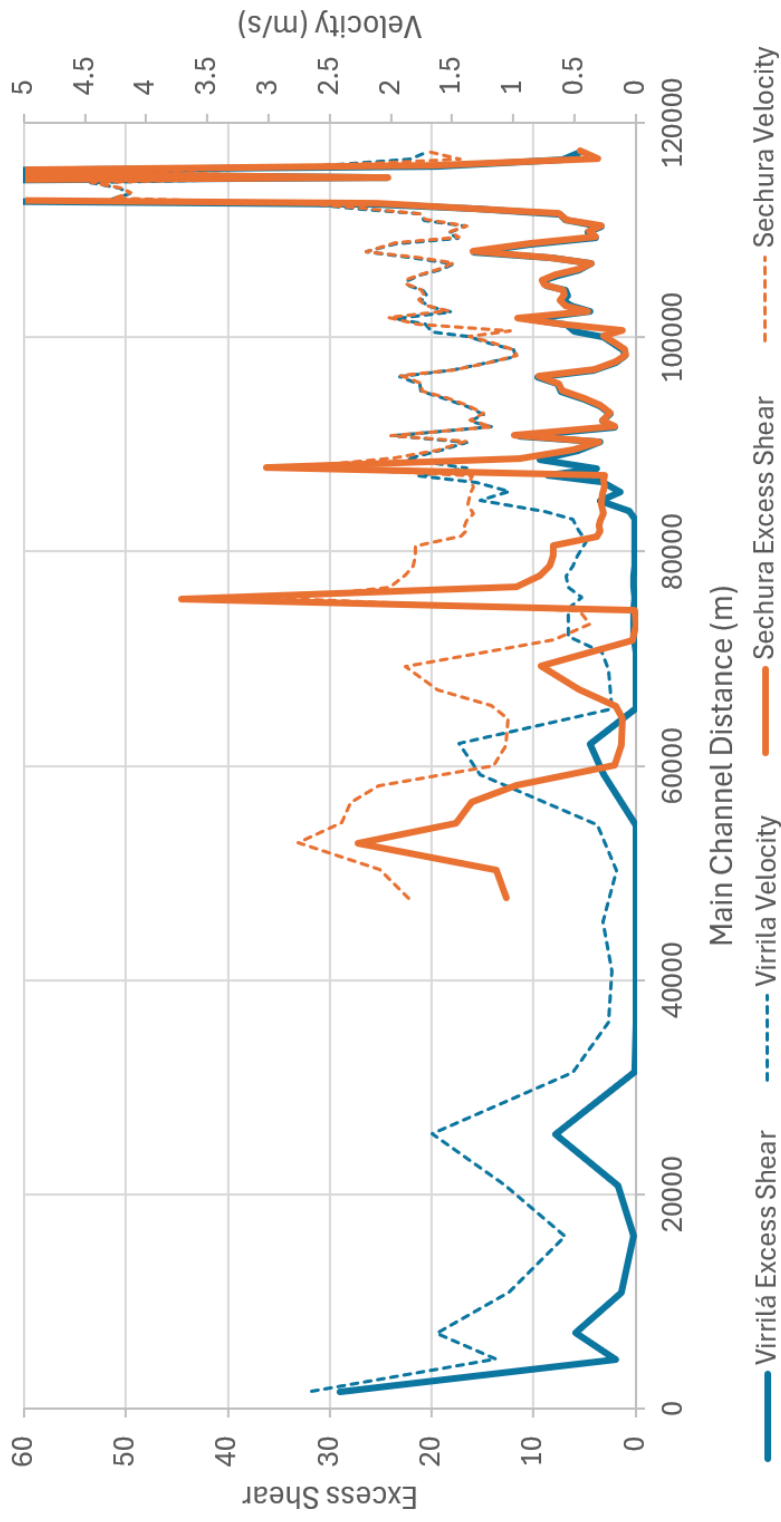*Figure 1- Excess shear based on drag law for Q=1,000m³/s*

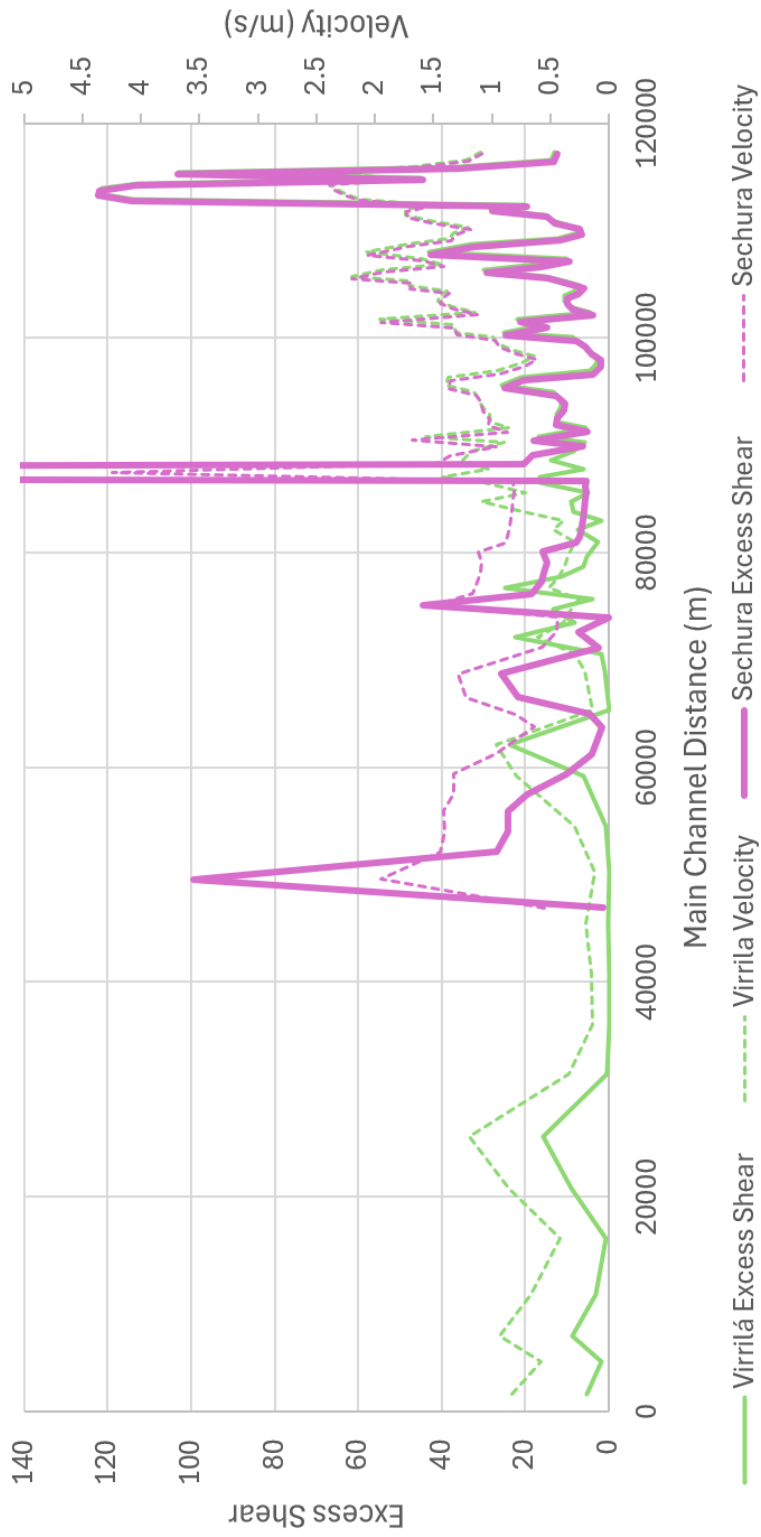*Figure 2- Excess shear based on drag law for Q=3,200m³/s*
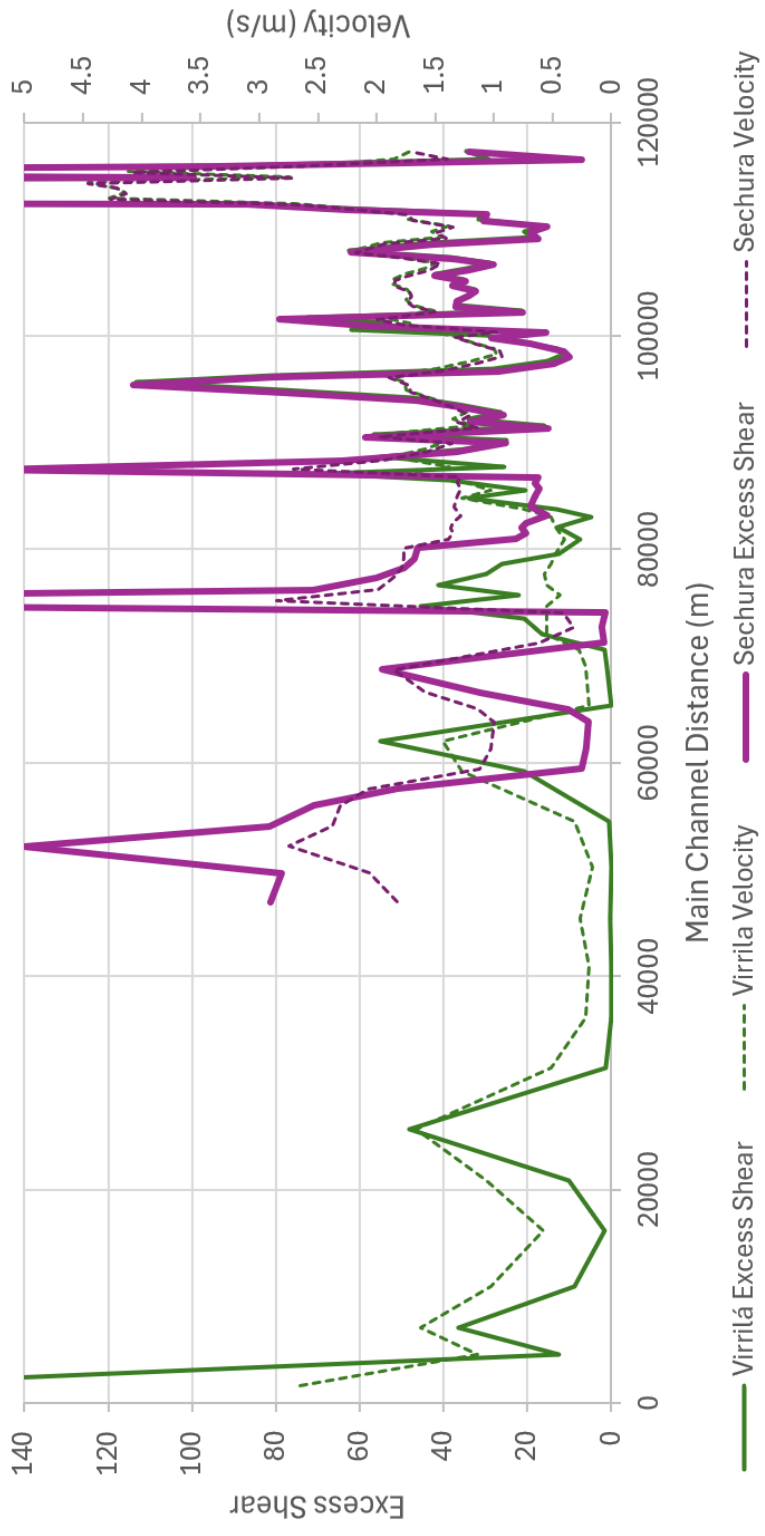
11

Figure 3- Excess shear based on HEC-RAS output for Q=1,000m3/s

Figure 4- Excess shear based on HEC-RAS output for Q=3,200m3/s

13